Blinding the CYCLOPS – Neuroblastoma vulnerabilities unveiled by 1p loss

Dissertation

Dipl. Biol. Alica Torkov

Biowissenschaften

Dissertation

submitted to the

Combined Faculty of Natural Sciences and Mathematics

of the Ruperto Carola University Heidelberg, Germany

for the degree of

Doctor of Natural Sciences

Presented by

Dipl. Biol. Alica Torkov

Born in: Moscow

Oral examination: 14.12.2018

Blinding the CYCLOPS – Neuroblastoma vulnerabilities unveiled by 1p loss

Referees: Prof. Dr. Thomas Höfer

PD Dr. Frank Westermann

Declaration

The work presented in this thesis was carried out from July 2013 until October 2018 in the group of Neuroblastoma Genomics at the German Cancer Research Center (DKFZ) in Heidelberg, Germany. It was supervised by Prof. Dr. Thomas Höfer PD and Dr. Frank Westermann.

I declare that this thesis, and the research to which it refers, are the product of my own work that has not been previously submitted for a degree or a diploma at any university. To the best of my knowledge this thesis contains no material previously published or written by another person except where due acknowledgement is made in the thesis itself.

_____

Alica Torkov
Heidelberg, October 2018

Table of Contents

Zusammenfassung

Das Neuroblastom ist der häufigste solide Tumor bei Kindern und tritt vor allem in der Embryonalentwicklung oder kurz nach der Geburt auf. Ein immer wiederkehrendes Ereignis ist die Deletion des Chromosomenarms 1p, was auf etwa 35% aller Hochrisikopatienten zutrifft. In den letzten Jahren hat sich die Forschung darauf konzentriert Tumorsuppressorgene in diesem Bereich zu identifizieren, jedoch stellten sich therapeutische Ansätze als kaum wirksam heraus. Neben den Tumorsuppressorgenen geht mit der Deletion auch eine große Anzahl an Passagiergenen verloren. Zellen mit hemizygoter Deletion von überlebensnotwendigen Passagiergenen und mit einhergehender reduzierter Genexpression, sind sensitiv gegenüber einer weitereren Reduktion. Gene, die diesem Muster entsprechen, werden CYCLOPS (**c**opy number alterations **y**ielding **c**ancer **l**iabilities **o**wing to **p**artial los**s**) genannt.

Diese Studie hat zum Ziel, CYCLOPS Gene auf Chromosomenarm 1p im Neuroblastom zu identifizieren. Nachdem der 1p-Status in 35 Neuroblastomzelllinien charakterisiert wurde, wurden fünf Zelllinien mit 1p-Deletion und fünf ohne ausgewählt. Um Kandidatengene zu identifizieren, wurde ein siRNA Screen für 184 potenziell therapeutisch adressierbare Gene auf dem distalen Ende von 1p durchgeführt. Sechs Kandidatengene mit differentieller Genabhängigkeit ($1p^{del} > 1p^{norm}$) und differentieller Expression ($1p^{del} < 1p^{norm}$) wurden ausgewählt. Am Ende setzte sich ein Gen durch, nämlich *EPHB2.* Dieses Gen ist von großer Bedeutung für embryonale Zellen und der Entwicklung des Nervensystems. In 1p deletierten Zelllinien hatte EphB2 Runterregulierung mittels siRNAs eine große Auswirkung auf die Viabiliät, zusätzlich stellte sich Zellzyklusarrest in G_1/G_0 ein. Es überlebte ein kleiner Anteil von Zellen, deren Resistenz durch das Aktivieren des HGF/c-MET Signalwegs und über MAPK/Akt-Aktivierung gesteuert wurde. Induzierbare EphB2-Expression rettete die Zellen vor dem Tod durch siRNA vermittelte EphB2 Runterregulierung, was darauf hinweist, dass 1p deletierte Zellen ein nötiges Minimum dieses Gens exprimieren.

In der Kontrollgruppe der 1p normalen Zellen hatte EphB2 Runterregulierung minimalen Einfluss. Die Viabilität der Zellen war nicht eingeschränkt, jedoch wurde Zellzyklusarrest in G_1/G_0 beobachtet.

Zusammenfassend beschreibt diese Studie EphB2 als einen vielversprechenden CYCLOPS Kandidaten im Neuroblastom. Da 1p-Deletion in ~35% aller Hochrisikopatienten auftritt, könnten mit diesem Ansatz weit mehr Patienten erreicht werden als mit Therapien, die auf andere Aberrationen im Neuroblastom abzielen. Auch könnten Nebenwirkungen reduziert werden, denn 1p-normale Zellen werden nicht negativ beeinflusst. Generell kann diese Studie als Grundsatzbeweis für die Identifikation neuer

zielgerichteter Therapieformen betrachtet werden und ist erweiterbar auf alle Krebsarten mit häufiger 1p-Deletion.

Summary

Neuroblastoma is the most common solid tumor in infants arising during embryonal development or early post-natal life. A frequently recurrent event is the deletion of chromosome arm 1p, which accounts for ~35% of all high stage cases. In the past years research focused on identification of potential 1p tumor suppressor genes but therapeutic targeting of these was shown to be difficult. With tumor suppressor gene deletion also a wide range of passenger genes get lost. As some of these are cell essential, hemizygous loss and associated reduced expression renders cells vulnerable to further impairment. Genes fulfilling these requirements are referred to as CYCLOPS (**c**opy number alterations **y**ielding **c**ancer **l**iabilities **o**wing to **p**artial los**s**) genes and may open a new therapeutic window.

In this study we aimed at identifying CYCLOPS genes on chromosome arm 1p in neuroblastoma. After detailed characterization of the 1p status in 35 neuroblastoma cell lines, we selected five cell lines with and five without 1p-deletion. For candidate gene identification, an siRNA screen for 184 druggable genes mapping to the distal end of 1p was done. Six candidates which showed high dependency in 1p-deleted but not in 1p non-deleted cells and differentially expression ($1p^{del} < 1p^{norm}$) were selected for further validation. In the end one gene met our requirements, *EPHB2*. This gene is especially important for embryonic cells and the developing nervous system. In 1p-deleted cell lines, EphB2 knock-down induced cell cycle arrest in G_1/G_0 and impaired cell survival. A small proportion of cells remained alive after activating HGF-induced c-MET signaling and MAPK/Akt pathway-mediated survival mechanisms. Induced EphB2 overexpression rescued the cells from cell death upon knock-down, supporting that *EPHB2* expression is at a minimum level for survival in 1p-deleted cell lines.

In the control group of 1p non-deleted cell lines the impact on viability and gene expression after EphB2 knock-down was minimal. We observed also G_1/G_0 arrest but viability was not impaired.

Taking together, this study revealed *EPHB2* as a promising 1p CYCLOPS candidate in neuroblastoma. As 1p is deleted in ~35% of all high-risk cases, a much wider range of patients may benefit from therapy approaches compared to strategies targeting other neuroblastoma-specific aberrations. Side effects of such approaches may be reduced as 1p non-deleted cells are not affected negatively. In general, this is a proof-of-principle for new drug target identification and is expandable to all cancers carrying frequent 1p-deletions.

1. Introduction

1.1 The genetic background of cancer

All cells of an organism underlie careful mechanisms to control and regulate the homeostasis of cell survival, division or differentiation. Any disturbance of these processes may result in the killing of the respective cell or, in contrast, lead to malignancy and tumor initiation. Acquired capabilities which are involved in tumor initiation and progression are resistance to cell death and growth suppression, potential immortality, uncontrolled proliferation, invasion and metastasis, induction of angiogenesis, avoidance of immune destruction, tumor-promoting inflammation and deregulation of cellular energetics (Hanahan and Weinberg 2011).

The course of tumor initiation is related to genomic alterations which may be induced by endogenic factors as defects of DNA replication, for example base pair mismatching, or reactive oxygen species produced during cellular metabolism. However, most of the defects are caused by exogenic factors which induce DNA damage (Lieber 1998; Mills, et al. 2003). These may be UV radiation, chemical substances as arsenic or asbestos or several viruses as the human papilloma virus (HPV) known to cause cervical cancer (Hubaux, et al. 2012; Pearce, et al. 2015; zur Hausen 1977). Whereas healthy cells show in average one mutation per cell in non-coding areas, cancer cells accumulate thousands of alterations (Loeb 2001). This process may start with one initial mutation in a crucial gene for tumor development which results in growth advantage compared to neighboring non-affected cells. The cell starts to proliferate leading to clonal expansion. Additional mutation events caused by endogenous or exogenous factors may lead to further growth advantage in affected cells which finally leads to the evolution of a tumor making carcinogenesis a multistep process (Vogelstein and Kinzler 2004). It is thought that at least four mutations that result in perturbation of critical signaling pathways are required to turn a cell into malignancy. Advanced tumor stages show strong genomic instability which goes along with heterogeneity of cells in one tumor cell population (Vogelstein and Kinzler 1993).

There are two types of mutations inducing tumor development. One is the gain-of-function mutation, amplification or overexpression of oncogenes, the other the loss-of-function mutation, deletion or epigenetic silencing of tumor suppressor genes.

1.1.1 Oncogenes

Oncogenes encode proteins which are involved in cell growth, differentiation, division or programmed cell death. They can be classified in to six categories: Growth and

transcription factors, growth factor receptors, proteins remodeling chromatin structure, signaling pathway transducers and regulators of apoptosis. The non-altered precursor genes of oncogenes are called proto-oncogenes. The activation of an oncogene leads to over expression of the corresponding protein giving the cell an advantage in proliferation and growth over other non-transformed cells. There are three basic ways to activate oncogenes: translocation, mutation and amplification (Anderson, et al. 1992; Croce 2008).

The translocation process may occur in two different types. The first event relocates a proto-oncogene to a new chromosomal site which may induce its expression. The second event is a fusion of a proto-oncogene and another gene which leads to a fusion protein with increased oncogenic activity. Oncogene activation via translocation was mainly observed in hematological diseases and childhood carcinomas (Mitelman, et al. 2007). The most prominent example is the Philadelphia Chromosome discovered by Peter Nowell and David Hungerford in 1960. Here, the broken end of chromosome 22 containing the *BCR* (RhoGEF and GTPase activating protein) gene fuses with the broken end of chromosome 9 containing the *ABL-1* gene (ABL proto-oncogene 1). The fused gene encodes for the fusion protein “BCR-ABL1” which shows high protein tyrosine kinase activity and recruits other proteins that are involved in cell cycle and division and leading uncontrolled cell proliferation. The Philadelphia Chromosome was observed in Chronic Myelogenous Leukemia and other forms of leukemia (Fitzgerald, et al. 1963; Heisterkamp, et al. 1985).

A mutation within a proto-oncogene causes changes in the protein structure which may increase the activity or lead to the loss of its regulation. The first oncogene in human beings was identified by Robert Allan Weinberg in 1981. *Ras* (rat sarcoma gene) gets activated by point mutation, is involved in signal transduction and the mutated form was observed in many carcinomas including lung, colon and pancreas (Balmain 1985; Fernandez-Medarde and Santos 2011).

Amplification of oncogenes increases their gene expression and contributes significantly to the progression of many solid tumors (Brison 1993). The amplification may occur as amplified DNA within one chromosome, known as homogeneously stained region (HSR) or as non-centromeric and non-telomeric extrachromosomal structure called double minutes (DMs). These events were first discovered in neuroblastoma where the transcription factor *MYCN* (v-myc avian myelocytomatosis viral related oncogene) was amplified up to 140 times (Schwab, et al. 1983). Another example for an amplified oncogene is *HER2* (human epidermal growth factor receptor 2), which plays a crucial role in 30% of aggressive breast cancers (Slamon, et al. 1987).

1.1.2 Tumor Suppressor Genes

Tumor suppressor genes (TSGs) are genes which loss drives the multistep process of tumor development (Boyd and Barrett 1990). In 1971 Knudson analyzed statistically the incidence of sporadic and hereditary retinoblastomas and observed that the inherited form is generally diagnosed at younger age compared to the sporadic form. Additionally, the hereditary cases often show tumor development in both eyes, whereas only one eye is affected in sporadic cancers. This observation led him to postulate the “two-hit hypothesis” for carcinogenesis which implies that two independent events are required for tumor development. Hereditary retinoblastomas inherit the “first hit” in the germline, the “second hit” occurs later in the somatic cell. Sporadic cases develop the “first” and “second hit” in somatic cells. The mutation rate is the same for all events, which explains the higher age of diagnosis in the non-inherited form (Knudson 1971; Weinberg 1989). Later, it was shown that the “first” and “second hit” occur in one gene, namely *Rb1* (retinoblastoma 1). The “first hit” occurred by loss of chromosomal region carrying *Rb1* (loss of heterozygosity, LOH) in the germ line and the second copy was mutated in somatic cells (“second hit”). As long as only one copy of the gene is altered, the expression of the other allele can compensate the protein level. In other words, whereas mutant oncogenes are typically dominant, these kinds of mutations are recessive requiring inactivation of both alleles (Cavenee, et al. 1983).

Next to the described genetic mechanisms, epigenetic silencing was observed, which is thought to be and early and driving event in tumorigenesis (Gauthier, et al. 2007; Yan, et al. 2006). The process is associated with a multi-step dynamic reprograming primarily in promoter regions which lead to transcriptional shut-down. One example is the TSG *RASSF1A* (Ras association domain family member 1) which shows widespread methylation of the promotor CpG islands in 65% of primary breast tumors and in many other cancer types (Honorio, et al. 2003; Liu, et al. 2002; Lo, et al. 2001). Another tool for TSG inactivation is post-transcriptional shut-down via microRNAs (miRNAs). Here, deregulated miRNAs bind to the messenger RNA (mRNA) of a TSG and inhibit the protein translation or induce direct cleavage. The miRNA *mir-21* suppresses several TSGs including *TPM1* (tropomyosin 1) and *PDCD4* (programmed cell death 4) in breast cancer cell lines (Zhu, et al. 2007; Zhu, et al. 2008).

However, the homozygous loss of TSGs is a too rare event to explain the high incidence of cancers. Nowadays it is known that the loss of one copy of many TSGs is sufficient to drive the cells into malignancy or promote tumor development. Indeed, most tumors are related to the hemizygous loss of TSGs which can be achieved by gene mutation, copy number changes, transcriptional repression, epigenetic silencing or post-transcriptional

shut-down through miRNAs leading to haploinsufficiency. This effect was suggested for many TSGs as *p53* (tumorprotein 53), *CAMTA1* (calmodulin binding transcription activator 1) or *PTEN* (phosphatase and tensin homolog). Whereas *p53* undergoes missense mutations, *CAMTA1* and *PTEN* can be inactivated by multiple ways including LOH, mutation, deletion, miRNAs or epigenetic silencing (Berger, et al. 2011; Henrich, et al. 2012; Kazanets, et al. 2016; Quon and Berns 2001; Wang, et al. 2015). In contrast to the "two-hit hypothesis", many TSGs are "obligate haploinsufficient" meaning that partial loss is tumorigenic but complete loss induces cell death. One example for this dose-responsive TSGs is *DICER1* (dicer 1, ribonuclease III) which is hemizygously deleted in many cancers. Mono-allelic deletion enhanced lung tumorigenesis in murine models but complete inactivation of *DICER1* improved survival of the mice (Kumar, et al. 2009; Lambertz, et al. 2010). The effect of TSG deletion is also highly tissue specific. Whereas some cells do not express a gene at all, others may be dependent on its activity for certain processes. Hence, a deletion of such TSGs will not alter non-expressing cells but will contribute to tissue specific cancer development in gene-dependent cells. Moreover, the tumorigenic power of a TSG is not only copy number or tissue-dependent but also relates on the genetic background of the cell. More precisely, combinations of TSG (and oncogene) alterations lead to divergent phenotypes. One example for this context-dependency is the interaction between *PTEN* and *p53*. In wild-type *p53*, prostate cancer haploinsufficient *PTEN* is more tumorigenic than the loss of both copies. In advanced cancers with *p53* mutation, complete inactivation of *PTEN* enhances tumor progression much stronger than *PTEN* haploinsufficiency. It was also shown that even a reduction of 20% of the expressed *PTEN* levels in murine prostate and mammary cells acts as a hit as it promotes the development of cancer ("quasi insufficiency") (Alimonti, et al. 2010; Berger, et al. 2011; Chen, et al. 2005).

Functionally, TSGs can be divided in to two groups: "gatekeepers" and "caretakers". Gatekeepers encode for genes that control cell growth and their loss leads to enhanced cell proliferation. An example is the previously mentioned *Rb1* gene, which is a key regulator of the entry into cell division. Caretakers are responsible for genetic stability and prevent and/or repair mutations. *MLH1* (MutL homolog 1) and *MSH2* (MutS homolog 2) are involved in mismatch repair of DNA bases which have been failed during DNA replication. Mutations in *MLH1* and *MSH2* induce microsatellite instability and increase the likelihood for tumor initiation. However, the differentiation between gatekeeper and caretaker is not always possible. For example, *p53* directly regulates cells growth on one hand; on the other hand it is involved in genome recovery after damaging mutations (Deininger 1999; Kinzler and Vogelstein 1997). An additional function group of TSGs has been proposed, namely the "landscaper" genes. These do not contribute to cancer

development directly but generate a tumor-supportive microenvironment. Landscapers may regulate extracellular matrix proteins, cellular surface markers, growth factors or cellular adhesion molecules (Michor, et al. 2004). An example is *PTEN* which is involved in apoptosis-inducing pathways and its loss reduces the sensitivity to extracellular death signals as TNFα (tumor necrosis factor α) (Stambolic, et al. 1998).
Nevertheless, direct targeting of TSGs for therapeutic reasons has turned out to be difficult. Approaches to address interaction partners of TSGs delivered more promising results. For example, MDM2 (mouse double minute 2 homolog) is a negative regulator of p53. The chemical compound nutlin inhibits the interaction of MDM2 and p53, which has anti-tumoric effects. Nutlin and some of its more potent derivates are currently tested in preclinical studies (Michaelis, et al. 2011; Morris and Chan 2015).

1.2 Neuroblastoma

Neuroblastoma is an embryonal tumor which arises during fetal or early post-natal life. It is the most common solid extracranial childhood cancer and represents about 7% of all pediatric malignancies under the age of 15. The incidence is 1 case per 100,000 children with a median age of diagnosis of 17 months (Howlader N 2011; London, et al. 2005). Tumors can develop anywhere along the sympathetic nervous system but 65% are present in the abdomen including neck, chest and pelvis with a majority occurring in the adrenal medulla or paraspinal ganglia (Maris 2010; Maris, et al. 2007). Neuroblastoma is a clinically heterogeneous disease. Whereas older children have generally a poor prognosis despite chemo- and radiation therapy, it also shows the highest rate of spontaneous regression of all cancers, especially for infants under 18 months (Hero, et al. 2008; Maris, et al. 2007). This goes along with the fact that low-risk patients show a long-term survival probability greater than 95% but high-risk cases only 40 – 50% (Maris 2010; Oberthuer, et al. 2015). To determine the patients risk level and outcome probability the International Neuroblastoma Staging System (INSS) was published in 1988 and revised in 2007 (Tab. 1.1) (Brodeur, et al. 1988; Maris, et al. 2007). Tumors of stages 1-3 and 4S are associated as low- or intermediate-risk cases with a much better survival prognosis than stage 4 showing an overall survival probability of 20 – 30% (Berthold and Hero 2000). Stage 4S accounts for 5% of cases and has a striking clinical phenotype (S = special) as it almost always regresses spontaneously (D'Angio, et al. 1971; Maris, et al. 2007). However, this phenomenon was also observed in rare cases of stage 1-3 neuroblastomas (Berthold F 1998). Next to localization of the tumor and patient´s age at diagnosis also certain genetic alterations have an impact on patient´s survival. One of these is the copy number status of the *MYCN* oncogene which is amplified in 20% of all neuroblastoma cases (Westermann and Schwab 2002). Irrespective of stage, *MYCN*

amplification leads to patient's assignment to the high-risk group. *MYCN* is a transcription factor which enhances cell proliferation and cell growth, metastasis, genomic instability, angiogenesis, reduces cell adhesion and inhibits proliferation. Thus its overexpression leads always to poor prognosis for the patient´s outcome (Adhikary and Eilers 2005). Next to the *MYCN* copy number, the tumor-cell DNA index (ploidy) and specific recurrent segmental chromosomal aberrations are prognostic biomarkers for neuroblastoma (Janoueix-Lerosey, et al. 2009).

Tab. 1.1: International Neuroblastoma Staging System (Maris, et al. 2007)

Stage	Description
1	Localized tumor with complete gross excision, with or without microscopic residual disease; representative ipsilateral lymph nodes negative for tumor microscopically (nodes attached to and removed with the primary tumor could be positive).
2A	Localized tumor with incomplete gross excision; representative ipsilateral non-adherent lymph nodes negative for tumor microscopically.
2B	Localized tumor with or without complete gross excision, with ipsilateral non-adherent lymph nodes positive for tumor. Enlarged contralateral lymph nodes must be negative microscopically
3	Unresectable unilateral tumor infiltrating across the midline, with or without regional lymph node involvement; or localized unilateral tumor with contralateral regional lymph node involvement; or midline tumor with bilateral extension by infiltration (unresectable) or by lymph node involvement.
4	Any primary tumor with dissemination to distant lymph nodes, bone, bone marrow, liver, skin, and/or other organs, except as defined for stage 4S.
4S	Localized primary tumor in infants younger than 1 year (as defined for stage 1, 2A, or 2B), with dissemination limited to skin, liver or bone marrow (<10% malignant cells).

1.2.1 Genomic alterations in neuroblastoma

Recent DNA sequencing projects revealed that recurrent somatic mutations in neuroblastoma are rare. Common cancer-driving mutations are limited, e.g. *MYCN* (1.7%) and *ALK* (ALK tyrosine kinase receptor) (7%). These findings suggest that tumorigenesis is more related to larger events as chromosomal rearrangements, including genomic gain or loss, or changes in ploidy (Molenaar, et al. 2012; Pugh, et al. 2013).

1.2.1.1 Ploidy

Cytogenetic analyses revealed four ploidy levels in neuroblastoma: near-diploid, near-triploid, near-tetraploid and near-pentaploid. The near-diploid and near-tetraploid stages usually are associated with structural abnormalities as 1p-deletion or *MYCN* amplification and are found mainly in infants older than one year. These patients most frequently have advanced tumor stages and are poor responders to chemotherapy. In contrast, near-triploid and near-pentaploid tumors, which show three or respectively five almost complete haploid sets of chromosomes with only few structural abnormalities, were found in children with high survival rates. Hence, the DNA content of neuroblastoma tumors can be linked to tumor stage and prognosis (Hayashi, et al. 1989; Janoueix-Lerosey, et al. 2009; Kaneko, et al. 1987).

1.2.1.2 Genomic gain

Gain of genomic material occurs via gain of whole or partial chromosome arms or simply, the duplication or amplification of single genes. About 50 to 72% of all neuroblastomas show an additional 17q segment, mainly 17q21.32-25.3, making it the most frequent genetic alteration in neuroblastoma. This event is more often detected in advanced stages of di- or tetraploid tumors which also show 1p loss and *MYCN* amplification. In contrast, gain of the whole chromosome 17 in triploid cases is associated with favorable clinical outcome (Bown, et al. 1999; Bown, et al. 2001; Ho, et al. 2018; Plantaz, et al. 1997). Partial gain happens mostly through translocation of an additional segment of 17q to a partner chromosome leading to the loss of genetic information at the fusion area. More than 20 chromosome regions were identified to bind translocated 17q, with the highest incidence seen for chromosome arm 1p followed by 11q (Bown, et al. 1999). It has been implicated that dosage effects of certain genes located on 17q are involved in tumor formation but the large size of the gained area makes it difficult to identify these. Nevertheless, 17q gain has been proposed as a marker for poor prognosis, as well as gain of 1q, 2p, 7q and 11p (Cheung and Dyer 2013; Vandesompele, et al. 2005). The recurrent gain of whole chromosomal segments leads to the assumption that several genes are located there which may contribute to tumor initiation or progression. Next to this, also duplication or amplification of single genes was observed which underlies their role as driving events. The most prominent example is the oncogene *MYCN* which plays a crucial role in a few cancer types, but especially in neuroblastoma. Amplified *MYCN* is found in around 25% of cases with values between 5 and 500 fold. The initial copies of *MYCN* remain after amplification at their original chromosomal locus, 2p24. The additional copies can either stay at the chromosomal site as homogeneously staining regions

(HSRs) or as extrachromosomal amplified DNA (double minutes, DMs) (Schwab, et al. 1983). *MYCN* amplification (> 10 copies) is present in 40% of high-risk patients and correlates with rapid tumor progression and poor prognosis. Therefore, it is a powerful prognostic marker (Brodeur, et al. 1984; Seeger, et al. 1985). However, it has turned out that *MYCN* itself is difficult to target therapeutically, which is true for most transcription factors. Current research focusses on addressing *MYCN* partners, for example *BRD4* (bromodomain containing 4) which can be inhibited by *JQ1* (Chayka, et al. 2015; Fowler, et al. 2014).

1.2.1.3 Genomic loss

Loss of whole or partial chromosomes is a major event in many tumors including neuroblastoma (Frohling and Dohner 2008). Recurrently deleted chromosomal regions with different ratios depending on the study and used methods are 2q, 3p, 4p, 9p, 14q, 16p and 18q (Bown 2001). The most frequently deleted chromosome arms are 11q (up to 40%) and 1p (~ 35%) (Mlakar, et al. 2017). While 11q is more often deleted than *MYCN* amplified, these alterations are almost mutually exclusive (Plantaz, et al. 2001). Totally, 70 to 80% of stage 4 neuroblastomas have either a *MYCN* amplification or 11q deletion (Mlakar, et al. 2017). Loss of whole chromosome 11 is associated with low stage, whereas unbalanced deletion is mostly observed in high stage tumors (Guo, et al. 2000). Loss of 11q is often associated with 17q gain as it is the second most common partner (after 1p) for 17q translocation (Van Roy, et al. 1994). Such translocations account for approximately half of all segmental 11q losses (Vandesompele, et al. 2001). The frequent loss of 11q led to the suggestion that TSGs may be located at this site. However, former attempts to validate candidates such as *CADM1* (cell adhesion molecule 1), *ATM* (ATM serine/threonine kinase) and *H2AFX* (H2A histone family member x) to have tumor-suppressing functions following Knudson´s “two-hit hypothesis” failed as no further (smaller) deletion, mutation or methylation events could be detected on the second chromosome. It has been proposed that 11q deletion could be a case of haplo-insufficiency but this still remains to be proven (Mandriota, et al. 2015; Michels, et al. 2008; Mlakar, et al. 2017). Interestingly, 11q also harbors several oncogenes as *CCND1* (cyclin D1) and *NCAM* (neural cell adhesion molecule 1). Copy number gains and rearrangements were identified in many tumors and hence appear to play important roles in neuroblastoma (Korja, et al. 2009; Molenaar, et al. 2003).

Allelic loss of 1p accounts for approximately 35% and 70% of advanced stages. Most of the deletions happen through the attachment of a translocated 17q chromosome arm (Caron, et al. 1994; Savelyeva, et al. 1994). In contrast to loss of 11q, 1p deletion correlates with *MYCN* amplification and other high-risk events such as di- or tetraploidy.

Only 15 - 20% of *MYCN* single copy cases show 1p loss (De Brouwer, et al. 2010; Fong, et al. 1989; Maris, et al. 2000). The size of the deleted chromosome part is associated with the *MYCN* status. *MYCN* amplified cases show large 1p deletions at the distal end and have worse outcome than patients with *MYCN* single copy with short or interstitial deletions (Takeda, et al. 1994). Many research groups have focused on the identification of the smallest region of overlapping deletion (SRO). Most studies agreed on a common deletion site at 1p36 (summarized by Henrich, et al. 2012; Fig. 1.1). A more recent study confirmed these findings by identification of a SRO at 1p36.33 – 1p13.3 in 25 – 40% of analyzed neuroblastoma tissue samples (Ho, et al. 2018). Enrichment of potential TSGs in frequently lost regions and a low density of oncogenes through all cancers have been reported and led to the proposal of a “cancer gene island model” (Solimini, et al. 2012).

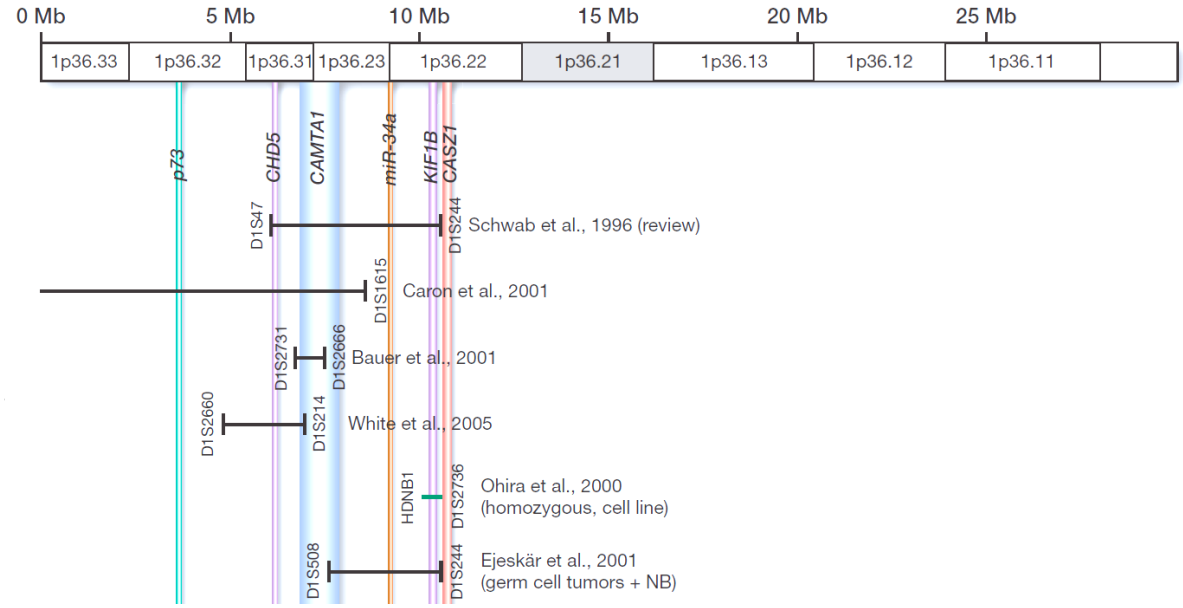

Fig. 1.1 Chromosome arm 1p36 with detected deletion sites and potential TSGs in neuroblastoma. The horizontal bars represent deletion sites identified by several research groups; vertical colored bars indicate the location of TSG candidates; adapted from Henrich, et al. 2012.

The frequent loss of chromosome arm 1p and the size of the SROs indicate that this location may also carry multiple genes shoes disruption promotes tumor development and progression. Indeed, several genes on 1p36 have been proposed as TSGs. However, the tumor-driving effect of these genes is difficult to proof as they do not follow the “two hit” model but are dosage-dependent. As there is no straight forward approach to prove dosage-sensitivity, the only way so far is to accumulate data and indications from genetic, epigenetic and transcriptional studies. Henrich and his colleagues reviewed supportive evidence for six TSG candidates: *TP73* (tumor protein 73), *CHD5* (chromodomain helicase DNA binding protein 5), *CAMTA1* (calmodulin binding transcription activator 1),

miR-34a (microRNA 34a), *KIF1B* (kinesin family member 1B) and *CASZ1* (castor zinc finger 1) (Henrich, et al. 2012). Other studies proposed TSG candidates as *NBPF1* (neuroblastoma breakpoint family member 1) or *DMAP1* (DNA methyltransferase 1 associated protein 1) (Vandepoele, et al. 2005; Yamaguchi, et al. 2014). Next to the loss of chromosome arm 1p, also aberrant methylation patterns at the distal end were observed leading to epigenetic silencing of encoded TSGs (Henrich, et al. 2016) (further discussed in 1.2.1.4).

1.2.1.4 Epigenetic alterations

Besides genetic alterations, epigenetic modifications play an important role in neuroblastoma development and progression. Here, the DNA sequence remains unchanged but local chromatin modification (e.g. aberrant DNA methylation or histone modification) or high-order chromatin structure rearrangements alter the expression of cancer-driving genes.

In general, DNA methylation of CpG islands is a stable modification and its pattern can be inherited through many cell divisions and is often associated with gene silencing. The methylation status changes actively during development and cell differentiation, depending on the required genes, or plays a role in epigenetic memory (reviewed in Durinck and Speleman 2018). The first DNA methylation study in neuroblastoma identified high methylation of the TSG *CASP8* (caspase 8) which goes along with *MYCN* overexpression and resistance to chemotherapy (Teitz, et al. 2000). Later, these findings were confirmed by Alaminos and his colleagues, who analyzed promoter hypermethylation of 45 candidate genes in 10 neuroblastoma cell lines and 10 candidate genes in 118 primary neuroblastoma tumors. The CpG island hypermethylation portrait was different for *MYCN*-amplified versus non-amplified tumors, including the TSG *CASP8* (Alaminos, et al. 2004).

Additionally, aberrant histone modification has been shown to play a role in tumorigenesis, including neuroblastoma (Lochmann, et al. 2018; Wong, et al. 2017). Histones serve as DNA packaging units associated with chromatin condensation and thereby regulate gene transcription. Post-translational modifications of N-terminal tails of the core histone proteins happen through, among others, methylation and acetylation. Whereas acetylation of lysine is associated with gene transcription, methylation of lysine and arginine residues induces either transcriptional activation or suppression, depending on the pattern (eg. di- or trimethylation) and exact position (Kornberg and Lorch 1999; Kouzarides 2007; Luger and Richmond 1998; Strahl and Allis 2000; van Groningen, et al. 2017). Several histone-modifying proteins are involved in methylation/acetylation processes, such as the polycomb repressive complex 2 (PRC2) which trimethylates histone H3 on lysine 27

(H3K27me3) leading to chromatin compaction and transcriptional repression. Many H3K27 trimethylation targets are genes required for stem cell differentiation and embryonic development (reviewed in Chase and Cross 2011). In high-risk neuroblastomas, PRC2 components have been described to play a role in the downregulation of tumor-suppressive and differentiation-related genes via promoter hypermethylation, e.g. *SPOCK2* (SPARC (Osteonectin), Cwcv and Kazal like domains proteoglycan 2) and *SLC18A2* (solute carrier family 18 member A2; Henrich, et al. 2016).

Taken together, chromatin accessibility is controlled by the CpG methylation level and the methylation/acetylation status of histones. Expression-activating hypomethylation and chromatin decondensation have been shown in so-called enhancer regions, DNA regulatory elements with multiple transcription factor (TF), cofactor and chromatin regulator binding. Enhancers control the expression of a gene from a distance, whereat these genes are required to define cell identity (Lister, et al. 2009). Mislead activation of enhancers which are connected to proto-oncogenes is a known epigenetic event in tumorigenesis (reviewed in Hnisz, et al. 2013; Pott and Lieb 2015). Recently, our group has combined the analysis of methylation and transcription profiles and copy number variations in 105 neuroblastomas with primary tumor- and cell line-derived global histone modification analyses. Divergent enhancer methylation has been identified in different patient subgroups, with respect to patient prognosis, including *MYCN* amplification. An important high-risk phenomenon was the hypermethylation of TSG candidates located on 1p36 as *CAMTA1*, *KIF1B* and *CHD5* (Fig. 1.1). Next to epigenetic down-regulation of potential TSGs, activation of oncogenes via hypomethylation has been described, such as *PRAME* (preferentially expressed antigen in melanoma) or *CCND1* in another study (Henrich, et al. 2016; Mayol, et al. 2012).

Large clusters of multiple enhancers with unusually high levels of TFs and coactivator binding and histone-modifications leading to very high chromatin accessibility are defined as super-enhancers (SEs). SEs induce strong expression of the associated genes which encode for TFs defining cellular identity (Hnisz, et al. 2013; Pott and Lieb 2015). In tumors, oncogenes may acquire SEs through chromosomal rearrangements, such as *TERT* (telomerase reverse transcriptase) located on chromosome 5p15.33. In 31% of high-risk neuroblastoma cases translocation of 5p15.33 occurs to juxtapose active enhancer elements to boost *TERT* transcription (Peifer, et al. 2015).

Many different TFs are involved in SE-induced gene transcription, however only a few of them, termed as core TFs, define the cell-specific network (Saint-Andre, et al. 2016). These TFs bind to their own promoters and those of other core TFs which leads to an auto-regulatory loop (Boyer, et al. 2005). It was shown that SE-associated TF regulatory circuits define lineage identity in intratumoral heterogeneity. Most neuroblastomas consist

of two types of tumor cells with divergent gene expression profiles. Here, undifferentiated mesenchymal and adrenergic- committed neuroblastoma types were described. Among others, *PRRX1* (paired related homeobox 1) and *SOX9* (SRY-box 9) were shown to be master regulators in the mesenchymal state, whereas the adrenergic state was driven by *GATA3* (GATA binding protein 3) and *HAND1* (heart and neural crest derivatives expressed 1). Interestingly, induction of *PRRX1* expression in adrenergic cells led to a switch to the mesenchymal state (van Groningen, et al. 2017).

1.3 The concept of CYCLOPS

As described in 1.1.2 and 1.2.1.3 the loss of genomic material is often associated with the deletion of genes which promote tumorigenesis, namely TSGs. Any genetic change which contributes to tumor development or progression is referred as “driver event”. However, the loss of a whole chromosome arm containing one or more TSGs always goes along with an accompanied loss of multiple neighboring genes. Their loss does not drive malignancy but is a collateral damage and is therefore referred as “passenger event” (Fig. 1.2). Nevertheless, these genes may function as general housekeepers or be involved in the accommodation of cancer-specific stress. Tumor cells rely in a much stronger manner than normal cells on genes that abrogate challenges induced by DNA replication damages, mitotic, metabolic or oxidative stress (Solimini, et al. 2007). In other words, the loss of one copy of such a gene through the deletion of a whole chromosome arm leads the cell to a high dependency on the remaining one. Some of these genes are expected to be cell essential and complete loss may not be tolerated by compensatory mechanisms.
Nijhawan and his colleagues described the potential therapeutic window which might be opened by addressing these genes. They hypothesized that there is a set of genes which hemizygous loss leads to a reduced protein level but that is still high enough to sustain viability. Further external suppression of these should induce cell death in cells with deletion but will not harm cell without loss (Fig. 1.2). They termed these new candidates CYCLOPS (copy number alterations yielding cancer liabilities owing to partial loss). For this approach they screened 86 cancer cell lines and identified 56 CYCLOPS candidates which were mainly encoding for spliceosome, proteasome or ribosome proteins. Finally,

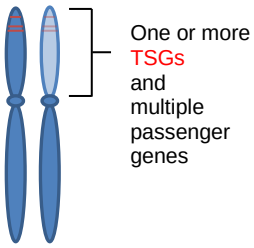

Fig. 1.2: Loss of a chromosome arm containing one or more tumor suppressor genes (driver genes) and multiple passenger genes.

they validated *PSMC2* (proteasome 26S subunit, ATPase 2) as a CYCLOPS gene which encodes and essential member protein of the 19S proteasome (Nijhawan, et al. 2012). In a recent follow-up study across 501 cancer cell lines the research group confirmed the previously found candidates in a total set of 399 identified potential CYCLOPS (Tsherniak, et al. 2017). Paolella et al. analyzed gene dependency date from Project Achilles with copy-number calls for 23,124 genes across 179 cancer cell lines. They show that CYCLOPS dependencies are the most frequent copy-number associated gene dependency. Again, CYCLOPS genes were mainly encoding for spliceosome components, which also accounts for their selected and validate candidate gene *SF3B1* (splicing factor 3b subunit 1) (Paolella, et al. 2017).

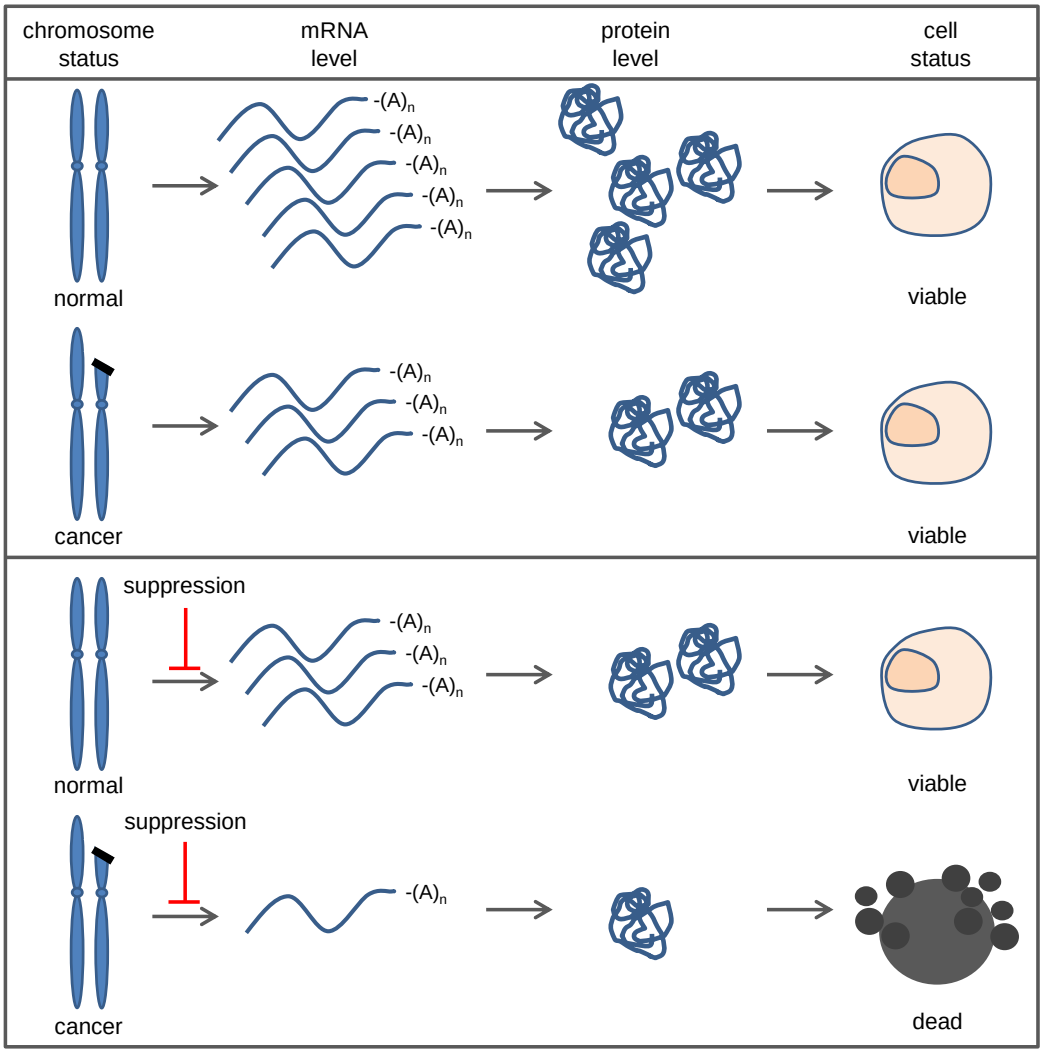

Fig. 1.3: The concept of CYCLOPS.

The expression ratio of CYCLOPS genes is reduced when one copy gets lost by hemizygous deletion but still the protein level is high enough to sustain viability. Further suppression of the remaining copy leads to such a strong reduction of the protein amount that viability cannot be maintained anymore whereas non-deleted cells stay unharmed.

1.4 Aim of the project

In contrast to many other cancers, neuroblastoma shows rare recurrent somatic mutations making it difficult to address this disease with commonly used targeting chemotherapeutics. Malignant transformation seems to develop from larger chromosomal events, e.g. genomic loss or gain. However, approaches to address these, for example targeting amplified *MYCN* failed so far, as transcription factors are generally difficult to regulate. The same is true for TSGs which have been many years in the focus of research, especially on chromosome arms 1p, 3p and 11q but did not deliver satisfying results towards therapy. The loss of the majority of genes on these chromosome arms likely does not contribute to cancer development but is due to collateral damage. We propose that many of these so-called passenger events are required for cell survival and hypothesize that their partial loss can be exploited as drug targets themselves. Hemizygous deletion of essential genes may render cells highly vulnerable to further suppression whereas cells without deletions remain unharmed. The group of potential candidates following this paradigm is termed CYCLOPS (copy number alterations yielding cancer liabilities owing to partial loss). Metaphorically speaking, like the Cyclops of the Greek mythology has only one eye (Fig. 1.4), the hemizygously deleted cells are left with one copy of an essential gene. Both, the mythical creature and the cancer cell, are highly related on their remains to survive. Previous studies identified many potential CYCLOPS across different cancer types. However, we propose that neuroblastoma may be related on different genes than the mainly adult cancers, leading to a different output of candidates. This study aims to identify CYCLOPS genes on chromosome arm 1p in neuroblastoma and show a new approach towards cancer therapy. In other words, we are blinding the CYCLOPS.

Fig. 1.4 Polyphemus, by Johann Heinrich Wilhelm Tischbein, 1802.

2. Material and Methods

2.1 Materials

2.1.1 Chemicals

4,6-diamidino-2-phenylindol (DAPI)	Sigma Aldrich, Munich
Agar agar	Carl Roth, Karlsruhe
Agarose	Carl Roth, Karlsruhe
Ammonium persulfate (APS)	Merck, Darmstadt
β-Mercaptoethanol	Merck, Darmstadt
Bacto-tryptone	Carl Roth, Karlsruhe
Boric acid	Sigma Aldrich, Munich
Bovine serum albumin (BSA)	Sigma Aldrich, Munich
Bromphenol blue	Sigma Aldrich, Munich
Chloroform	Sigma Aldrich, Munich
Deionized formamide	AppliChem, Darmstadt
Dextran sulfate	Carl Roth, Karlsruhe
Dimethyl sulfoxide (DMSO)	Carl Roth, Karlsruhe
DTT	Carl Roth, Karlsruhe
EDTA	Carl Roth, Karlsruhe
Ethanol	Sigma Aldrich, Munich
Formaldehyde	AppliChem, Darmstadt
Giemsa Azure Eosin Methylen Blue	Merck, Darmstadt
Glutaraldehyde	Sigma Aldrich, Munich
Glycine	Carl Roth, Karlsruhe
Goat serum	Jackson ImmunoResearch, West Grove, USA
HEPES KOH	Sigma Aldrich, Munich
Hoechst	Thermo Fisher Scientific, Waltham, USA
Isopropanol	Sigma Aldrich, Munich
Laemmli Sample buffer x4	Bio-Rad, Munich
Lipofectamine RNAiMAX	Thermo Fisher Scientific, Waltham, USA
Magnesium acetate	Sigma Aldrich, Munich
Magnesium chloride	Sigma Aldrich, Munich
Methanol	Sigma Aldrich, Munich

Midori Green Direct	Biozym, Hessisch Oldendorf
Milk powder	Sigma Aldrich, Munich
Phenol/ chloroform/ isoamylalcohol	Carl Roth, Karlsruhe
Propidium iodide staining solution (PI)	Miltenyi Biotec, Bergisch Gladbach
Polyacrylamide	Serva Electrophoresis, Heidelberg
Polyethylengycol 6000	Sigma Aldrich, Munich
Potassium acetate	Sigma Aldrich, Munich
Potassium chloride	Carl Roth, Karlsruhe
Sodium acetate	Merck, Darmstadt
Sodium chloride	Sigma Aldrich, Munich
Sodium citrate	Sigma Aldrich, Munich
Sodium dodecyl sulfate (SDS)	Sigma Aldrich, Munich
Sodium hydrogen carbonate	Merck, Darmstadt
Sodium hydrogen phosphate	Sigma Aldrich, Munich
Sodium hydroxide	Carl Roth, Karlsruhe
Sucrose	Sigma Aldrich, Munich
TEMED	AppliChem, Darmstadt
Tris base	AppliChem, Darmstadt
Tris-HCl	AppliChem, Darmstadt
Triton X-100	AppliChem, Darmstadt
Trypan Blue	AppliChem, Darmstadt
Tween	Sigma Aldrich, Munich
Vectashield Antifade Mounting Medium	Vector Laboratories, Burlingame, USA
Yeast extract	GERBU, Heidelberg

2.1.2 Drugs and inhibitors

Cysmethynil	Biomol, Hamburg
KaryoMax Colcemide	GIBCO, Invitrogen, Karlsruhe
Necrostatin-1	Sigma Aldrich, Munich
Ferrostatin-1	Sigma Aldrich, Munich
z-VAD-FMK	Sigma Aldrich, Munich
Bafilomycin A1	Sigma Aldrich, Munich
FR180204	Sigma Aldrich, Munich

2.1.3 Enzymes

DNA-Polymerase I	Thermo Fisher Scientific, Waltham, USA
DNase I	Fermentas, St.Leon-Rot, NEB, Schwalbach
Pepsin	Sigma Aldrich, Munich
Proteinase K	GERBU, Heidelberg
RNase A	Roche, Basel, Switzerland
DNA restriction enzymes	Fermentas, St.Leon-Roth, NEB, Schwalbach

2.1.4 Kits

BM Chemiluminescence Blotting Substrate kit	Roche, Basel, Switzerland
CellTiter-Blue® Cell Viability Assay	Promega, Madison, USA
ECL Select Western Blot Detection Reagent	GE Healthcare, Munich
Effectene transfection Reagent	Qiagen, Hilden
First Strand cDNA Synthesis Kit	Thermo Fisher Scientific, Waltham, USA
Gateway® LR Clonase Enzym mix	Thermo Fisher Scientific, Waltham, USA
HGF Human ELISA Kit ab100534	Abcam, Cambridge, UK
Platinum SYBR Green qPCR SuperMix-UDG	Thermo Fisher Scientific, Waltham, USA
Protein Assay kit	Bio-Rad, Munich
Qiagen Plasmid Isolation kits (Mini, Maxi)	Qiagen, Hilden
QIAquick Gel Extraction kit	Qiagen, Hilden
QIAquick PCR purification kit	Qiagen, Hilden
RNeasy mini kit	Qiagen, Hilden
Senescence β-galactosidase assay	Cell Signaling, Danvers, USA
Ribo-Zero rRNA Removal Kit	Illumina, San Diego, USA
NEBNext Ultra Directional RNA Library Prep Kit	New England BioLabs, Frankfurt a.M.

2.1.5 Buffers and solutions

1x PBS	137 mM NaCl	10 mM Na_2HPO_4
	2.7 mM KCl	pH 7.4

2.1.5.1 Separation of DNA in horizontal agarose gels

Agarose gel	1% Agarose 1x TBE
1x TBE	89 mM Tris 89 mM Boric acid 2 mM EDTA

2.1.5.2 Total protein isolation, separation and western blot analysis

Lysis buffer	20 mM Tris pH 8.5 1% Triton X-100 7 M Urea 0.1 M DTT 2.5 mM $MgCl_2$ Protease inhibitor cocktail (1 tablet per 25 ml)
1x TBS-T	50 mM Tris, pH 7.6 150 mM NaCl 5% Tween 20
10x Running buffer	25 mM Tris 192 mM Glycine 20% SDS
1x Transfer buffer	25 mM Tris 192 mM Glycine 20% Methanol
Blocking solution	5% Milk powder in H_20_{dd}
Stacking gel	375 µl Acrylamide 1.4 ml Tris [1.5 M], pH 6.8 Bromphenol blue 2.74 ml H_2O_{dd} 25 µl 20% SDS 150 µ 10% APS 6 µl TEMED
Separation gel (10%)	3.78 ml Acrylamide 3.75 ml Tris [1.5 M], pH 8.8 7.32 ml H_2O_{dd} 75 µl 29% SDS 150 µl 10% APS 6 µl TEMED

2.1.5.3 Fluorescence *in situ* hybridization (FISH)

Hybridization buffer	4x SSC 20% Dextran sulfate pH 7.0
Nick translation	0.5 M Tris-HCl, pH 8.0 50 nM MgCl2 0.5 mg/ml BSA
dNTP mix	50 µl dNTP (dATP, dCTP, dGTP) [1 nM] 25 µl dTTP [1 nM] 25 µl labeled dUTP [1 nM]
Hypotonic solution	0.55% KCl 1% NaCitrate

Fixative solution	Methanol Acetic acid Proportion 1:1	**20x SSC**	3 M NaCl 300 mM Sodium citrate, pH 7.0

2.1.5.4 Fluorescence-activated cell sorting (FACS)

Citric acid buffer	2.1% citric acid in $H20_{dd}$ 0.5% Tween 20

2.1.5.5 Molecular cloning

Lysis buffer	25 mM Tris-HCl, pH 7.5 10 mM EDTA 15% Sucrose	**Annealing Buffer**	100 mM potassium acetate 30 mM HEPES KOH 2 mM magnesium acetate

2.1.6 Media and supplements for cell culture

Versene	0.02% EDTA 1x PBS	**Freezing medium**	50% FCS 50% RPMI 1640 10% DMSO of total volume

All media and reagents were purchased as sterile ready-to-use solutions.

Blasticidin	MP Biomedichals, Heidelberg
Doxycycline	BD Clontech, Heidelberg
Fetal bovine serum (FCS)	GIBCO, Invitrogen, Karlsruhe
G418	Sigma, Munich
Penicillin/ Streptomycin (10,000 U/ml / 10,000 µg/ml)	Bio Whittaker, Walkerville, USA
RPMI 1640	GIBCO, Invitrogen, Karlsruhe
Zeocin	Invitrogen, Karlsruhe

2.1.7 Media and supplements for *E.coli* cultivation

SOC medium	Invitrogen, Karlsruhe

LB medium 5 g/l yeast extract
10 g/l bacto tryptone
5 g/l NaCl

For LB plates preparation agar agar was added to the medium prior autoclaving.
All antibiotics were added to the autoclaved media after cooling down to 50 °C.

Tab. 2.1: List of antibiotics and concentrations for the cultivation of *E.coli*.

Antibiotic	Stock Concentration	Final concentration	Supplier
Ampicillin	100 mg/ml	100 µg/ml	Serva, Heidelberg
Chloramphenicol	25 mg/ml	25 µg/ml	Serva, Heidelberg
Kanamycin	50 mg/ml	50 µm/ml	Serva, Heidelberg
Zeocin	100 mg/ml	50 µm/ml	Invitrogen, Karlsruhe

2.1.8 Bacteria strains and vectors

E.Coli OneShot Top10 Thermo Fisher Scientific, Waltham, USA
Genotype: F- mcrA Δ(mrr-hsdRMS-mcrBC)Φ80lacZΔM15 Δ lacX74 recA1 araD139 Δ(araleu)7697 galU galK rpsL (StrR) endA1 nupG

pcDNA/6TR	Invitrogen, Karlsruhe
pTER+	van de Wetering et al., 2003
pT-Rex^{TM}-DEST30	Invitrogen, Karlsruhe

2.1.9 Bacterial artificial chromosomes (BACs)

All BACs have been purchased from the BACPAC Resource Center of the Children´s Hospital Oakland Research Institute in Oakland, USA.

Tab. 2.2: List of BACs and their localization on 1p.

BACs	Localization (hg19)
RP11-547D24	1,891,455 – 2,024,338
RP11-368C17	25,034,711 – 25,212,781
RP11-159C21	53,128,015 – 53,289,181
RP11-415A20	77,205,366 – 77,334,921
RP11-643M22	119,770,060 – 119,925,166

2.1.10 Antibodies

Tab. 2.3: List of primary and secondary Antibodies for protein detection.

Specificity	catalog number	Host	supplier
primary antibodies			
MAP2	ab5392	chicken, polyclonal	Abcam, Cambride, UK
EphB2	14389	rabbit, polyclonal	Cell Signaling, Danvers, USA
EphA2	6997	rabbit, monoclonal	Cell Signaling, Danvers, USA
TUBB3	ab18207	rabbit, polyclonal	Abcam, Cambride, UK
GAPDH	MAB374	mouse, monoclonal	Merck Millipore, Darmstadt
α-Tubulin	ab40742	mouse, monoclonal	Abcam, Cambride, UK
β-Actin-HRP	ab20272	mouse, monoclonal	Abcam, Cambride, UK
NEFL	ab108363	rabbit, monoclonal	Abcam, Cambride, UK
HGF	ab83760	rabbit, monoclonal	Abcam, Cambride, UK
Phospho-Akt	9271	rabbit, monoclonal	Cell Signaling, Danvers, USA
Phospho-MAPK	9101	rabbit, monoclonal	Cell Signaling, Danvers, USA
Akt	9271	rabbit, monoclonal	Cell Signaling, Danvers, USA
MAPK	4695	rabbit, monoclonal	Cell Signaling, Danvers, USA
secondary antibodies			
anti mouse-HRP	115-035-003	goat, polyclonal	Dianova, Hamburg
anti rabbit-HRP	115-035-144	goat, polyclonal	Dianova, Hamburg
anti chicken-HRP	103-035-155	goat, polyclonal	Dianova, Hamburg
anti rabbit-FITC	111-095-003	goat, polyclonal	Dianova, Hamburg
molecular weight marker			
PageRuler Prestained Protein Ladder	26616	-	Thermo Fisher Scientific, Waltham, USA

2.1.11 Nucleic acids

C_ot1 DNA Roche, Basel, Switzerland

Fluorescence-conjugated dUTP Fermentas, St.Leon-Rot; NEB, Schwalbach

GeneRuler 1 kb DNA Ladder Thermo Fisher Scientific, Waltham, USA

GeneRuler 100 bb DNA Ladder Thermo Fisher Scientific, Waltham,USA

Salmon Sperm DNA Roche, Basel, Switzerland

Tab. 2.4.: Oligonucleotides for shRNA hairpins.

Oligonucleotidess for shRNA hairpins	Sequence 5´-3
EphB2 #2_for	GATCCACATCGATCCTTTCACCTATTCAAGAGATAGGTGAAA GGATCGATGTTTTTTTGGAAA
EphB2 #2_rev	AGCTTTTCCAAAAAAGCGTGATCCTGGACTATGATCTCTTGA ATCATAGTCCAGGATCACGCG
EphB2 #3_for	GATCCAGATGATCCGCAATCCCAATTCAAGAGATTGGGATTG CGGATCATCTTTTTTTGGAAA
EphB2 #3_rev	AGCTTTTCCAAAAAAAGATGATCCGCAATCCCAATCTCTTGAA TTGGGATTGCGGATCATCTG

Tab. 2.5: Oligonucleotides for RT-PCR.

Primer	Sequence 5´-3
ja HPRT1 for	TGACACTGGCAAAACAATGCA
HPRT1 rev	GGTCCTTTTCACCAGCAAGCT
SDHA for	TGGGAACAAGAGGGCATCTG
SDHA rev	CCACCACTGCATCAAATTCATG
Primer	QuantiTect Primer Assay *
EphB2	Hs_EPHB2_1_SG
HGF	Hs_HGF_1_SG
LRRC4B	Hs_LRRC4B_1_SG
MAP2	Hs_MAP2_1_SG
NEFL	Hs_NEFL_1_SG
PRAME	Hs_PRAME_2_SG
SRGAP3	Hs_SRGAP3_1_SG
TUBB3	Hs_TUBB3_1_SG

*QuantiTect Primer Assays were obtained from Qiagen, the sequences are not provided.

Tab. 2.6: siRNAs for transient gene knock-down.

Target gene	siRNA ID	Sense sequence 5´-3´
AURKAIP1	s195269	AGAUCAAGUUCGAGAAAGAtt
AURKAIP1	s29953	GCAGAUCAAGUUCGAGAAAtt
AURKAIP1	s29954	CCACCGCAAUCCUACCAGUtt
EphA2	s4564	UGAUGAUCAUCACUGAGUAtt
EphA2	s4565	GGAAGUACGAGGUCACUUAtt
EphA2	s4566	GUAUCUUCAUUGAGCUCAAtt
EphB2	s4740	GCGUGAUCCUGGACUAUGAtt
EphB2	s4741	ACAUCGAUCCUUUCACCUAtt
EphB2	s4742	AGAUGAUCCGCAAUCCCAAtt
ICMT	s23871	GGUUAGAGUUCACACUUGAtt
ICMT	s23872	CAGCCUGGAGUAUACAGUAtt
ICMT	s23873	CGAUCGAACAGAAGAAGAAtt
RSC1A1	s12369	GAAUCUUGCCCGUCUAUAAtt
RSC1A1	s12370	GGAUCUCACUUUAGAUAAUtt
RSC1A1	s12371	GCUCAACAGUCCCUAGUUAtt
SDF4	s27560	GGAGUUUGAGGAGCUCAUUtt
SDF4	s27561	AGGUGGAUGUGAACACUGAtt
SDF4	s27562	GAGUAUAAGGUGAAGUUUUtt
PLK1	s448	CCAUUAACGAGCUGCUUAAtt
Negative Control No. 1 siRNA – non target	4390843	Proprietary, not provided

All siRNA are Silencer Select siRNAs and have been purchased from Ambion, Austin, USA. The sequences of the all 990 siRNAs used in the screen are listed in the supplementary information (Tab. S1).

Tab. 2.7: Sequencing primers.

Primer	Sequence 5´-3
CMV_for	CGCAAATGGGCGGTAGGCGTG
T7	TAATACGACTCACTATAGGG
H1	TCGCTATGTGTTCTGGGAAA
BGH_rev	TAGAAGGCACAGTCGAGG
pCAG	GCAACGTGCTGGTTATTGTG

2.1.12 Tissue culture cell lines

CHLA-90	(Keshelava, et al. 1998)
CHLA-20	(Keshelava, et al. 1998)
CHP-126	(Schlesinger, et al. 1976)
CHP-134	(Schlesinger, et al. 1976)
CLB.Ga	(Combaret, et al. 1995)
GI-M-EN	(Donti, et al. 1988)
HD-N-16	(Schwab, unpublished)
HD-N-33	(Schwab, unpublished)
IMR-32	(Tumilowicz, et al. 1970)
IMR-5/75	(Tumilowicz, et al. 1970)
Kelly	(Schwab, et al. 1983)
LAN-1	(Seeger, et al. 1977)
LAN-2	(Seeger, et al. 1977)
LAN-5	(Seeger, et al. 1982)
LAN-6	(Wada, et al. 1993)
LS	(Rudolph, et al. 1991)
MHH-NB11	(Pietsch, et al. 1988)
NB69	(Mena, et al. 1989)
NBL-S	(Cohn, et al. 1990)
NBS-124	(Westermann, unpublished)
NGP	(Brodeur, et al. 1977)
NMB	(Brodeur, et al. 1977)
SH-EP	(Ross, et al. 1983)
SH-SY5Y	(Biedler, et al. 1978)
SIMA	(Marini, et al. 1999)
SJ-NB-12	(Van Roy, et al. 2006)
SK-N-AS	(El-Badry, et al. 1989)
SK-N-BE(2)	(Biedler and Spengler 1976)
SK-N-BE(2)c	(Biedler and Spengler 1976)
SK-N-DZ	(Sugimoto, et al. 1984)
SK-N-FI	(Sugimoto, et al. 1984)
SK-N-SH	(Biedler, et al. 1973)
SMS-KCNR	(Reynolds, et al. 1986)
TR14	(Cowell and Rupniak 1983)
Vi-856	(Ambros, unpublished)

2.1.13 Laboratory equipment

2100 Bioanalyzer	Agilent Technologies, Santa Clara, USA
Analytical Balances PM 4600	Mettler, Gießen
ChemiSmart 5100	Vilber Lourmat, Marne-la-Vallée, France
CO_2 Incubator Steri-Cult	Thermo Fisher Scientific, Waltham, USA
Gel documentation system (Geldoc)	Bio-Rad, Munich
Horizontal mini-gel systems	GIBCO/BRL Eggenstein Renner, Darmstadt
Horizontal mixer RM5	CAT, Staufen
Incubator Function Line	Heraeus, Wehrheim
Incubator Shaker, Innova 4300	New Brunswick Scientific, Enfield, USA
LightCycler 480	Roche, Basel, Switzerland
Luna Automated Cell Counter	Logos biosystems, Annandale, USA
MACSQuant VYB flow cytometer	Miltenyi Biotec, Bergisch Gladbach
Magnetic Mixers	Heidolph-Elektro, Kehlheim
Microplate dispenser	Thermo Fisher Scientific, Waltham, USA
Mini trans-blot cell	Bio-Rad, Munich
Mini-PROTEAN 3 electrophoresis system	Bio-Rad, Munich
NanoDrop Spectrophotometer ND-1000	Peqlab, Erlangen
pH-Meter Ph 540 GLP	WTW, Weilheim
Pipetting Robot Microlab STAR	Hamilton, Reno, USA
Plate Loader SWAP	Hamilton, Reno, USA
Platereader FLUOstar OPTIMA	BMG Labtech, Ortenberg
Power supply units, Phero-stab 500	Biotec Fischer, Reiskirchen
Shaking platform, IKA KS250	Janke & Kunkel, Staufen
Spectrophotometer GeneQuant 1300	GE Healthcare, Munich
Sterile bench SAFE 2020	Thermo Fisher Scientific, Waltham, USA
Thermo block mixer compact	Eppendorf, Hamburg
Thermo water bath GFL 1083	GFL, Burgwedel
Thermocycler GeneAmp 9700	Applied Biosystems, Darmstadt
Vacuum concentrator, RVC2-18	Christ, Osterode am Harz

Vortex Reax top	Heidolph Instruments, Schwabach

Centrifuges and rotors

Avanti-JS-25-I	Beckman Coulter, Sinsheim
Allegra X-12	Beckman Coulter, Sinsheim
Biofuge fresco	Hereaus, Wehrheim
J2-21 M/E	Beckman Coulter, Sinsheim
Mini Star	Neolab, Heidelberg
Rotor JA-10	Beckman Coulter, Sinsheim
Rotor JA-20	Beckman Coulter, Sinsheim
Rotor JS-4.2	Beckman Coulter, Sinsheim

Microscopes

Leica DMRA2	Leica, Wetzlar
Zeiss Z1	Zeiss, Jena
Olympus IX81	Olympus, Hamburg
Olympus CKX41	Olympus, Hamburg
Axiovert 10	Zeiss, Jena

2.1.14 Further materials

Cell culture dishes	TPP, Trasadingen, Switzerland
Cell culture flasks	TPP, Trasadingen, Switzerland
Cover slips	Menzel, Braunschweig
Cryo tubes, 2 ml	NalgeneNunc, Wiesbaden
Cuvettes Semi-Micro	Greiner Bio-One, Kremsmünster, Austria
FACS tubes with cell-strainer cap	Corning, Tewksbury, USA
Filter tips, graduated (10, 100, 200, 1000 µl)	Star Lab, Hamburg
Fixogum	Marabuwerke, Tamm
Glass slides	Thermo Fisher Scientific, Waltham, USA
Luna Cell Counter Slides	Logos biosystems, Annandale, USA
Nitrocellulose membranes 0.45 µm	GE Healthcare, Munich
Plastic pipettes (5, 10, 25, 50 ml)	Corning, Tewksbury, USA
qPCR 96 well plates, white	Biozym, Hessisch Oldendorf
qPCR optical adhesive film	Applied Biosystems, Darmstadt

Reaction tubes (0.5, 1.5, 2.0 ml)	Eppendorf, Hamburg
Reaction tubes (15, 50 ml)	Greiner Bio-One, Kremsmünster, Austria
Tissue culturing plates (black, clear bottom 384 wells)	BD Biosciences, Bedford, USA
Tissue culturing plates (transparent, 6, 24, 96 wells)	TPP, Trasadingen, Switzerland
Whatman 3MM paper	Whatman, Dassel

2.1.15 Software

FLUOstar Optima	BMG Labtech, Ortenberg
Microsoft Office package 2010	Microsoft Crop., Redmond, USA
Cell B Image Software	Olympus, Hamburg
ScanR acquisition software	Olympus, Hamburg
IGV viewer	Broad Institute, Cambridge, USA
FlowJo version 10	FlowJo, LLC, Ashland, USA
IDES 480	Roche, Basel, Switzerland
Leica CW 4000 FISH Software	Leica Microsystems
ImageJ version 1.51d	Wayne Rasband
ISIS MetaSystems version 5.0	MetaSystems
Chromas Lite 2.1	Technelysium Pty Ltd
SignalMap version 1.9	Roche, Basel, Switzerland
R studio	Comprehensive R Archive Network
Sigma Plot 13.0	SPSS Inc., Chicago, USA

2.1.16 Databases

DAVID Bioinformatics Resources	http://david.abcc.ncifcrf.gov
Ensembl genome browser	http://www.ensembl.org/index.html
Addgene	https://www.addgene.org
National Center for Biotechnology (NCBI)	http://www.ncbi.nlm.nih.gov/
R2	https://hgserver1.amc.nl
UCSC Genome Browser	http://genome.ucsc.edu/

2.2 Methods

2.2.1 Methods of cell biology

2.2.1.1 Culturing and cryoconservation of human neuroblastoma cells

All cell lines were cultured in a humidified cell incubator at 37 °C in a 5% CO_2 atmosphere. RPMI 1640 medium was supplemented with 100 U/ml penicillin, 100 µg/ml streptomycin and 10% FCS. Every four days the cell culture medium was substituted and the cells were split at ratios from 1:3 to 1:10, depending on the cell confluence and proliferation rate. Adherent cells were detached from the surface by versenization. For cryoconservation cells were harvested at a density of 70% and resuspended in 1 ml cryoconservation medium, dispensed in cryovials and immediately transferred to -80 °C in a freezing container. After one week, the cryovials were located to nitrogen tanks at -96°C for long-term storage. To recultivate the cells the frozen suspension was thawed quickly and added into fresh warm growth medium. After cell detachment the medium was substituted with fresh growth medium to remove the DMSO.

2.2.1.2 Determination of amount and viability of neuroblastoma cells

To calculate the number of living cells in a cell culture, trypan blue assay was used. After siRNA or drug treatment the cell density was estimated by cell confluency assays and the viability was determined by CellTiter-Blue assay.

Trypan blue viability assay

Trypan blue is a membrane non-permeable dye which accumulates only in dying cells with lost membrane integrity. In contrast to the non-colored healthy cells, dead cells appear blue making it easy to count the amount both, dead and living cells.

Adherent cells were removed from the surface by versenization. Then, 10 µl of the cell suspension were mixed 1:1 with 0.1% trypan blue/ PBS and counted in an automated cell counter.

CellTiter-Blue viability assay

Cells were seeded in 94 well plates and treated with siRNA or drugs after 24 hs. To assess the cell viability after 96 hs CellTiter-Blue reagent was added in a ratio of 1:5 and incubated for 5 hs. In a flouroscan platereader the fluorescence was read using 540 nm excitation and 580 nm emission filters (acquisition time 0.2 s, automatic gain). Auto fluorescence of the CellTiter-Blue reagent in RPMI medium of blank wells was subtracted

from all samples. The relative fluorescence values served as an indicator of the amount of viable and metabolically active cells.

Cell confluency assay

To determine the effectivity of gene knock-down or drug activity cell confluency was assessed after treatment. The cells were seeded and treated in 96 well plates in 100 µl medium. After 96 h 30 µl of an 11% glutaraldehyde fixation solution in 1x PBS were added for 30 min. The medium was removed and cells were washed two times with 1x PBS. Each well was then stained with 100 µl of a 10% Giemsa Azure Eosin Methylen Blue solution in 1x PBS and incubated overnight and then washed two times with *Aqua dest*. To calculate the cell confluency the plates were scanned and analyzed by the ImageJ software using the Colony Formation plugin.

2.2.1.3 Cell transfection and selection

Transfection is the process to introduce foreign DNA into eukaryotic cells. Here, we generated doxycycline-inducible, stable overexpression of EphB2 with the pT-Rex™-DEST30 and doxycycline-inducible, stable knock-down of EphB2 in IMR32_6TR cells through the pTER30+ vector. IMR32_6TR contained the stably expressing tetracycline repressor protein (pcDNA/6TR). A very efficient method is binding the plasmids to lipids that can fuse with the cell membrane, releasing the DNA into the cell. We used “Effectene Transfection Reagent” and associated reagents from Qiagen. Cells were seeded 24 h before transfection in 15 cm plates. First, 1 µg of plasmids was diluted in 100 µl EC-buffer and 3 µl of the enhancer solution. After 2 min of incubation at RT, 7.5 µl of Effectene was added to the DNA/ enhancer mix. The solution was vortexed and incubated for 15 min at RT. Then, it was filled up with 1 ml cell culture medium and the whole mixture was added dropwise to the cells. The transfection medium was replaced after 24 h by fresh one. After 48 h the selection process was initiated by addition of appropriate antibiotics into the growth medium. The selection took 7 – 10 days resulting in cell death of non-transfected cells whereas the transfected formed colonies. The polyclonal culture was reseeded in 96 well plates with an average concentration of 1 cell per well. The separated cells were raised to monoclonal cultures and the expression of the introduced vectors was determined. The expression of pTER30+-EphB2 and the knock-down efficiency of pEXP30-EphB2 after doxycycline treatment were determined by western blot.

2.2.1.4 Gene knock-down with siRNA

To study if a candidate gene has cell essential functions we performed knock-down experiments with short interfering RNAs (siRNAs). siRNAs are small double-stranded RNAs (21-25 bp) which get processed by the RNA-induced silencing complex (RISC). The target-complementary siRNA leads RISC to the mRNA of the transcribed gene of interest and induces cleavage by ribonucleases.
Cells were seeded 24 h before the transfection in 96 well plates or 10 cm dishes. siRNA from a 50 µM stock solution was dissolved in serum- and antibiotic-free medium in a ratio of 1:250. In the same amount of medium Lipofectamine RNAiMAX was diluted 1:100 – 1:25 (depending on the cell line). Both solutions were mixed 1:1 and incubated at RT for 5 min. The 96 well plates were treated with 10 µl of the siRNA-lipid mix per well or 1 ml was added drop wise to the 10 cm the dishes.

2.2.1.5 siRNA screening

To identify candidate genes we screened 184 druggable genes on 1p in 10 neuroblastoma cell lines. We used three different siRNAs per gene in independent experiments. The cells were seeded 24 h prior transfection in 384 well plates and treated as described in 2.2.1.4. After 96 h the cells were fixated 30 min with an 11% glutaraldehyde solution and washed three times with 1x PBS. The nuclei were stained with Hoechst solution (1:4000 in 1x PBS) over night at RT. Afterwards, the plates were imaged with a ScanR system by taking 9 images of each well to acquire a 3x3 matrix over the well. The total fluorescent area was determined and normalized for plate effects (B-scoring) and to the controls present on each plate. Replicates were combined by calculating the mean, the median value for the three siRNAs was calculated to show the general effect. Finally, the mean value for 1p-deleted and 1p non-deleted cell lines was determined and the distance between the cell line groups was calculated by subtracting these values.
The experimental part of the CYCLOPS screen was done in cooperation with the Advanced Biological Screening Facility (BioQuant, Heidelberg); data analysis was performed by Manuel Gunkel. The genome-wide siRNA screen in IMR5/75 was done by Sina Gogolin, data analysis by Chunxuan Shao.

2.2.1.6 Senescence β-galactosidase assay

In contrast to quiescent or immortal cells, senescent cells overexpress lysosomal β-galactosidase required for the hydrolysis of β-galactosides to monosaccharides. The

cleavage of the chromogenic substrate X-Gal results in intracellular accumulation of a blue-dyed precipitate in senescent cells. In order to investigate if cells turn senescent after siRNA treatment the “Senescence β-Galactosidase Staining Kit” from Cell Signaling was used and all experiments were done following the company´s protocol. To amount of blue dye was assessed microscopically.

2.2.2 Nucleic acids manipulation

2.2.2.1 Whole genome sequencing

Whole genome sequencing was performed by Elisa Wecht and Moritz Gartlgruber, data analysis was done by Chunxuan Shao according to a published protocol (Peifer, et al. 2015).

2.2.2.2 Comparative genomic hybridization arrays

Comparative genomic hybridization (CGH) arrays have been performed by Elisa Wecht according to the NimbleGen Array User´s Guide (Roche, Madison USA)

2.2.2.3 Total RNA extraction

Cellular RNA was isolated with the “miRNeasy” kit from Qiagen using the QIAzol lysis reagent. QIAzol is a phenol/guanidine-based solution which dissolves cellular components. After addition of chloroform, the solution separates into an organic and an aqueous phase. The later one contains the RNA which can be easily recovered by precipitation.

First, the cells were harvested by versenization and centrifuged (800 RPM; 5 min). The pellet was dissolved in 700 µl QIAzol and 140 µl chloroform were added. The reaction tube was shaken vigorously for 15 s and then allowed to rest for 3 min an RT. After centrifugation (10,000 RPM; 4 °C; 15 min) the upper aqueous phase containing the RNA was transferred to a new reaction tube. One volume of 70% ethanol was added and mixed thoroughly by vortexing. The mixture was then pipetted in a RNaesy Mini spin column placed in a collection tube and centrifuged (10,000 RPM; 15 s; RT). The flow-through was discarded and the pellet in the spin column was washed with 350 µl RWT buffer and centrifuged again (10,000 RPM; 15 s; RT). To digest remaining DNA, 80 µl of DNase I solution (10 µl DNase I stock, 70 µl RDD buffer) was pipetted on the spin column and incubated for 15 min at RT. Again, the pellet in the spin column was washed with 350 µl RWT, centrifuged (10,000 RPM; 15 s; RT) and the flow-through discarded followed by an additional washing and centrifugation step with 500 µl RPE. The spin column was then

placed in a new collection tube and centrifuged for 1 min at full speed. To elute the RNA from the membrane the spin column was placed in a new reaction tube and 30-50 µl of RNase-free water were added and again centrifuged (10,000 RPM; 15 s; RT). The RNA amount in the flow-through was estimated in a spectrometer, reading the absorbance at 260 nm.

2.2.2.4 RNA sequencing

Total RNA was isolated as described in 2.2.2.3 and afterwards depleted from ribosomal RNA using the Ribo-Zero rRNA removal Kit according to the manufacture´s protocol. The NEBNext Ultra Directional RNA Library Prep Kit was used to prepare RNA libraries following the manufacture´s protocol including the following changes: the RNA fragmentation has been carried out for 20 min at 94 °C; the first strand cDNA synthesis reaction was expanded to 50 min at 42 °C. The adaptor-ligated DNA was purified and size-selected on a DynaMag^{TM}-2 magnetic device (Thermo Fisher Scientific, Waltham, USA) with AMPure XP Beads (Beckman Coulter, Brea, USA) according to the manufacture´s protocol using first 40 µl, then 20 µl of bead volume. To analyze the quality, quantity and size of the RNA library we used a DNA High Sensitivity DNA chip on a 2100 Bioanalyzer. The libraries were sequenced on an Illumina sequencing platform (50 bases single-end, German Cancer Research Center core facility).
The data analysis of IMR-32, TR14 and IMR32_shRNA clones was performed by Umut Toprak as describe briefly. All genes below 1 count per million (CPM) were removed and the results were normalized with the TMM method (Robinson and Oshlack 2010). Then, the CPM from the normalized values was calculated and log2(x+1) transformation applied. These values were grouped into controls or intervention samples and the fold-change was calculated (mean and trimean) followed by a log2 transformation. The rank-based Kruskal-Walis test (Wallis 1952) was used to calculate statistical significances under no assumption of the underlying distribution.
RNA sequencing of neuroblastoma primary tumors and cell lines was done by Elisa Wecht, data analysis was performed by Chunxuan Shao and Naveed Ishaque using TPM normalization and log2 transformation. Statistical significance was calculated with t-test.

2.2.2.5 Quantitative RT-PCR

To estimate the expression of genes in neuroblastoma cell lines, real time PCR (RT-PCR) was performed. First, the total RNA was isolated from cells and reversely transcribed to cDNA using the “First Strand cDNA synthesis” kit (Thermo Fisher Scientific, Waltham,

USA) Scientific according to the company´s protocol. To avoid degradation of enzymes or the RNA, all steps were performed on ice. One standard reaction contained:

250 ng RNA

1 µl Random Hexamer Primer [100 µM]

Fill up to 11 µl with H_20_{dd}

To the RNA/ oligo mixture, the following master mixture was added:

4 µl 5x Reaction Buffer

1 µl RiboLock RNase Inhibitor (20 U/µl)

2 µl dNTP Mix [10 mM]

2 µl M-MuLV Reverse Transcriptase (20 U/µl)

The reaction was carried out by the following conditions:

25 °C – 5 min

37 °C – 60 min

5 min – 70 °C

The samples were diluted and stored at -20 °C for maximum one week.

To perform the RT-PCR the “Platinum SYBR Green qPCR SuperMix-UDG” from Invitrogen was used together with “QuantiTect” Primers from Qiagen. To detect the housekeeping genes SDHA and HPRT1 the following components were mixed:

13 µl Platinum SYBR Green PCR SuperMix UDG (2x)

0.75 µl forward primer [10 µM]

0.75 µl reverse primer [10 µM]

2.5 µl template cDNA

8 µl H_2O_{dd}

For all other genes the qPCR reaction mix is shown below:

13 µl Platinum SYBR Green PCR SuperMix UDG (2x)

2.5 µl 10x QuantiTect Primer

2.5 µl template cDNA

7 µl H_2O_{dd}

The reaction was carried out in a LightCycler 480 from Roche with the following conditions:

50 °C – 20 s
95 °C – 2 min
95 °C – 15 s
60 °C – 30 s } x 50

A melting curve was assessed at 97 °C. The results for all genes were normalized by HRPT1 and SDHA housekeeping genes qPCR results.

2.2.3 Molecular Cloning

Standard methods like separation of DNA fragments in agarose gel, enzymatic DNA manipulations or culturing and cryo-conservation of *E.coli* were conducted according to Sambrook J, Russell D (2002) and will not be emphasized here.

2.2.3.1 Cloning of EphB2 cDNA into a Gateway® eukaryotic expression plasmid

The Entry clone pENTR^{TM}223 containing the EphB2 open reading frame (ORF) was obtained from the Genomics & Proteomics Core Facilities at the DKFZ. The EphB2 ORF was cloned into a Gateway® eukaryotic expression vector pTRex™-DEST30 by using the Gateway® LR system. The recombination reaction was performed as followed:

300 ng pTRex™-DEST30 vector
300 ng pENTR^{TM}223-EphB2
4 µl 5x LR Clonase^{TM} Reaction Buffer
To 16 µl TE Buffer, pH 8.0
4 µl LR Clonase^{TM}

The reaction mix was then incubated for one hour at 25 °C and afterwards 2 µl of Proteinase K were added and incubated for 10 min at 37 °C.
Then, 3 µl of the recombination reaction were transformed in *E.Coli* OneShot Top10 (2.2.3.3).

2.2.3.2 Cloning of EphB2 shRNAs into the pTER+ plasmid

First, the pTER+ plasmid was linearized for 3.5 hs at 37 °C by using the following mix:

3.5 µg pTER+ plasmid
4.5 µg Bgl II restriction enzyme
4.5 g Hind III restriction enzyme
10 µl Buffer R+
77.5 µl H_20

To inactivate the enzymes the mixture war incubated for 20 min at 60 °C. The resulting fractions of the solution were then separated on a 1% agarose gel and the vector was extracted from the corresponding band with the Qiagen “QIAquick Gel Extraction Kit”.
To anneal the oligonucleotides encoding for the forward and reverse shRNA 3 µg of each were mixed in 5 µl annealing buffer and 43 µl H_2O. The reaction was carried out on a PCR cycler for 3 min at 95 °C and then for one hour at 37 °C.
The cloning reaction of the linearized vector and the annealed oligonucleotides was assembled over night at 16 °C. Following compounds were mixed:

1 µl annealed oligonucleotides
250 ng linearized pTER+
1 µl ligation buffer (10x)
4.5 µl H_2O.

2.2.3.3 Transformation of competent *E.coli* cells

Chemically competent *E.coli* were obtained from Invitrogen. After thawing, 25 µl of the bacteria solution was mixed with 2.5 µl DNA (20 – 50 µg DNA in H_2O) and incubated for 30 min on ice. The bacteria were then subjected to heat shock (30 s; 42 °C) and returned on ice for 3 min. To the suspension 100 µl of SOC medium was added and placed on a shaker with mild agitation for 30 min at 37 °C. LB plates containing appropriate antibiotics were inoculated with the transfected bacteria and incubated overnight at 37 °C. The next day, colonies were selected and picked with a sterile inoculation loop and transferred to 5 ml (mini culture) or 300 ml (maxi culture) LB medium supplemented with antibiotics and grew overnight in an incubation shaker (160 rpm; 37 °C).

2.2.3.4 Isolation and purification of plasmid DNA from *E.coli*

For plasmid isolation from *E.coli* we used the QIAprep kits, according to the supplier´s protocols. Depending on the estimated DNA yield the Mini or Maxi kit was chosen. The plasmid DNA used to transfect neuroblastoma cell cultures was prepared with the “Endo-free DNA isolation” kit from Qiagen to remove bacterial oligosaccharides and glycans.

DNA concentration and purity were assessed by reading the absorbance at 260 and 280 nm.

2.2.3.5 Isolation and purification of BAC DNA from *E.coli*

E.coli transfected with BAC DNA were incubated overnight at 37 °C in 300 ml LB medium with antibiotics. The next day the culture was centrifuged (5,000 RPM; 4 °C; 15 min), the supernatant discarded and the pellet resuspended in 7 ml lysis buffer. The bacterial suspension was chilled for 20 min on ice, then 12 ml of 0.2 M NaOH/ 1% SDS were added and again placed on ice for 10 min. Afterwards, 7.5 ml of 3 M sodium acetate (pH 4.6) were added followed by another 10 min on ice. The lysate was centrifuged (18,000 RPM; 20 min; 4 °C) and the supernatant was transferred into a new reaction tube. For RNA digestion RNase A (80 µl) was added and incubated for 1h at 37 °C. The solution was mixed with one volume of phenol/ chloroform/ isoamylalcohol (25:24:1) and centrifuged (3,500 RPM; 10 min). The upper aqueous phase contained the DNA and was therefore transferred into a new reaction tube and again mixed with phenol/ chloroform/ isoamylalcohol (25:24:1) and centrifuged. For DNA precipitations 2 volumes of 100% ethanol were added and kept for 1h at -20 °C. After centrifugation (8,500 RPM; 5 min; RT) the DNA pellet was dissolved in 1.68 ml water. For another precipitation process 350 µl NaCl and 2 ml of 13% polyethylengycol were added and chilled 60 min on ice. The mixture was centrifuged (8,500 RPM; 15 min; RT) and the precipitate was washed with 70% ethanol, air-dried and dissolved in 1 ml *Aqua dest*.

2.2.4 Protein methods

2.2.4.1 Separation of proteins by SDS-PAGE

SDS Page (sodium dodecyl sulfate polyacrylamide gelelectrophoresis) followed by western blot analysis is a method to separate and detect expressed proteins within cell cultures. The presence of SDS denatures proteins and gives a negative charge which is in proportion to their mass. In an electric field the proteins move to the cathode with a running speed proportional to size and charge and get separated from each other.

Protein extraction and sample preparation

For protein sample preparation all cultured cells were harvested (floating cells and adherent by versenization), pelleted, washed with 1x PBS and resuspended in protein extraction buffer. After centrifugation the pellet consisting of cellular debris was discarded. The total amount of proteins in the supernatant was determined by the method of Bradford

(1976) using the “Protein Assay kit” from BioRad. A protein amount of 40 µg was supplemented with 4x Laemmli Sample buffer and incubated for 5 min at 95 °C.

Protein separation

The samples were loaded on a SDS gel for size separation which was prepared in prior. Each gel contained two different layers, first the stacking gel, second the resolving gel. The stacking layer is needed to bring all proteins in one sample to the same height level by concentrating. The resolving gel separates the proteins by their size and a PAA concentration of 10% was used for all experiments. The resolving gel solution was filled in between of two glass plates and covered with isopropanol to remove bubbles. The polymerization process was finished after 30 min and the isopropanol removed. Next, the resolving gel solution was added on top and sample preparation combs were inserted. After 30 min the combs were removed and the glass sandwiches were assembled in a Mini-Protean 3 chamber from BioRad and filled up with Tris-Glycine buffer (by Laemmli). The samples were loaded into the gel slots and an electric potential of 100 V was applied for 2 h.

Western blotting and protein detection

After the separation via electrophoresis the proteins need to be blotted on a nitrocellulose membrane. The gel was released from the glass plates and transferred on two Whatman papers in a BioRad Mini Gel Holder Cassette and covered with a nitrocellulose membrane followed by two additional Whatman papers. After assembling of the cassette in the Mini-Protean 3 chamber the tank was filled up with transfer buffer and an electric potential of 100 V was applied for 2 h. After the blotting process the membranes were incubated on a shaker in blocking buffer for 1 h at RT and covered with primary antibody dilutions for 1 h at RT or 4 °C over night. The membranes were washed two times with PBS-T for 10 min and incubated for 1h at RT with 1:1000 secondary antibody dilutions followed by another washing step. The protein bands were detected using the BM Chemiluminescence kit.

2.2.4.2 Enzyme-linked immunosorbent assay (ELISA)

Extracellular quantitative protein measurements were assessed via enzyme-linked immunosorbent assay (ELISA). For this, the Human ELISA kit from Abcam was used. All steps were conducted according the manufacture´s protocol.

2.2.4.3 Immunocytochemistry

Morphologic changes of cells after gene knock-down can be detected by using fluorescent markers against proteins of the cytoskeleton (here TUBB3). For this, the cells were seeded and treated in 8 well chamber slides with removable chamber walls. After 30 min the medium was substituted with 11% glutaraldehyde fixation solution and the cells were permeabilized with 1x PBS + 0.1% Tween 20 for 15 min. To block unspecific binding sites the samples were incubated for 1h with 1% goat serum in PBS. Then, the primary antibody was applied for 1h in a 1:100 dilution followed by a 1:200 FITC-labeled secondary antibody dilution for 1h. The cells were finally treated with DAPI solution (1:10,000 in PBS) for nuclei staining. After each step the samples were washed twice with 1x PBS. Finally, the chamber walls were removed, the slides were mounted with antifade solution and covered by a slip. For protein visualization, a fluorescent microscope was used with appropriate filters.

2.2.5 Fluorescence *in situ* hybridization (FISH)

Fluorescence *in situ* hybridization (FISH) is a technique to identify the number and the location of specific regions of a chromosome using sequence complementary fluorescent probes. We used six different probes mapping in equal distances on the chromosome arm 1p to determine the copy number status, location and length in neuroblastoma cell lines.

Fluorescent labeling of DNA probes

Sequence complementary DNA fragments were assessed from transfected *E.coli* with BAC DNA (see chapter 2.2.3.5). The DNA probes were enzymatically labeled with fluorescent dyes by nick translation. We used six different dyes linked to dUTP (FITC, DEAC, Cy3, Cy3.5, Cy5, Cy5.5). To avoid light-dependent degradation all steps were performed, as far as possible, in dark conditions. A standard nick translation reaction contains:

3 µg BAC DNA
10 µl β-Mercaptoethanol [0.1 M]
1 µl nick translation buffer
3 µl DNase I (0.03 U/µl)
2 µl DNA-Polymerase I
10 µl dNTP-mix
Fill up to 100 µl with H_20_{dd}

After 1 h of incubation at 15 °C 5 µl C_0t1 DNA and 2.5 µl salmon sperm DNA were added to block repeats. To precipitate the DNA a 2.5x volume of ethanol (20 min; -80 °C) was added and the probes were centrifuged (13,000 RPM; 15 min). The supernatant was discarded and the pellet was resuspended in 1 ml of 70% ethanol and again centrifuged (13,000 RPM; 15 min). Deionized formamide (50 µl; 65 °C) was used to dissolve the pellet and incubated for 5 min at 65 °C followed by another centrifugation step (13,000 RPM; 15 min). The supernatant was transferred to a new reaction tube and 50 µl of pre-warmed (75 °C) hybridization buffer was added. Finally, the probe mix was incubated for 10 min at 80 °C, cooled down on ice for 5 min and again incubated for 20 min at 37 °C. For long-term storage, the probes were kept at -20 °C.

Preparation of metaphases

In order to increase the amount of cells with metaphase chromosomes cell cultures were treated with 10 µg/ml colcemid (2 h; 37 °C) to arrest cell division. The cells were harvested by versenization and centrifuged for 5 min at 800 RPM. The supernatant was discarded and 3 ml of the hypotonic dilution were added dropwise to the pellet and finally filled up to 12 ml and incubated for 30 min at RT. Then, 2 ml of fixative solution were added followed by a centrifugation step (800 RPM; 5 min). The supernatant was discarded and the pellet dissolved in 10 ml fixative solution. After 10 min incubation at RT the suspension was centrifuged (800 RPM; 5 min) and the pellet again dissolved in 10 ml fixative solution and incubated for 10 min at RT. The solution was centrifuged (800 RPM; 5 min) and the supernatant was substituted with 5 ml fixative solution and stored at -20 °C.

Preparation of slides and *in situ* hybridization of chromosomes

Glass slides were washed, rinsed with *Aqua dest*. and dried at RT. Two to three drops of a cell suspension were pipetted on the slide and immediately flamed by a lighter. The heat bursts cell and nuclei membranes and leads to a release of chromosomes. The chromosomes were dried over night at 60 °C or two days at RT. To remove endogenous RNA which may influence the fluorescent signals 1 ml of 2x SSC + 20 µl RNAse A were added to each sample, covered with a cover slip and incubated for 1 h at 37 °C. The slides were rinsed three times for 5 min in 2x SSC at 42 °C. Afterwards, proteins were digested by 50 µg/ml pepsin in 0.01 M HCL (10 min; 42 °C) followed by a washing step in 1x PBS (5 min; 42 °C) and in 1x PBS + $MgCl_2$ (5 min; 42 °C). The chromosomes were fixated in 1% formaldehyde + $MgCl_2$ (20 min; RT) and washed in 2x SSC (5 min; 42 °C). To dehydrate the chromosomes the slides were incubated 5 min in an ethanol series

(70%; 90% and 100%; RT) and air dried. Then, 70% formamide was used to denature the chromosomes (1.5 min; 71 °C) followed by another incubation series in ethanol (70%; 90% and 100%; 5 min; -20 °C). After air-drying, previously prepared fluorescent-labeled DNA probes were spotted on the samples and carefully closed with cover slips for overnight hybridization at 37 °C in a humidified chamber. To prevent drying-out the edges of the cover slip were sealed with rubber cement (Fixogum). The cover slips were removed and the slides washed in 2x SSC (5 min; 42 °C). The chromosomes were dyed with a DAPI solution (0.05 mg/ml; 5 min; RT) and rinsed with *Aqua dest*. Finally, a drop of "Vectashield Antifade Mounting Medium" was applied on the slides to avoid light-mediated degradation of the fluorescent dyes and closed with a cover slip. The analysis was done with a fluorescent microscope using appropriate filters.

2.2.6 Fluorescence-activated cell sorting (FACS)

2.2.6.1 Cell cycle analysis

Gene knock-down and drug treatment can enhance or inhibit cell cycle progression. As the relative amount of DNA is in G_2/M phase twice as high as in G_0/G_1 we performed the cell cycle analysis by determination of the DNA content. For this, the DNA was stained with fluorescent dye (DAPI) and the amount was then estimated by fluorescence-activated cell sorting (FACS).

Sample preparation

Cells were harvested by versenization and centrifuged (800 RPM; 10 min). The excess medium was discarded leaving 500 µl in the tube to resuspend the pelleted cells. Then, 1 ml of citric acid solution was added to the cell suspension and inverted gently. All samples were stored at 4 °C for at least 24 h and maximum 1 week. Before measurement, the tube were centrifuged (800 RPM; 10 min), the supernatant was discarded and the pellets were up taken in 500 µl PBS. The cells were stained with 0.5 µg/ ml DAPI and incubated 30 min before measurement in the dark.

Sample acquisition

The cellular suspensions were analyzed with the MACSQuant VYB flow cytometer with the following instrument settings:

Tab. 2.8: Basic flow cytometer instrument settings.

Detector (channel)	Voltage	Acquisition mode
Forward scatter (FSC)	245	linear
Side scatter(SSC)	317	linear
Fluorescent signal (V1)	385	linear

The FSC and SSC gains were adjusted to place the cell population in the middle of the dot plot and in each sample the voltage and gain of V1 were adjusted to run the G_1 peak on 10^3. In each experiment 20,000 events were measured. Data was analyzed with the FlowJo software cell cycle platform using the Watson pragmatic algorithm.

Cell death analysis

To investigate if gene knock-down induces cell death, we measured the DNA content via PI staining. Whereas dead cells accumulate PI due to the disruption of membranes, healthy cells show no staining as the dye cannot enter through intact membranes.

Sample preparation

Cells were harvested 96 h after treatment and centrifuged (1000 RPM; 5 min). The pellets were washed with 10 ml PBS and centrifuged again. The pellets were then resuspended in 1 ml PBS and 200 µl were transferred to FACS tubes. Directly before measurement 2 µl PI were added to the cell suspension and 20,000 events were acquired.

Sample acquisition

The samples were analyzed with FCS and SSC as described in 2.2.6.1. The fluorescent signal (channel B2) was acquired at 356 V.

3. Results

3.1 Initial indications of CYCLOPS genes in neuroblastoma on chromosome arm 1p

3.1.1 The expression of 1p-encoded genes is lower in 1p-deleted tumors than in 1p non-deleted

The concept of CYCLOPS is based on the assumption that the copy number of a gene correlates with its expression level. This means that cells with a hemizygously-deleted gene show a reduced expression compared to non-deleted cells. In this study, we focused on chromosome arm 1p as it is deleted in ~35% of patients (Bown 2001). There are mainly two types of deletions occurring, type 1 affects the first third of the distal end, the second includes almost the whole chromosome arm (Fig. 3.1 A). To assess the expression level in dependency to the copy number status, we analyzed an RNA sequencing data set from 573 primary tumors including 145 cases showing a type 1 or type 2 deletion. The expression level of genes in 1p-deleted tumors was set in contrast to the expression level in 1p normal tumors. The results show that the expression ratio of genes in hemizygously-deleted cases is lower than in 1p non-deleted tumors indicating that potential CYCLOPS may be localized on chromosome arm 1p (Fig. 3.1 B).

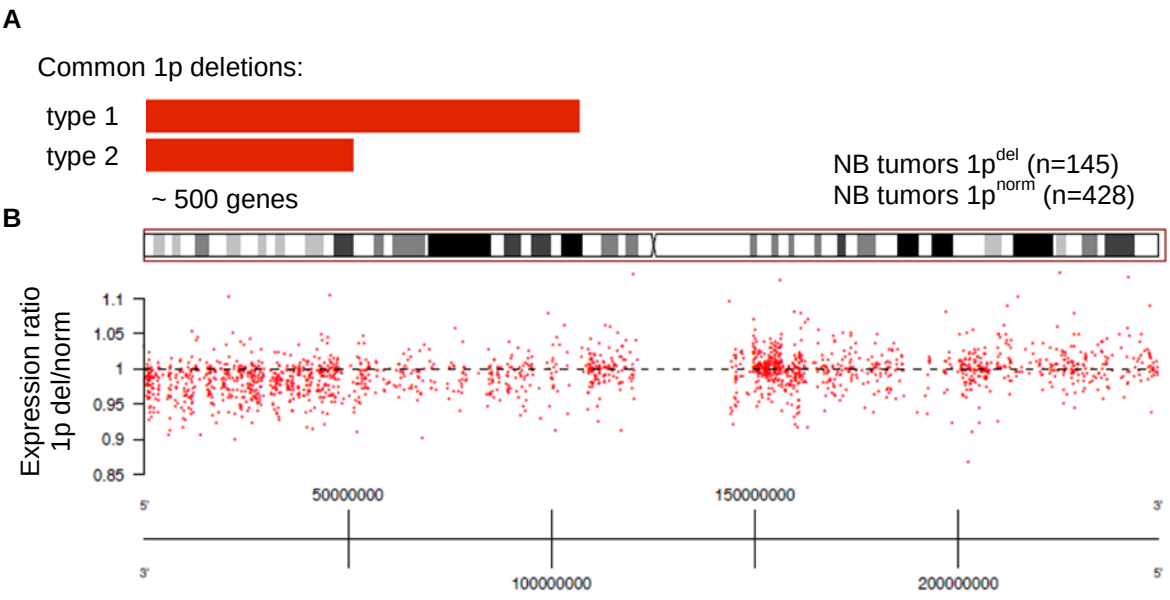

Fig. 3.1: The expression ratio of genes located on 1p depends on their copy number.
Neuroblastoma tumors show two types of deletions, type 1 affects one third of the distal end of chromosome 1p, type 2 includes almost the whole chromosome arm (A). The expression of genes on 1p in hemizygously-deleted tumors is lower compared to 1p non-deleted tumors (B).

3.1.2 Potential CYCLOPS genes preferentially map on chromosome arm 1p

To investigate if chromosome arm 1p has cell essential genes we analyzed data from an initial genome-wide siRNA screen in the neuroblastoma cell line IMR-5/75 addressing 2934 druggable genes. A hit was defined as a reduction of the mean cell number of >40% after knock-down for at least two out of three siRNAs. The results showed a hit to non-hit ratio of 34.2% on 1p, whereas this ratio of the remaining chromosomes is 27.7%. This difference is significant indicating that genes whose knock-down induces cell death are significantly enriched in chromosome arm 1p (Tab. 3.1).

Tab. 3.1: Genome wide analysis of hit to non-hit ratio in IMR-5/75 cells.

	1p	All chromosomes (1p excluded)
Hits	113	2821
Non-hits	217	7001
Ratio of hits	34.2%	27.7%

*****

p = 0.034

3.2 Characterization of the 1p copy number status in neuroblastoma cell lines

For this study 1p-deleted and 1p normal cell lines were selected. To assess if the cells have a 1p deletion and to determine the exact breakpoint whole genome sequencing (WGS) was performed in 34 neuroblastoma cell lines. The absolute copy number was estimated by fluorescence *in situ* hybridization (FISH).

3.2.1 Whole genome sequencing revealed the 1p status in neuroblastoma cell lines

We analyzed whole genome sequencing data from 34 neuroblastoma cell lines to characterize the copy number status of chromosome arm 1p (Fig. 3.2). This revealed that one half of the cell lines had a deletion of 1p and showed the exact breakpoints. However, the sequencing results do not distinguish between diploid and tetraploid conditions. For instance, a tetraploid cell with two deleted and two non-deleted 1p chromosomes (e.g. SIMA, GI-ME-N) has the same copy number ratio as a diploid cell line with one deleted and one non-deleted chromosome arm 1p (e.g. LAN-5, NBS-124). Also more complex rearrangements as translocations cannot be seen.

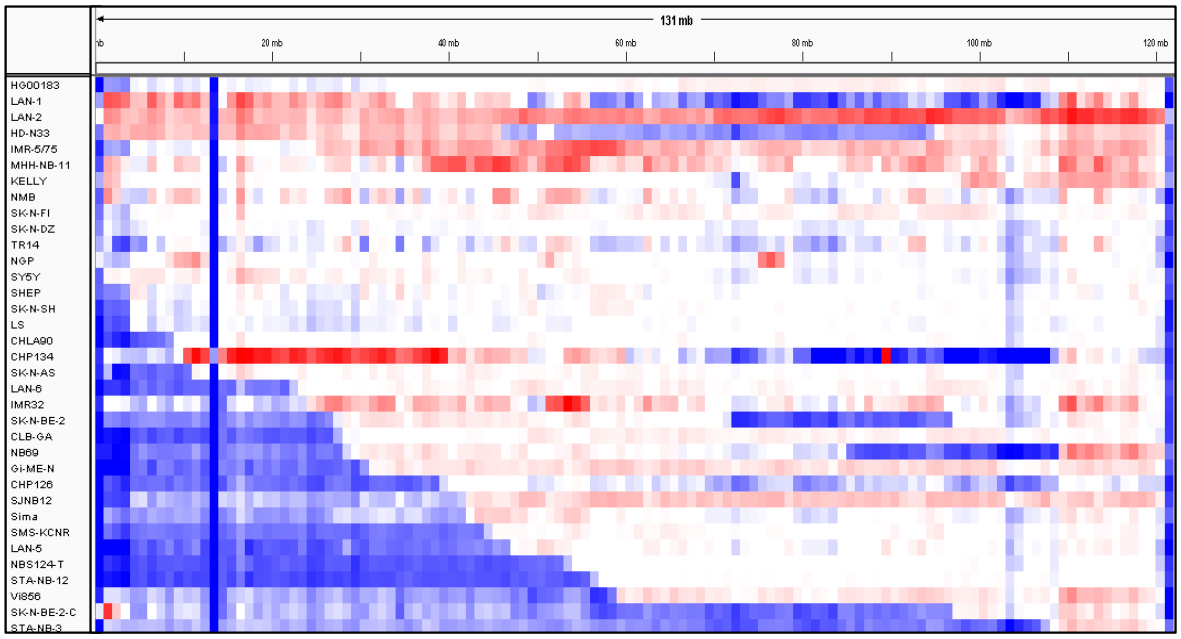

Fig. 3.2: Whole genome sequencing in neuroblastoma cell lines.

Whole genome sequencing in 34 neuroblastoma cell lines revealed the status of chromosome arm 1p. Blue: loss, red: gain.

3.2.2 FISH analysis revealed the absolute amount of 1p chromosome arms in neuroblastoma cell lines

To validate the WGS results, estimate the total copy number and identify translocations and rearrangements of chromosome arm 1p, we analyzed 35 neuroblastoma cell lines with FISH analysis. For this, we used six color probes mapping on predefined regions on 1p (Fig. 3.3 A, Tab. 3.2). An example of a non-deleted, non-translocated and non-rearranged chromosome arm 1p is shown in SH-EP cells (Fig. 3.3 B).

We identified five cell lines with normal 1p status which have been selected for this study: LS, SH-SY5Y, SK-N-AS, SK-N-FI, TR14 (Fig. 3.4). All cell lines showed two 1p chromosomes without gain, loss or rearrangements except of TR14 which has a gain of the proximal end shown by three blue probes.

The selected 1p-deleted cell lines are CHP-126, CBL.Ga, IMR-32, NB69 and SK-N-BE(2), the rearrangements were here more complex but the distal end including 1p36 was detected only once per cell (Fig. 3.5). All other tested cell lines showed more complicated 1p modifications or were difficult to handle in cell culture and have not been selected for this study (Fig. S 1, Tab. 3.3).

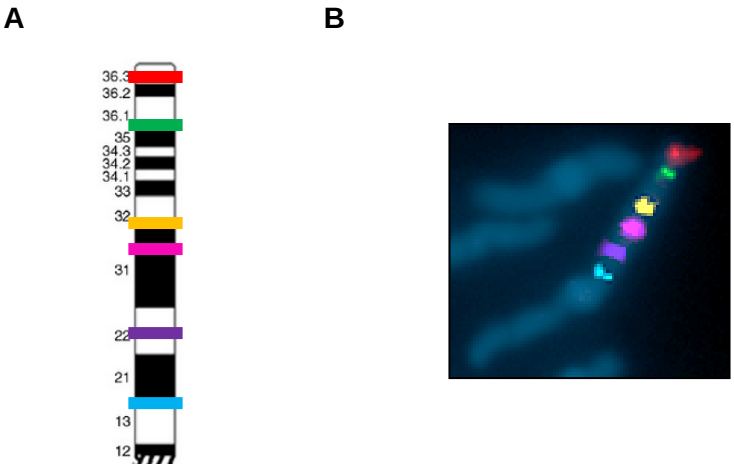

Fig. 3.3: FISH probes for chromosome arm 1p.
Six different probes mapping on pre-defined positions of chromosome arm 1p (A). Example of a structurally unchanged chromosome arm 1p in SH-EP cells (B).

Tab. 3.2: Positions and colors of FISH probes.

Dye	Color	Position (mb)	Band
Cy3	Red	1.89 – 2.02	1p36.33
FITC	Green	25.03 – 25.21	1p36.11
Cy5	Yellow	53.12 – 53.28	1p32.3
Cy3.5	Pink	77.20 – 77.33	1p.31.1
DEAC	Violet	97.50 – 97.70	1p21.3
Cy5.5	Blue	119.77 – 119.92	1p12

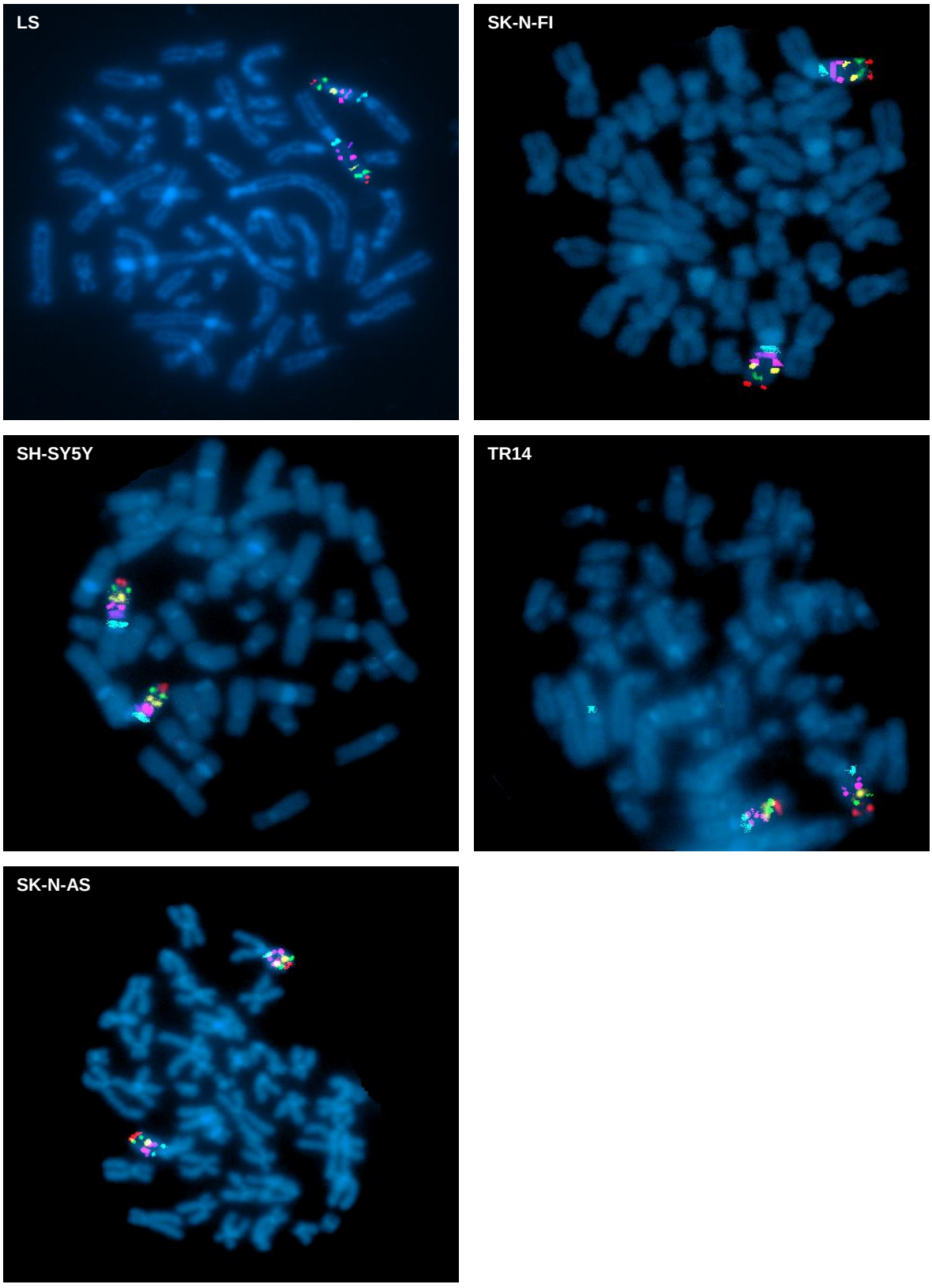

Fig. 3.4: FISH analysis in 1p non-deleted cell lines.

FISH analysis reveals that LS, SH-SY5Y, SK-N-AS, SK-N-FI, TR14 have normal 1p status for the distal end of the chromosome arm, blue: DAPI.

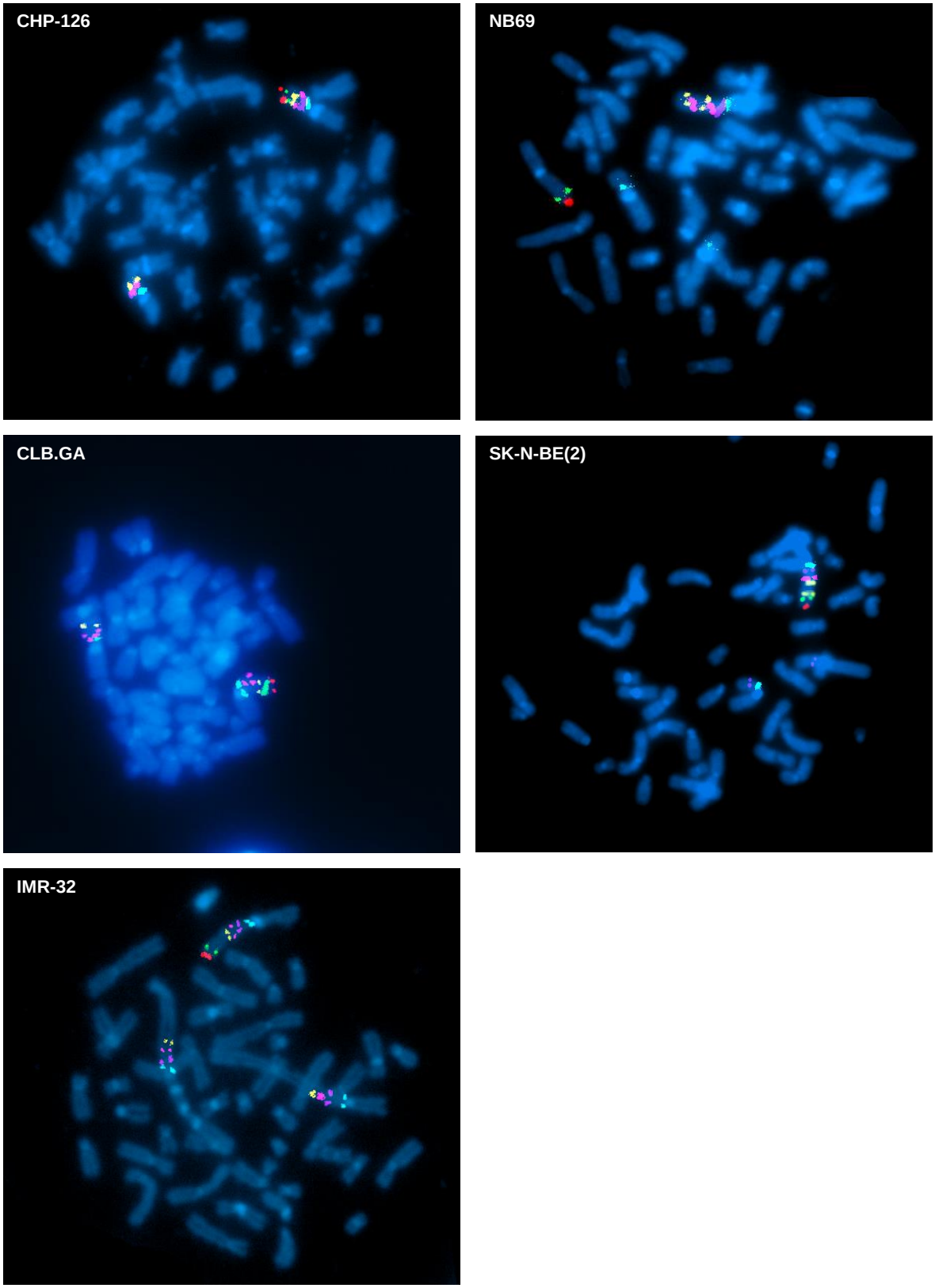

Fig. 3.5: FISH analysis in 1p-deleted cell lines.
FISH analysis reveals that CHP-126, CLB.Ga, IMR-32, NB69 and SK-N-BE(2) have a deletion on the distal end of chromosome arm 1p, blue: DAPI.

Tab. 3.3: Copy number at position of individual FISH probes in neuroblastoma cell lines.

Cell line	1p36.33	1p36.11	1p32.3	1p31.1	1p21.3	1p12
CHLA-90	1	2	2	3	3	3
CHLA-20	2	2	2	1	1	1
GI-M-EN	2	2	4	4	4	4
HD-N-16	3	2	2	2	2	2
CHP-134	1	3	2	2	1	2
HD-N-33	4	4	4	4	4	4
IMR-5/75	2	3	4	3	3	3
CHP-126	1	1	2	2	2	2
CLB.Ga	1	1	2	2	2	2
IMR-32	1	1	3	3	3	3
Kelly	3	2	2	2	2	3
LAN-1	3	3	3	3	3	5
LAN-2	5	5	5	5	7	7
LAN-5	1	1	2	2	2	2
LAN-6	1	2	2	2	2	2
LS	2	2	2	2	2	2
MHH-NB-11	3	3	6	6	6	6
NB69	1	1	2	2	1	3
NBL-S	2	2	2	2	2	2
NBS-124	1	1	1	2	2	2
NGP	2	2	2	2	2	2
NMB	1	3	3	3	3	3
SH-EP	2	2	2	2	2	2
SH-SY5Y	2	2	2	2	2	2
SIMA	2	2	4	4	4	4
SJNB-12	3	3	3	3	3	3
SK-N-AS	2	2	2	2	2	2
SK-N-BE(2)	1	1	2	2	2	2
SK-N-BE(2)c	4	2	2	2	4	4
SK-N-DZ	3	3	3	3	3	5
SK-N-FI	2	2	2	2	2	2
SK-N-SH	2	2	2	2	2	2
SMS-KCNR	1	1	2	2	2	2
TR14	2	2	2	2	2	3
Vi856	2	2	2	2	5	5

3.2.3 CGH arrays reveal an interstitial deletion in SK-N-AS

FISH analysis of the cell line SK-N-AS suggested two unaltered chromosome arms 1p (3.2.2). However, the WGS data identified a small deletion at the distal end (3.2.1). To elucidate this discrepancy, we included CGH array data to further characterize the 1p status and revealed an interstitial deletion in 1,859,899-11,034,099 (Fig. 3.6)

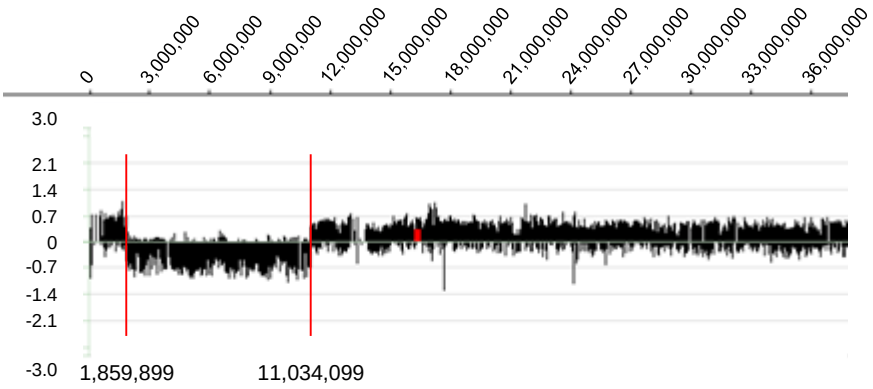

Fig. 3.6: CGH array of SK-N-AS.
The CGH array of SK-N-AS revealed a small interstitial deletion at the distal end.

3.3 Candidate gene identification

3.3.1 siRNA screen for CYCLOPS genes in neuroblastoma cell lines

To identify CYCLOPS genes on chromosome arm 1p, we performed an siRNA screen. We focused on 1p36 as this is the smallest region of overlapping deletion in our cell lines and patients and selected 184 druggable genes. Each gene was knocked down with three different siRNAs in triplicates in five 1-deleted and five 1p non-deleted cell lines. The cell confluency was assessed after 96 hours. After normalization for plate effects (B-scoring) and to a non-coding scrambled siRNA as negative control, the mean of the confluency replicates was calculated. The three siRNAs were combined by calculating the median of all means leading to the confluency score for one gene in one cell line. To assess the 1p status-related gene dependency the mean values of all 1p-deleted vs all 1p non-deleted cell lines were estimated. A negative confluency score indicated cell death or growth arrest after gene knock down which is an indicator for high gene dependency. Genes whose knock-down induced cell growth had a positive confluency score. Genes with a negative confluency score in 1p-deleted cells ($x \leq -0.15$) but little or no impact on 1p non-deleted cells ($-0.2 \leq x \leq 0.2$) were considered as hits (Fig. 3.7). Finally, the distance

between the dependency scores ($1p^{norm}$ – $1p^{del}$) was calculated. The bigger the distance, the stronger the effect on 1p-deleted cells while any impact on 1p normal cells was excluded by setting the parameters (Tab. 3.4).

Additionally we noticed that genes that impair viability upon knock-down in both, 1p-deleted and 1p non-deleted cell lines are mainly involved in cell growth and proliferation or are related to neuronal and embryonic development (Tab. S2). As these genes are likely to play important roles in neuroblastoma, this finding confirms the reliability of this siRNA screen.

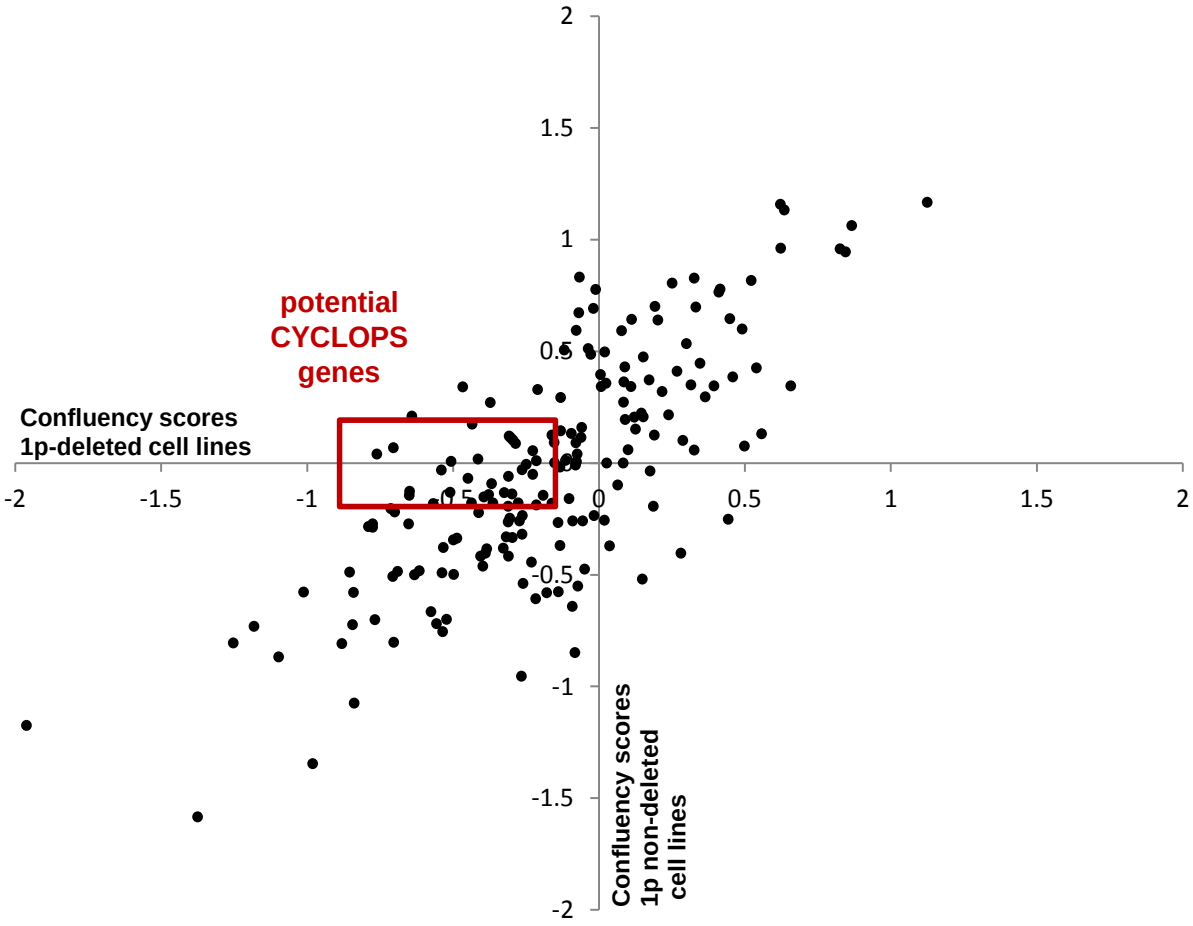

Fig. 3.7: CYCLOPS candidate screening results in neuroblastoma cell lines.

The confluency scores for 1p non-deleted cell lines were blotted over the confluency scores for 1p-deleted cell lines. Each dot represents one gene. A positive score indicates that siRNA knock-down of the gene induced cell growth; a negative score indicates cell death or growth inhibition. Genes whose knock-down induces cell death/growth inhibition in 1p-deleted cells ($x \leq -0.15$) but has no effect on 1p non-deleted cells ($-0.2 \leq x \leq 0.2$) were defined as CYCLOPS genes, therefore, the potential candidates map in the red square. All scores are normalized to a non-coding scrambled siRNA.

Tab. 3.4: Potential CYCLOPS genes sorted by distance.

Gene	Confluency scores $1p^{del}$	Confluency scores $1p^{norm}$	Distance ($1p^{norm} - 1p^{del}$)
AURKAIP1	-0.76	0.04	0.80
CALML6	-0.70	0.07	0.77
CAPZB	-0.43	0.17	0.61
SSU72	-0.65	-0.13	0.52
AJAP1	-0.51	0.01	0.51
ICMT	-0.54	-0.03	0.51
ATAD3B	-0.65	-0.15	0.50
RSC1A1	-0.41	0.02	0.43
USP48	-0.31	0.12	0.43
AKR7A2	-0.30	0.11	0.41
PRDM16	-0.29	0.10	0.39
CLCNKA	-0.57	-0.18	0.38
MMEL1	-0.45	-0.07	0.38
PEX14	-0.51	-0.13	0.38
NPPB	-0.29	0.09	0.37
LIN28A	-0.16	0.12	0.28
HSPG2	-0.23	0.05	0.28
PLOD1	-0.37	-0.09	0.27
ZBTB40	-0.44	-0.18	0.26
FBXO6	-0.31	-0.06	0.25
DNAJC11	-0.15	0.09	0.24
HSPB7	-0.25	-0.01	0.24
TP73	-0.39	-0.15	0.24
LDLRAD2	-0.38	-0.14	0.23
DHRS3	-0.26	-0.03	0.23
SDF4	-0.21	0.01	0.22
PLEKHM2	-0.32	-0.13	0.19
CDEL5	-0.36	-0.18	0.18
FBXO44	-0.23	-0.05	0.17
NECAP2	-0.30	-0.14	0.16
EPHA8	-0.15	0.00	0.15
TTLL10	-0.31	-0.20	0.11
EPHB2	-0.28	-0.18	0.10
EPHA2	-0.19	-0.15	0.04
KIF1B	-0.21	-0.19	0.03

3.3.2 Selection of candidates by gene function and expression ratio in neuroblastoma patients and cell lines

In the previously mentioned siRNA screen (3.3.1) genes whose siRNA-mediated knock-down reduced confluency in 1p deleted-cells but had no impact on 1p non-deleted cells were considered hits. Candidate gene prioritization was based on the following criteria:

- Confluency scores from the siRNA screen:
  1p-deleted cells: $x \leq -0.15$
  1p non-deleted cells: $-0.2 \leq x \leq 0.2$
- Gene expression in neuroblastoma patients:
  $1p^{del} < 1p^{norm}$
- Gene expression in neuroblastoma cell lines:
  $1p^{del} < 1p^{norm}$
- Druggability
  Genes for whom drugs are commercially available were preferred

3.3.2.1 Expression ratio analysis in neuroblastoma patients

A major characteristic of a CYCLOPS gene is its lower expression in hemizygously-deleted vs non-deleted tumors. For candidate prioritization, we analyzed RNA sequencing data of a cohort with 573 patients including 147 cases which show an 1p deletion or imbalance. Following the criteria in 3.3.2 three candidates with the best results for gene expression ($1p^{del} < 1p^{norm}$) were chosen: *SDF4*, *AURKAIP1* and *ICMT*. Additionally, we noticed that all genes belonging to the family of ephrin receptors which were included in the screen (*EPHA2*, *EPHA8*, *EPHB2*) were hits by our definition in 3.3.1, although the distance ($1p^{norm} – 1p^{del}$) was not as strong as for other candidates. However, we included them for validation as they function as key players in neuronal and embryonal development (Kania and Klein 2016; Nievergall, et al. 2012). *EPHA2* and *EPHB2* were significantly lower expressed in 1p-deleted/-imbalanced patients than in 1p non-deleted tumors, whereas the expression of *EPHA8* was higher in 1p-deleted/-imbalanced tumors (Fig. 3.8 B).

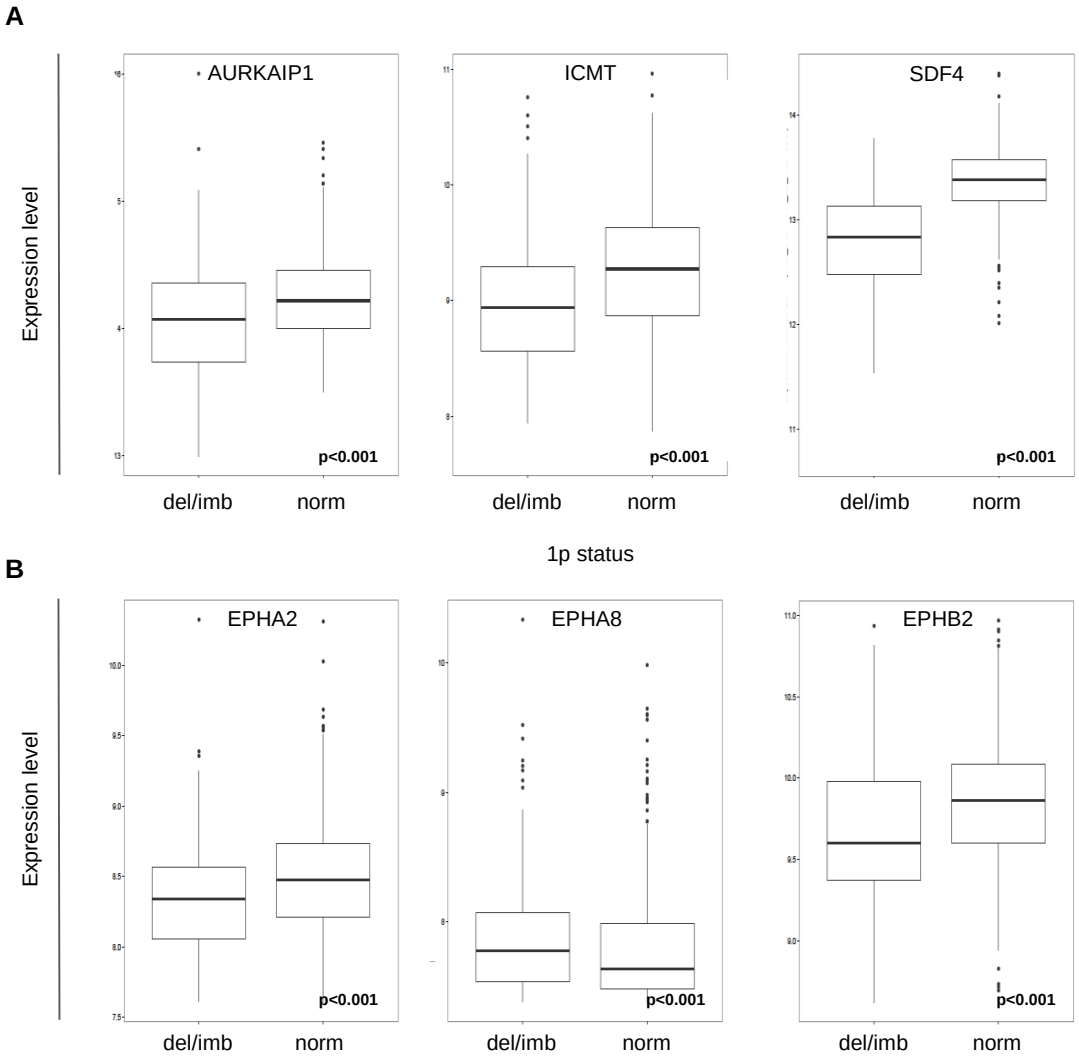

Fig. 3.8: Expression level analysis in primary neuroblastoma tumors.
To assess the expression level of the candidate genes *AURKAIP1*, *ICMT*, *SDF4* (A) and *EPHA2*, *EPHA8*, *EPHB2* (B) RNA sequencing data of 573 primary neuroblastoma tumors were analyzed; of these 147 show a deletion or imbalance of chromosome arm 1p; all results are highly significant.

3.3.2.2 Expression ratio analysis in neuroblastoma cell lines

To determine the expression ratio of the candidate genes in the selected neuroblastoma cell lines (3.2.2) we analyzed an RNA sequencing data set of five 1p-deleted (CLB.Ga, CHP-126, IMR-32, SK-N-BE(2), NB69) and five 1p non-deleted cell lines (TR14, LS, SK-N-AS, SK-N-FI, SH-SY5Y). All selected cell lines are either deleted or non-deleted for all genes with exception of SK-N-AS which has an interstitial deletion lacking one copy of *ICMT* (Tab. 3.5).
The median expression levels of the candidates *AURKAIP1*, *ICMT*, *SDF4*, *EPHA2* and *EPHB2* were lower in hemizygously-deleted than in 1p non-deleted cell lines. This effect

was significant for *AURKAIP1*, *SDF4* and *EPHA2*. The candidate *EPHA8* expression was higher in 1p-deleted compared to 1p non-deleted tumors (Fig. 3.9).

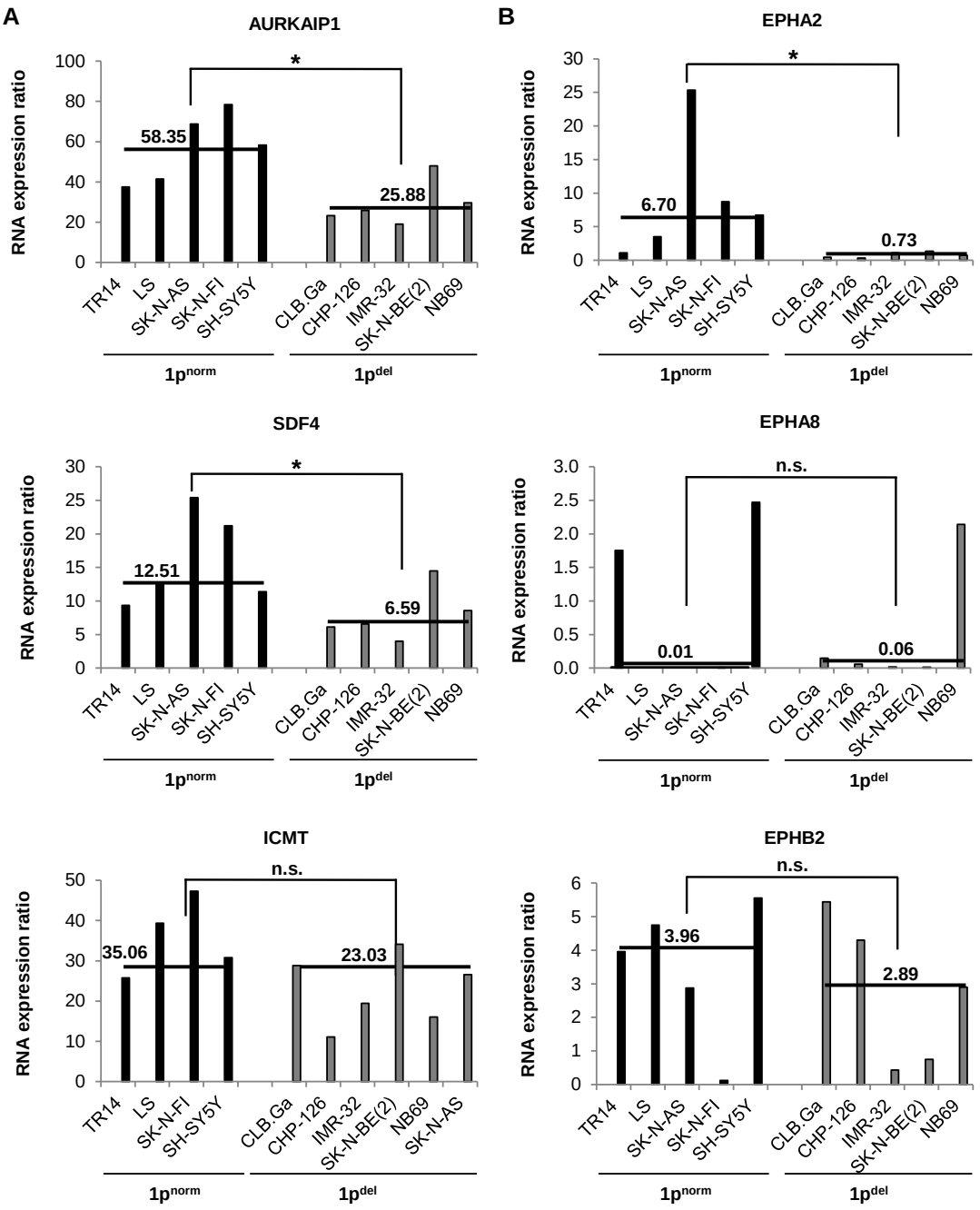

Fig. 3.9: Expression level analysis in neuroblastoma cell lines.

To assess the expression level of the candidate genes *AURKAIP1*, *ICMT*, *SDF4* (A) and *EPHA2*, *EPHA8*, *EPHB2* (B) RNA sequencing data of five 1p-deleted cell lines (CLB.Ga, CHP-126, IMR-32, SK-N-BE(2), NB69) and five 1p non-deleted (TR14, LS, SK-N-AS, SK-N-FI, SH-SY5Y) was analyzed and the median expression assessed; SK-N-AS has an interstitial deletion and is therefore counted as an 1p-deleted cell line in the *ICMT* context, n.s. = not significant., * = significant ($p<0.5$).

Tab. 3.5: Copy number of the selected candidate genes in ten neuroblastoma cell lines, wt: wild type, del: deleted.

Gene	*SDF4*	*AURKAIP1*	*ICMT*	*EPHA2*	*EPHA8*	*EPHB2*
Position	1,21 mb	1,37 mb	6,22 mb	16,12 mb	22,56 mb	22,71 mb
CHP-126	del	del	del	del	del	del
CLB.Ga	del	del	del	del	del	del
IMR-32	del	del	del	del	del	del
LS	wt	wt	wt	wt	wt	wt
NB69	del	del	del	del	del	del
SH-SY5Y	wt	wt	wt	wt	wt	wt
SK-N-AS	wt	wt	del	wt	wt	wt
SK-N-BE(2)	del	del	del	del	del	del
SK-N-FI	wt	wt	wt	wt	wt	wt
TR14	wt	wt	wt	wt	wt	wt

3.4 Candidate gene validation

3.4.1 Validation of AURKAIP1, ICMT and SFD4

3.4.1.1 Knock-down of candidate genes induces loss of viability in neuroblastoma cells

To validate the screening results AURKAIP1, ICMT and SDF4 were knocked down in four exemplary cell lines. We used IMR-32 and SK-N-BE(2) as 1p-deleted models and TR14 and LS as 1p non-deleted. Each gene was addressed with three different siRNAs and after 96 hours the viability was measured via CTB assays (Fig. 3.10). The distance between the viability values was calculated ($1p^{norm}$ – $1p^{del}$; Tab. 3.6).

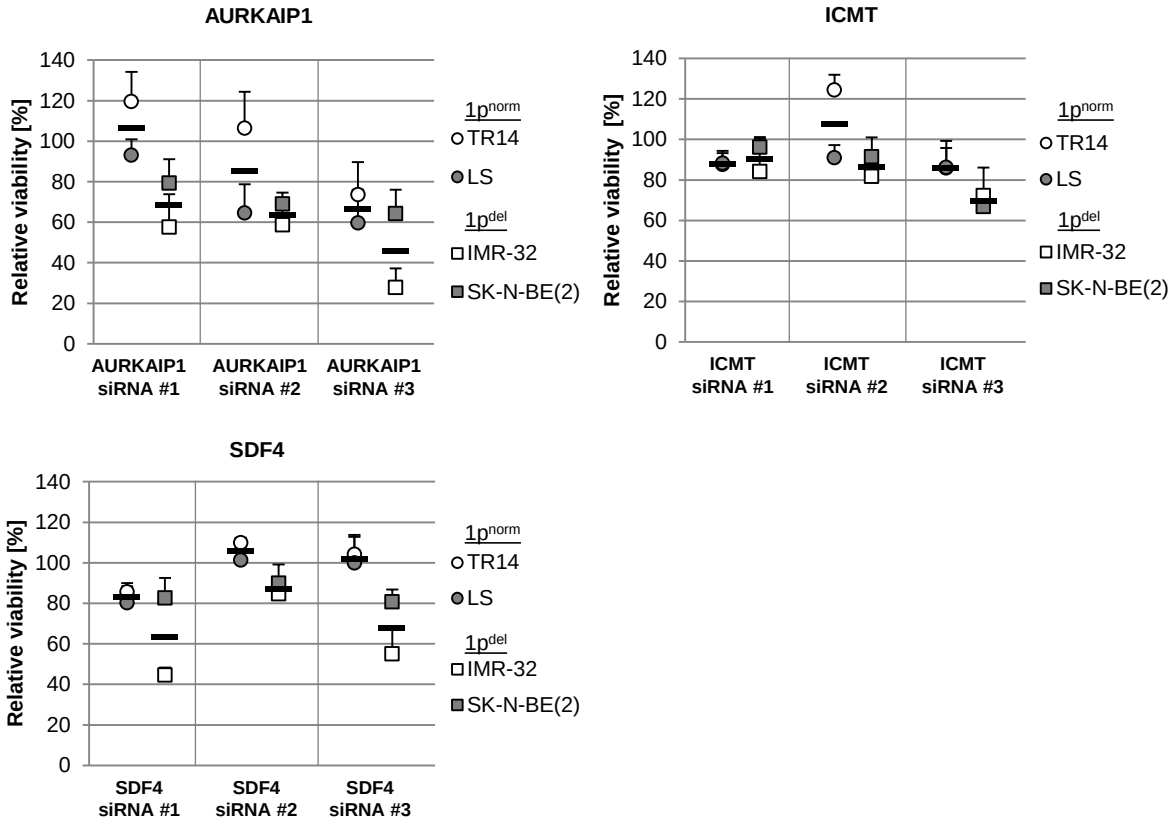

Fig. 3.10: Candidate gene knock-down induces loss of viability.
The candidate genes *AURKAIP1*, *ICMT* and *SDF4* were knocked down in two 1p non-deleted cell lines (TR14, LS) and two 1p-deleted cell lines (IMR-32, SK-N-BE(2)). For each approach three different siRNAs were used. The viability was assessed after 96 h with CTB assay and the mean of each result group was calculated. All results are normalized to a non-specific scrambled siRNA. The results are triplicates of three independent experiments, + SD.

Tab. 3.6: Means and distances of viability after siRNA knock-down of candidate genes.

Target gene	siRNA	Mean $1p^{norm}$ [%]	Mean $1p^{del}$ [%]	Distance ($1p^{norm} – 1p^{del}$)
AURKAIP1	#1	106.3	68.4	37.9
	#2	85.5	63.8	21.7
	#3	66.6	46.1	20.6
ICMT	#1	88.0	90.1	-2.2
	#2	107.1	86.6	21.2
	#3	86.1	69.5	16.5
SDF4	#1	82.9	63.6	19.4
	#2	105.6	87.3	18.3
	#3	102.0	67.9	34.1

Following criteria for a positive validation result were set:

- Mean viability $1p^{norm}$ >85%
- Mean viability $1p^{del}$ <75%
- Distance ($1p^{norm} – 1p^{del}$) >20
- At least two siRNAs have to fulfill these criteria

AURKAIP1 siRNA #1 and #2 fulfilled these requirements. The 1p-deleted cells were not differentially sensitive to ICMT knock-down and only siRNA #3 showed a positive result for SDF4 knock-down.

These results were in line with testing the selective ICMT inhibitor cysmethynil. In titration experiments cysmethynil was used in a range of 30 – 50 µM in IMR-32 and SK-N-BE(2) (1p-deleted) and TR14 and LS (1p non-deleted) cells and the viability was assessed after 96 hours (Fig. 3.11). TR14 had an IC_{50} of 39.3, LS 47.7. The values in IMR-32 and SK-N-BE(2) were 34.1 and 47.6 (Tab. 3.7). The IC_{50} indicates that the sensitivity to ICMT inhibition is not related to the 1p copy number status.

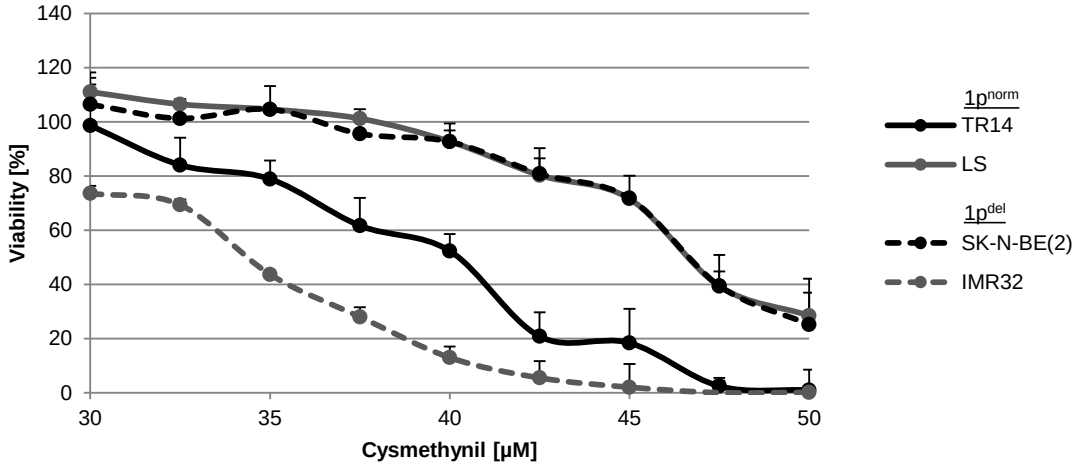

Fig. 3.11: Cysmethynil treatment reduces viability in neuroblastoma cell lines.
To inhibit ICMT selectively, we treated two 1p non-deleted cell lines (TR14, LS) and two 1p-deleted cell lines (SK-N-BE(2), IMR-32) with cysmethynil. We used concentrations of 30 – 50 µM and assessed the viability after 96 h with CTB assay. Measurements were done in triplicates in three independent experiments, + SD.

Tab. 3.7: IC_{50} values of cysmethynil treatment in neuroblastoma cell lines.

Cell line	1p Status	IC_{50}
TR14	non-deleted	39.3
LS	non-deleted	47.7
IMR-32	deleted	34.1
SK-N-BE(2)	deleted	47.6

3.4.1.2 Knock-down of candidate genes reduces cell confluency in neuroblastoma cells

To estimate the effect of candidate genes knock-down on cell confluency, plates used for viability assays (3.4.1.1) were Giemsa stained and the cell density was estimated. The same criteria as in 3.4.1.1 were used to determine positive results. Although the effect on 1p-deleted cells was strong in all cases (except ICMT siRNA #2), a considerable effect on cell confluency was also seen for two out of three siRNAs after knock-down of all candidates (Fig. 3.12, Tab. 3.8). As the concept of CYCLOPS assumes that only hemizygously deleted cells are sensitive to further knock-down but non-deleted cells remain unharmed, these results revalidate *AURKAIP1, ICMT* and *SDF4* as candidates. For this reason no further validation experiments were performed with these genes.

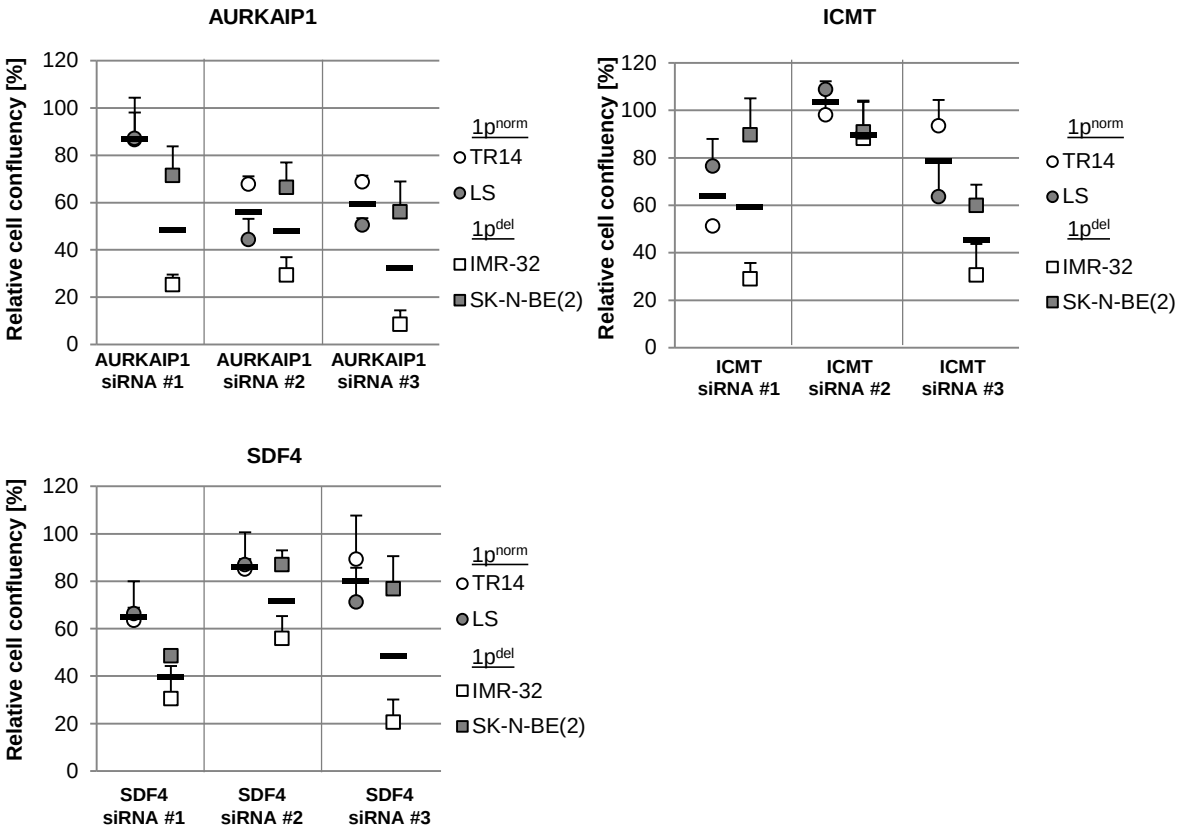

Fig. 3.12: Candidate gene knock-down reduces cell confluency.

The candidate genes AURKAIP1, ICMT and SDF4 were knocked down in two 1p non-deleted cell lines (TR14, LS) and two 1p-deleted cell lines (IMR-32, SK-N-BE(2)). For each approach three different siRNAs were used. The cell confluency was assessed after 96 h with Giemsa staining and the mean of each result group was calculated. All results are normalized to a non-specific scrambled siRNA. The results are triplicates of three independent experiments, +SD.

Tab. 3.8 Means and distances of cell confluency after siRNA knock-down of candidate genes.

Target gene	siRNA	Mean $1p^{norm}$ [%]	Mean $1p^{del}$ [%]	Distance ($1p^{norm} - 1p^{del}$)
AURKAIP1	#1	86.9	48.4	38.5
	#2	56.0	47.9	8.1
	#3	59.6	32.2	27.3
ICMT	#1	63.9	59.3	4.6
	#2	103.4	89.6	13.9
	#3	78.6	45.3	33.3
SDF4	#1	64.9	39.5	25.4
	#2	86.0	71.5	14.6
	#3	80.2	48.7	31.5

3.4.2 Validation of ephrin receptor family candidates (*EPHA2*, *EPHA8*, *EPHB2*)

Although the screening scores for genes of the ephrin receptor family (*EPHA2*, *EPHA8*, *EPHB2*) were moderate compared to the other candidates, we selected these genes for further validation as they play important roles in neuronal and embryonic development and this may have an impact on neuroblastoma biology. Per definition a CYCLOPS gene is lower expressed in deleted than in non-deleted tumors. We showed in 3.3.2.1 that this is the case for *EPHA2* and *EPHB2* but not for *EPHA8*, both in neuroblastoma primary tumors and cell lines. For this reason we excluded *EPHA8* from the validation pipeline and focused on the other two candidates.

3.4.2.1 Knock-down of EphA2 has little impact on neuroblastoma cell lines

We knocked down EphA2 with three different siRNAs and assessed viability (Fig. 3.13 A) and cell confluency (Fig. 3.13 B) after 96 hours. None of these siRNAs reduced viability in 1p-deleted or 1p non-deleted cells in line with our criteria in 3.4.1.1. Cell confluency in 1p-deleted cell was reduced to 72.6% upon siRNA #1 treatment but the effect on 1p non-deleted cells was also too strong by our definition (82.8%). Despite similar knock-down efficiencies of the siRNAs (Fig. 3.14) only siRNA #3 had a promising cell confluency reduction in 1p-deleted cells (65.9%) and almost no impact on 1p non-deleted cell lines (90.3%, Tab. 3.9). As one of the requirements in 3.4.1.1 was that at least two siRNAs have to meet the criteria but only siRNA #3 showed positive results here, *EPHA2* was discarded from the validation pipeline.

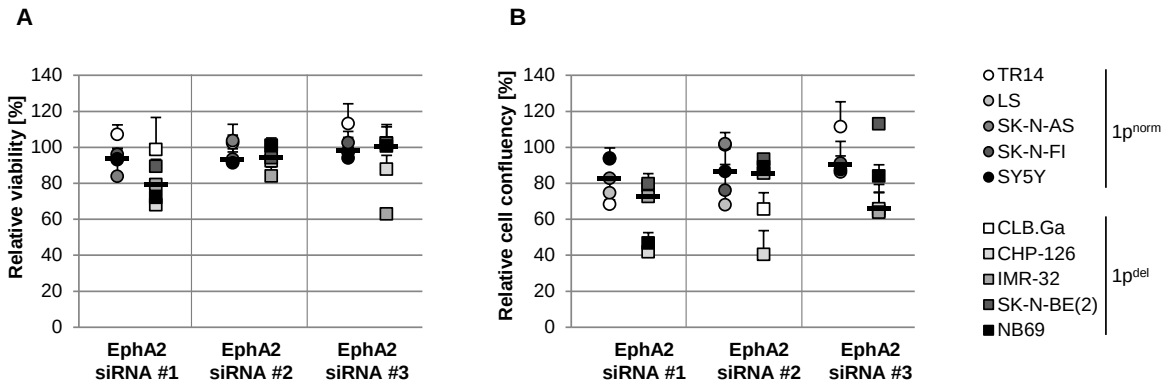

Fig. 3.13: EphA2 knock-down has little impact on neuroblastoma cell lines.
EphA2 was knocked down in five 1p non-deleted cell lines and five 1p-deleted cell lines. For each approach three different siRNAs were used. First, the viability was assessed after 96 h via CTB assay (A) and then the cells were stained with Giemsa to detect cell confluency (B). The median of each result group was calculated. All results are normalized to a non-specific scrambled siRNA. The results are triplicates of three independent experiments, + SD.

Tab. 3.9: Median values of viability and cell confluency in neuroblastoma cell lines after EphA2 knock-down.

Assay	siRNA	Median $1p^{norm}$ [%]	Median $1p^{del}$ [%]	Distance ($1p^{norm} – 1p^{del}$)
Viability	#1	93.5	79.3	14.2
	#2	93.4	94.2	-0.8
	#3	98.0	100.7	-2.7
Cell confluency	#1	82.8	72.6	10.2
	#2	86.6	85.6	1.0
	#3	90.3	65.9	24.4

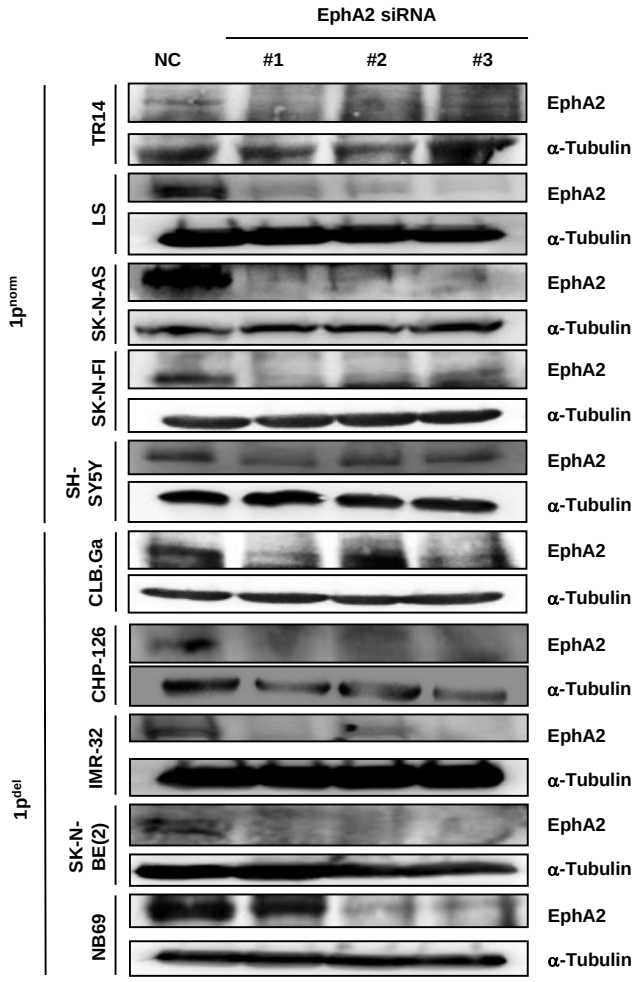

Fig. 3.14: Confirmation of EphA2 knock-down.

The knock-down of EphA2 was confirmed by western blot analysis. The results are compared to a non-specific scrambled siRNA as negative control (NC).

3.4.2.2 EphA2 knock-down had no impact on morphology of neuroblastoma cell lines

Here, we assessed cell morphology 96 hours after siRNA knock-down of EphA2. However, no morphological changes could be detected visually in neither 1p-deleted nor 1p non-deleted cells.

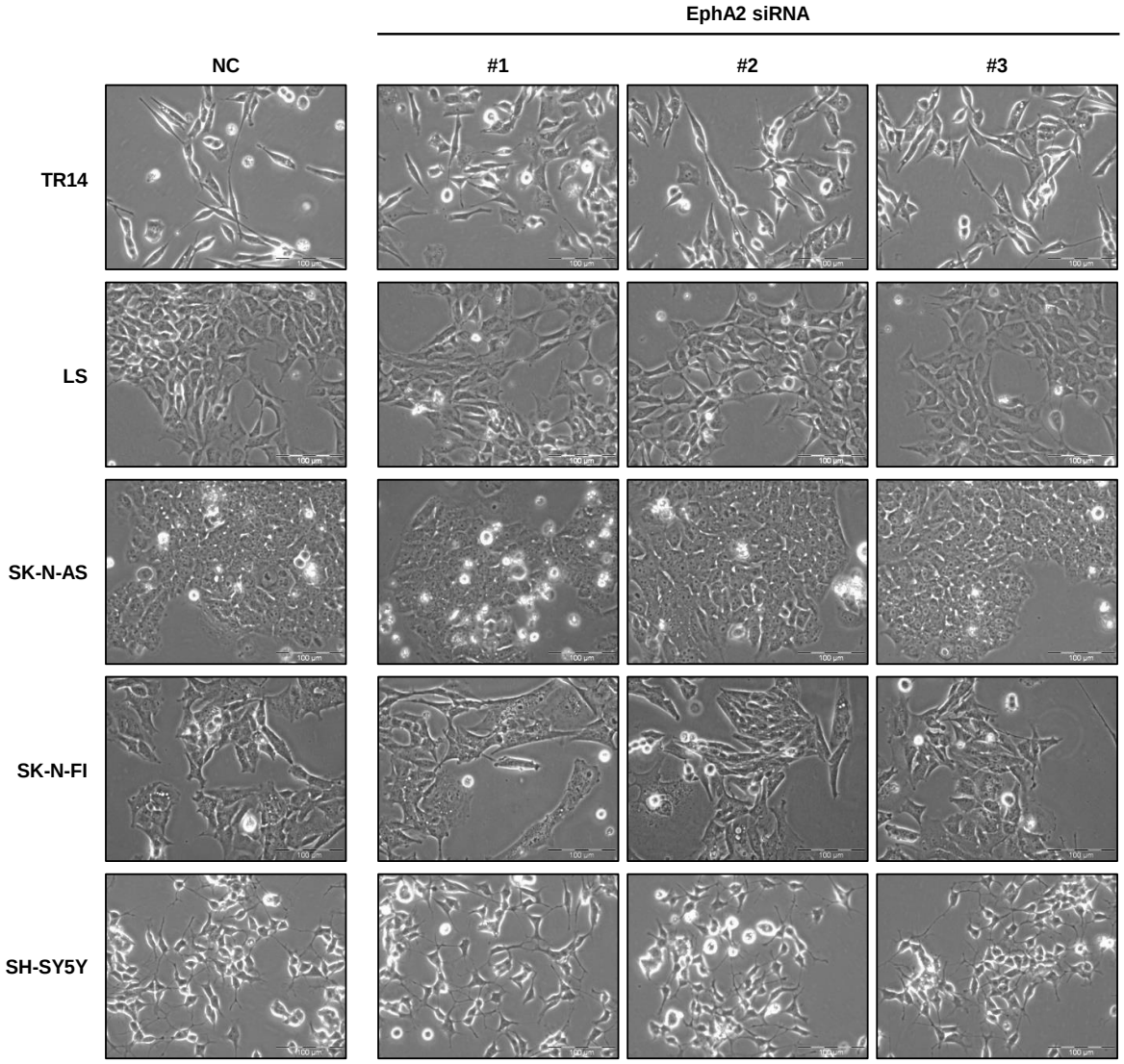

Fig. 3.15: EphA2 knock-down has no influence on the morphology of 1p non-deleted cells.
EphA2 was knocked down in five 1p-deleted cell lines with three different siRNAs. After 96 h the morphology of cells was assessed microscopically. All results are compared to a non-specific scrambled siRNA as negative control (NC), magnification x200.

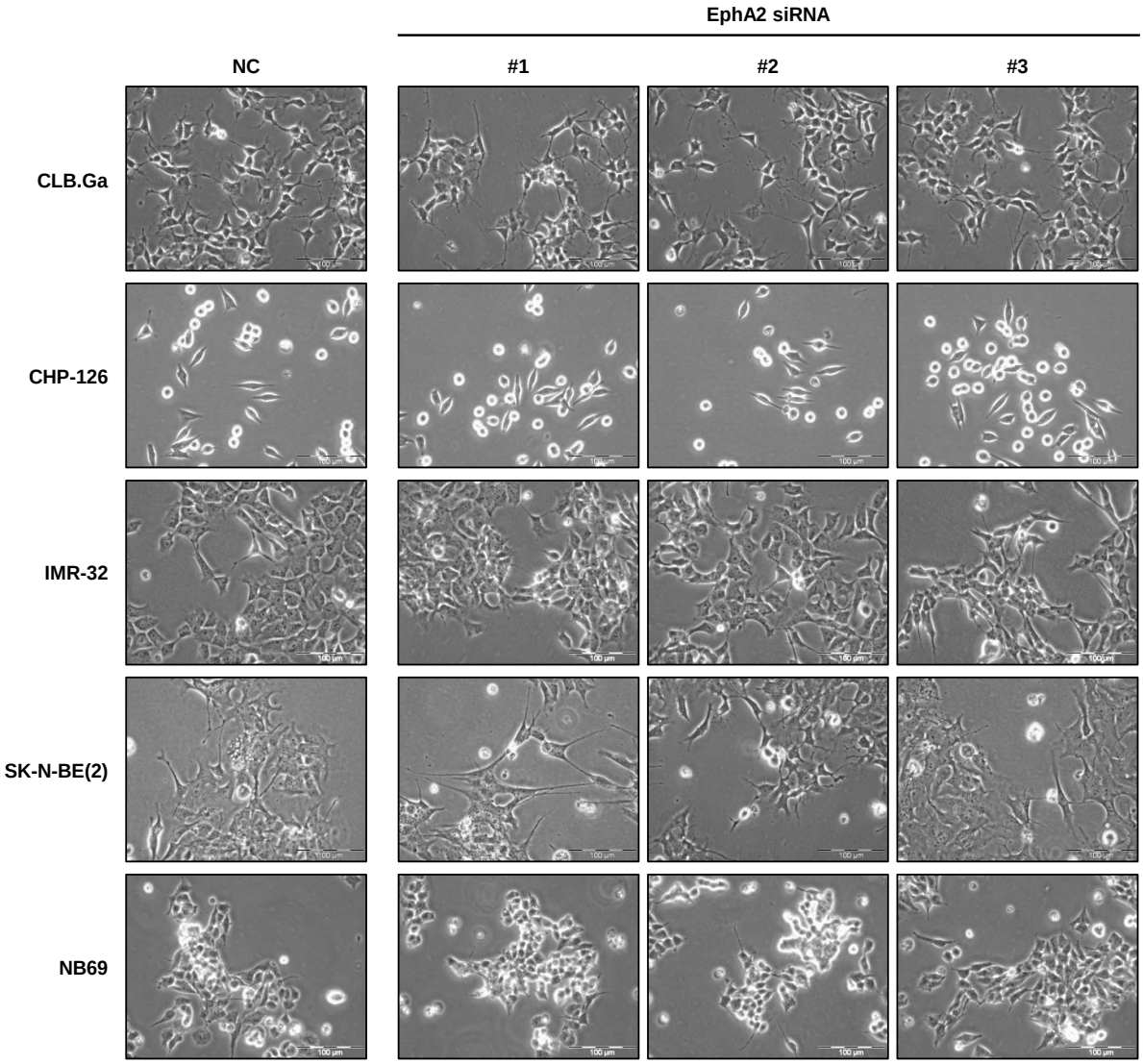

Fig. 3.16: EphA2 knock-down has no influence on the morphology of 1p-deleted cells.
EphA2 was knocked down in five 1p-deleted cell lines with three different siRNAs. After 96 h the morphology of cells was assessed microscopically. All results are compared to a non-specific scrambled siRNA as negative control (NC), magnification x200.

3.4.2.3 Knock-down of EphB2 reduces viability and cell confluency in neuroblastoma cell lines

We knocked down EphB2 with three single siRNAS in five 1p-deleted and five 1p non-deleted cell lines. After 96 hours, the viability was assessed via CTB assay (Fig. 3.17 A). For all three siRNAs, the median of viability was lower in 1p-deleted compared to 1p non-deleted cells. The same cells were then fixated and stained with Giemsa to determine cell confluency. The effect on 1p-deleted cells was stronger whereas the cell confluency of 1p normal cells remained unchanged (Fig. 3.17 B, C). In all cases the effect was not significant. However, LS showed outlying effects for cell confluency probably indicating 1p-additional factors determining EphB2-dependency in this cell line. Removing LS from the analysis leads to a highly significant result for siRNA #2 and #3 (both p=0.016).

In the cell confluency assays siRNAs #2 and #3 fulfilled the hit requirements of our definition in 3.4.1.1 (Tab. 3.10). We confirmed the knock-down effect by western blot analysis and RT-PCR (Fig. 3.18). As the EphB2 knock-down results were promising we continued with further experiments to confirm *EPHB2* as a CYCLOPS gene.

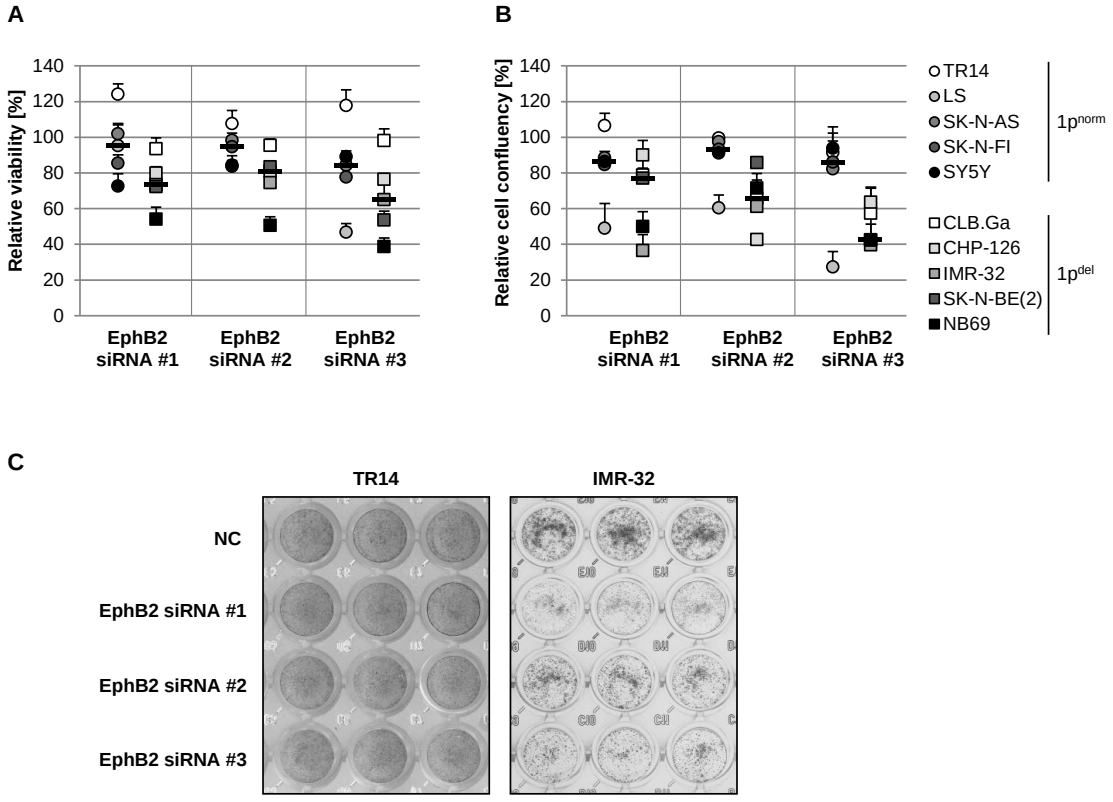

Fig. 3.17: EphB2 knock-down induces loss of viability and reduces cell confluency.

EphB2 was knocked down in five 1p non-deleted cell lines and five 1p-deleted cell lines with three different siRNAs. First, the viability was assessed after 96 h via CTB assay (A) and then the cells were stained with Giemsa to detect cell confluency (B). The median of each result group was calculated. All results are normalized to a non-specific scrambled siRNA. The results are triplicates of three independent experiments, + SD. Cell confluency results for TR14 (1p normal) and IMR-32 cells (1p-deleted) (C).

Tab. 3.10: Median values and distances of loss of viability and cell confluency after siRNA knock-down of EphB2.

Assay	EphB2 siRNA	Median $1p^{norm}$ [%]	Median $1p^{del}$ [%]	Distance ($1p^{norm} - 1p^{del}$)
Viability	#1	95.3	73.3	22.0
	#2	94.6	81.0	13.6
	#3	84.3	65.0	19.3
Cell confluency	#1	86.4	77.1	9.3
	#2	93.2	65.7	27.5
	#3	86.2	42.6	43.6

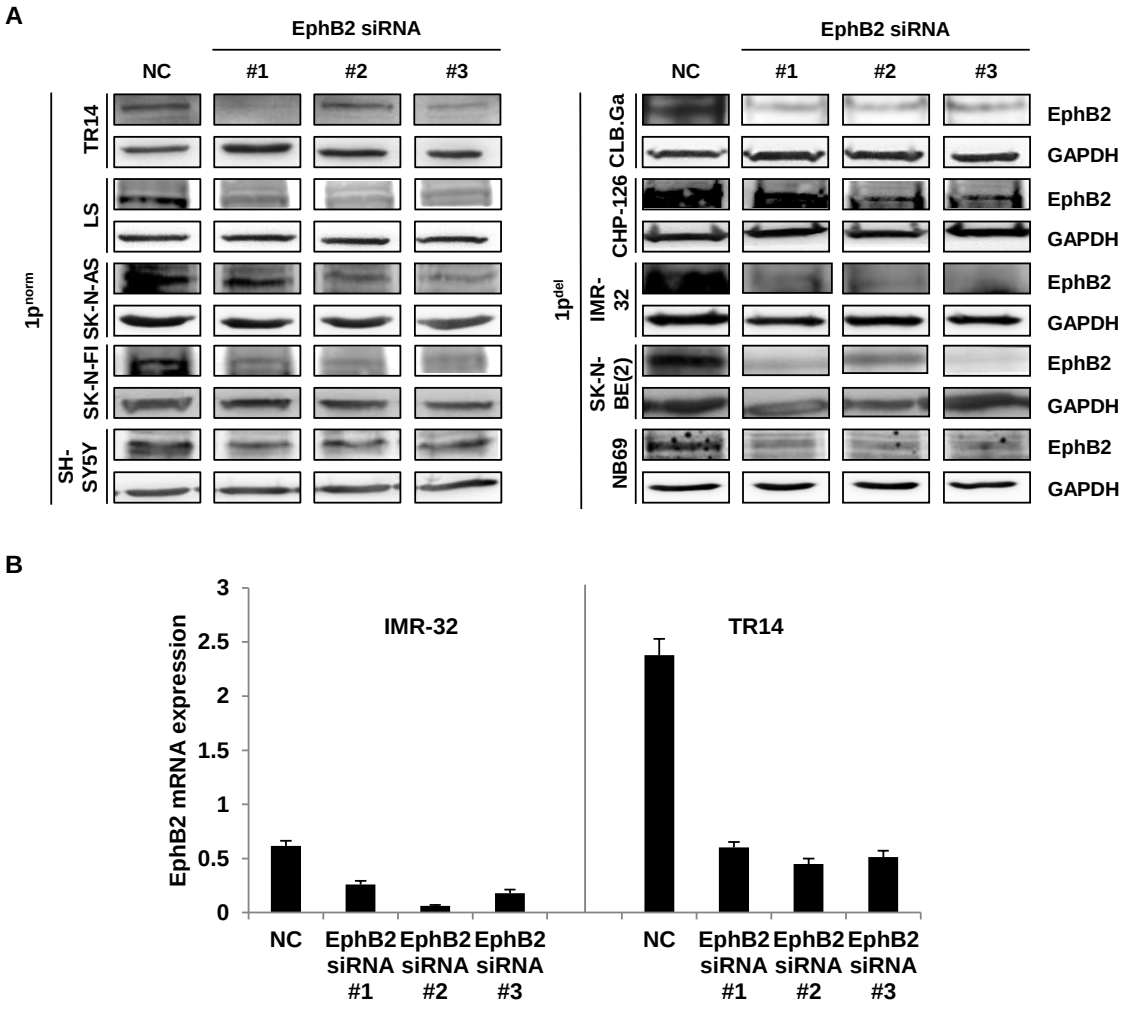

Fig. 3.18: Confirmation of EphB2 knock-down.

The knock-down of EphB2 was confirmed by western blot analysis (A) and RT-PCR (B) for the exemplary cell lines IMR-32 (1p-deleted) and TR14 (1p non-deleted), RT-PCR was performed in triplicates, one exemplary result is shown, +SD. All results are compared to a non-specific scrambled siRNA as negative control (NC).

3.4.2.4 EphB2 knock-down induces morphological changes in 1p non-deleted neuroblastoma cell lines

As described in 3.4.2.1 knock-down of EphB2 induced loss of viability and reduced cell confluency in 1p-deleted cells but had only minimal impact on 1p non-deleted cell lines. However, changes in morphology were mainly observed in 1p normal cells (TR14, SK-N-AS, SK-N-FI and SH-SY5Y, Fig. 3.19). This included extended fiber outgrowth and cell shape lengthening. Only LS showed no morphologic changes as well as the 1p-deleted cell lines CHP-126, CLB.Ga, IMR-32 and NB69 (Fig. 3.20). An exception is SK-N-BE(2) which is also 1p-deleted but started to grow fibers upon EphB2 knock-down.

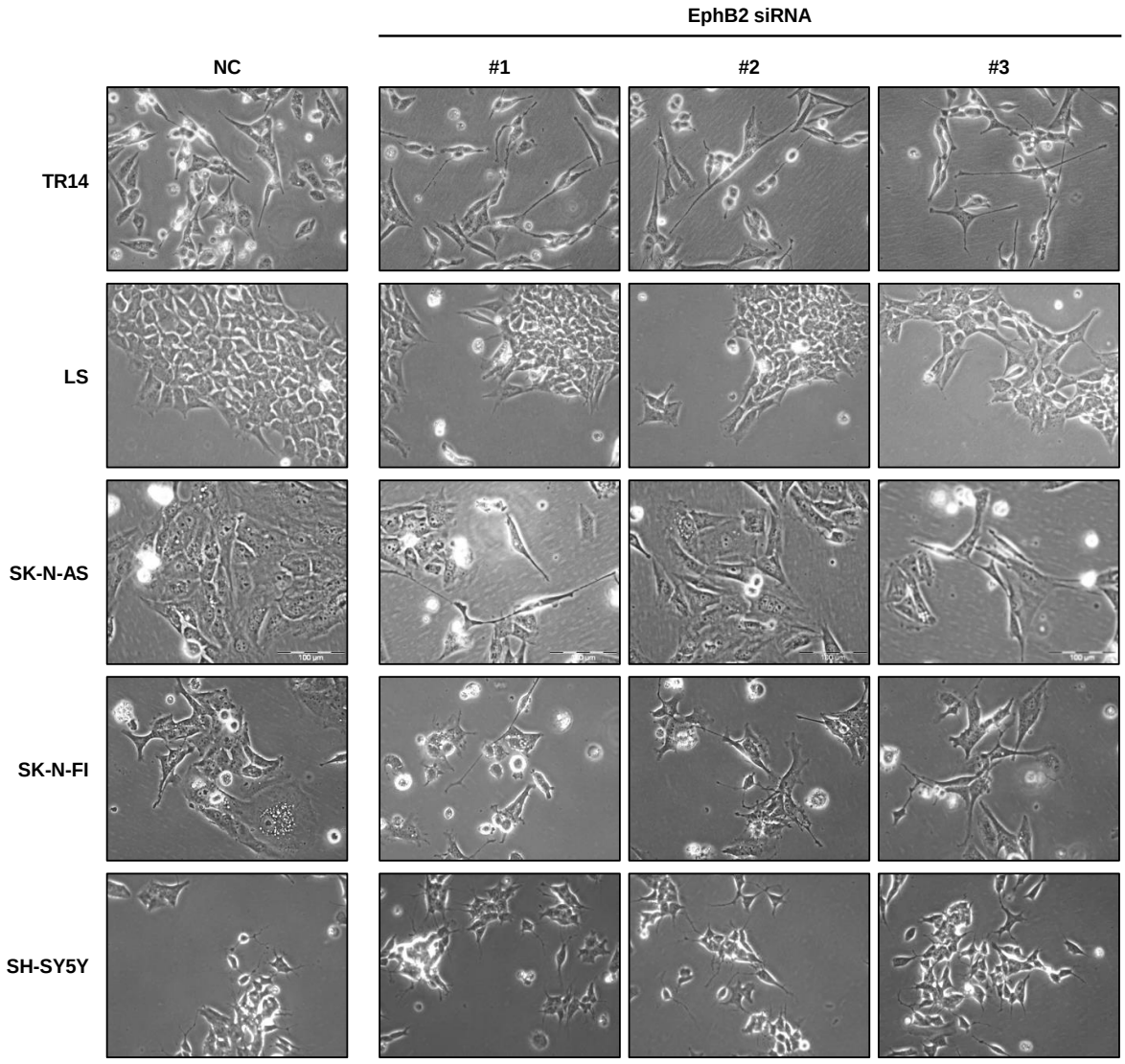

Fig. 3.19: EphB2 knock-down induces morphological changes in most 1p non-deleted cell lines. EphB2 was knocked down in five 1p non-deleted cell lines with three different siRNAs. After 96 h the morphology of cells was assessed microscopically. All results are compared to a non-specific scrambled siRNA as negative control (NC), magnification x200.

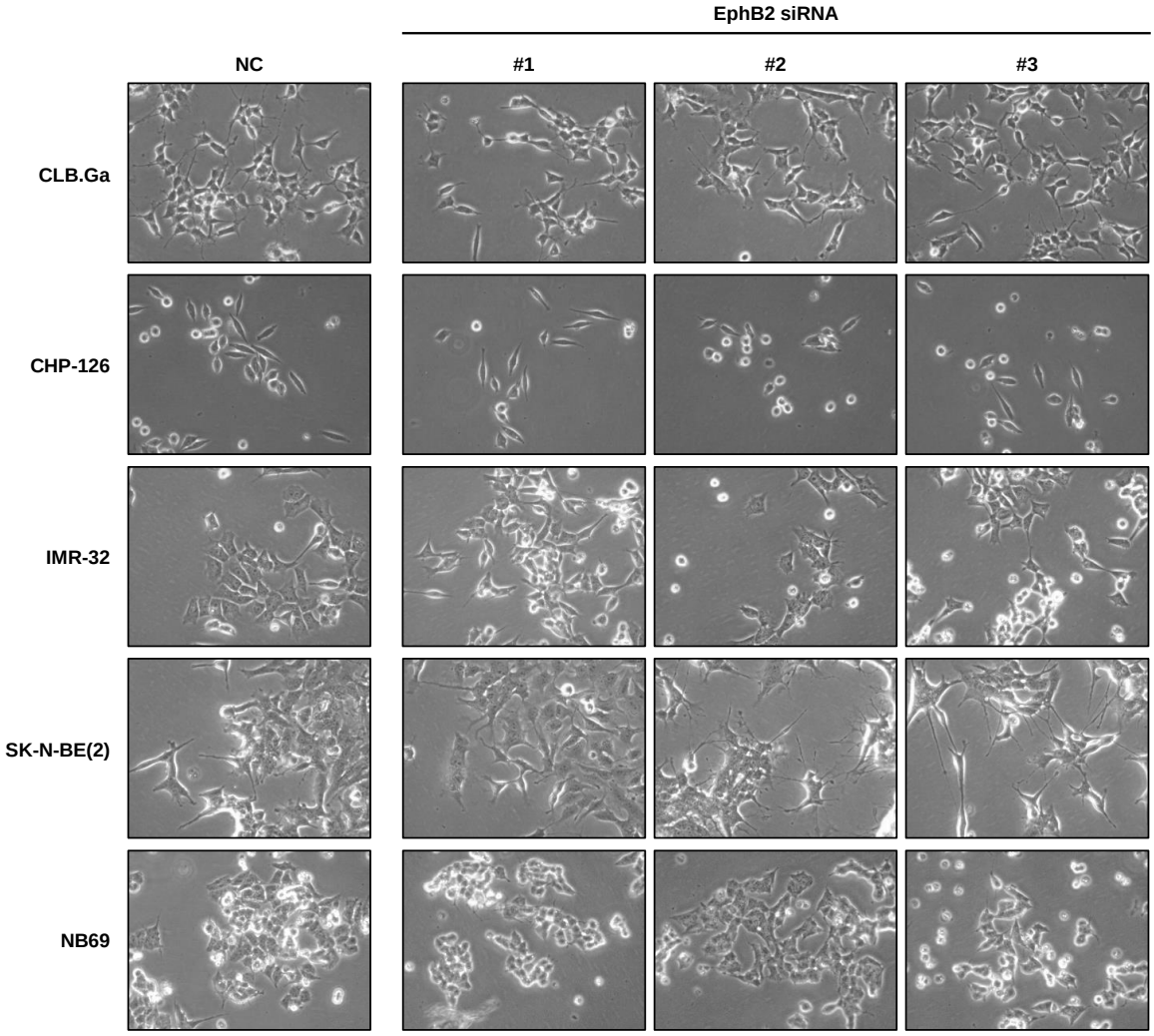

Fig. 3.20: EphB2 knock-down has no influence on morphology on most 1p-deleted cell lines.
EphB2 was knocked down in five 1p-deleted cell lines with three different siRNAs. After 96 h the morphology of cells was assessed microscopically. All results are compared to a non-specific scrambled siRNA as negative control (NC), magnification x200.

3.4.2.5 Characterization of 1p-deleted neuroblastoma cell lines after EphB2 knock-down

For all validation experiments of 1p-deleted cell lines, IMR-32 has been selected.

3.4.2.5.1 EphB2 knock-down induces cell cycle arrest in 1p-deleted cells

To analyze changes in cell cycle progression, we knocked down EphB2 with three different siRNAs and measured the DNA content after 96 hours via FACS. Compared to a non-targeting scrambled control the amount of cells in G_1/G_0 was higher after knock-down, which goes along with fewer cells in S and G_2 phase (Fig. 3.21)

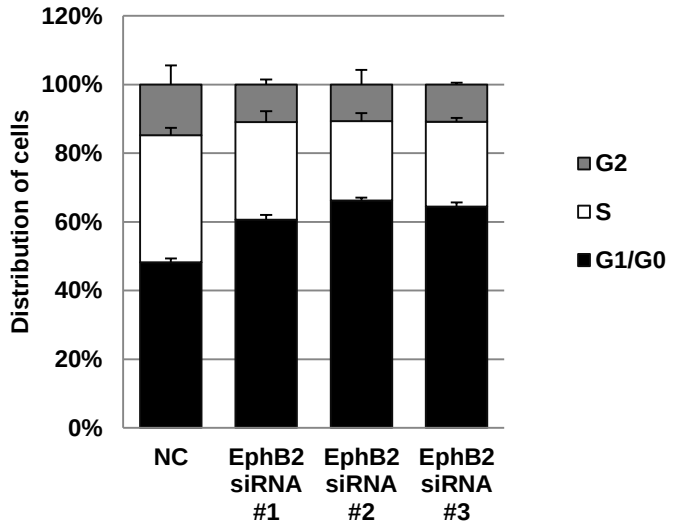

Fig. 3.21: EphB2 knock-down induces cell cycle arrest.
EphB2 was knocked down in IMR-32 (1p-deleted) and the amount of cells in G_1/G_0, S and G_2 phase was assessed via FACS after 96 h. All results were compared to a non-targeting siRNA as negative control (NC), on exemplary result out of three, +SD.

3.4.2.5.2 EphB2 knock-down induces cell death in 1p-deleted cells

In 3.4.2.1 we showed that knock-down of EphB2 via three different siRNAs led to reduced cell confluency in the 1p-deleted cell line IMR-32. Additionally, we noticed that this effect was accompanied by an increase of the amount of floating cells in the medium. Here, we wanted to determine the concrete number of detached cells and to analyze if these are dead or alive. This was addressed by PI staining and FACS analysis. Compared to cells treated with a non-targeting scrambled siRNA as negative control the amount of floating cells increased after EphB2 knock-down and in all cases the live to dead ratio was exactly 1:3 (Fig. 3.22 A).

To assess if the cells have the ability to regrowth, we reseeded 50,000 floating cells 96 hours after EphB2 knock-down. After ten days incubation the cells were stained with Giemsa and the number of colonies was estimated. Compared to the scrambled siRNA negative control, the amount of colonies regrown from floating cells is for all three siRNAs lower (Fig. 3.22 B). This indicates that a high proportion of the living EphB2 knock-down survivors died in a longer time manner.

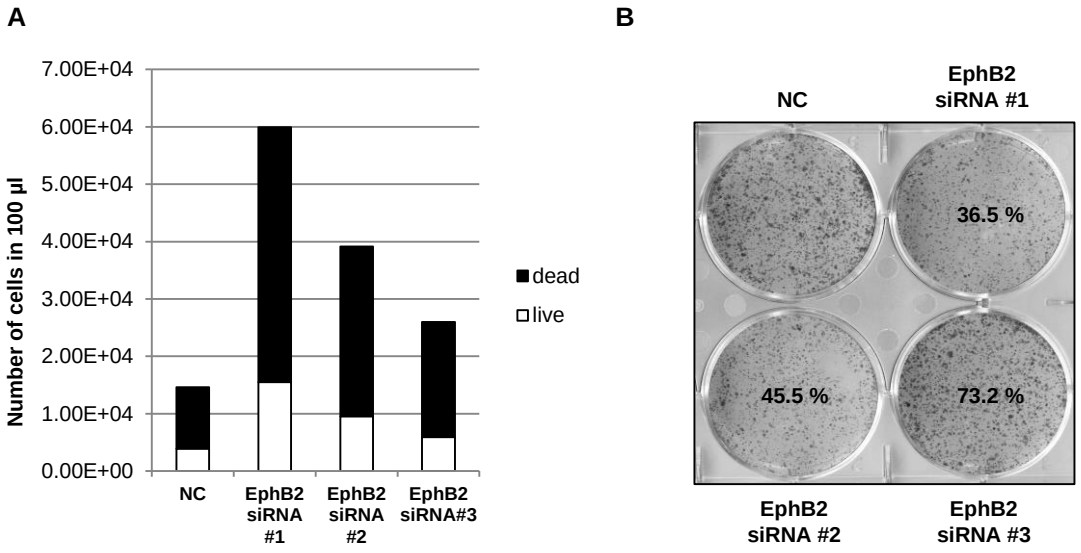

Fig. 3.22: EphB2 knock-down increases the number of floating dead cells and reduces the regrowth ability.

EphB2 was knocked down in the 1p-deleted cell line IMR-32 and after 96 h the number of detached cells estimated, the amount of living and dead was determined via PI staining and FACS analysis (A). Then, 50,000 cells from the same treatment were reseeded and after ten days the number of regrown colonies was count. The results are normalized to a non-targeting scramble siRNA as negative control (B). One exemplary result, NC: negative control.

3.4.2.5.3 Cell death of 1p-deleted cells after EphB2 knock-down cannot be prevented by cell death inhibitors

We showed previously that a high proportion 1p-deleted IMR-32 cells died after EphB2 knock-down (3.4.2.5.2). Here, we aimed at investigating what kind of cell death occurred in the cells. We treated the cells with three different siRNAs against EphB2 in presence or absence of four different cell death inhibitors or DMSO as control. Before, a killing curve of each inhibitor was assessed in titration experiments and the highest possible non-toxic concentration was used (data not shown). The following inhibitors were applied: Z-VAD-FMK (apoptosis inhibitor, 30 µM), Necrostatin-1 (necroptosis inhibitor, 20 µM), Ferrostatin-1 (ferroptosis inhibitor, 5 µM) and Bafilomycin-A1 (autophagy inhibitor, 2.5 nM). After 96 hours, the viability of cells was assessed via CTB assay. However, none of these inhibitors was able to prevent cells from death after EphB2 knock-down (Fig. 3.23).

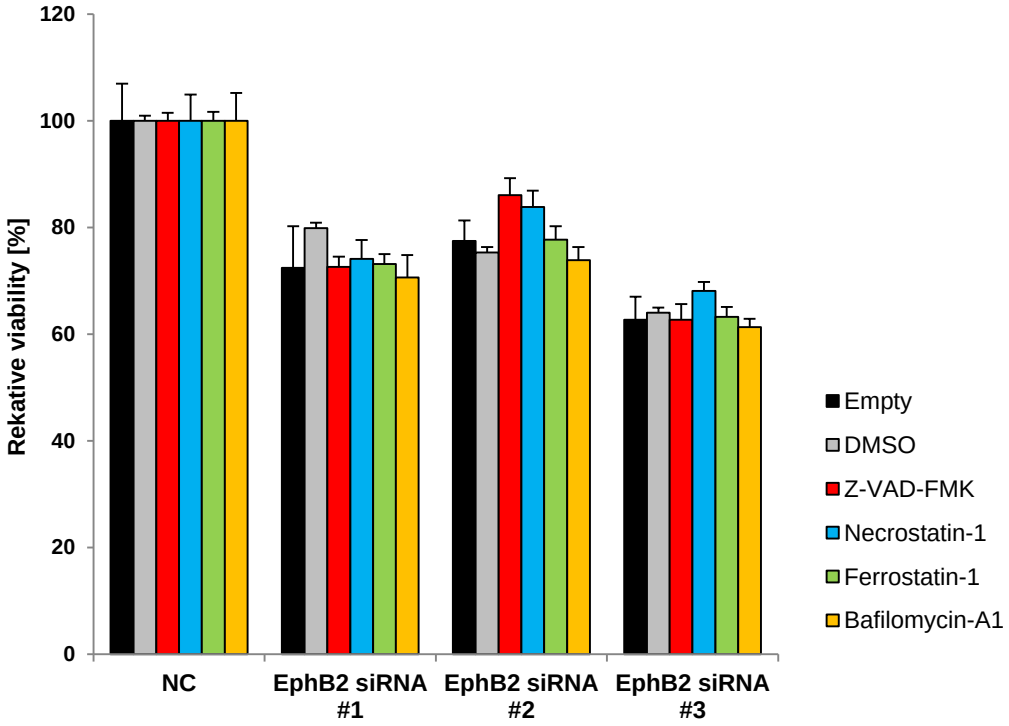

Fig. 3.23: Cell death upon EphB2 knock-down cannot be prevented by cell death inhibitors in 1p-deleted cells.

In the 1p-deleted cell line IMR-32 EphB2 was knocked down with three different siRNAs and a non-targeting scrambled siRNA as negative control (NC) in the presence/absence of Z-VAD-FMK [30 µM], Necrostatin-1 [20 µM], Ferrostatin-1 [5 µM] and Bafilomycin-A1 [2.5 nM]. Untreated cells and DMSO served as negative control. After 96 h, the viability was assessed with CTB assay. One exemplary experiment performed in triplicates, + SD.

3.4.2.5.4 RNA sequencing of 1p-deleted cells reveals differentially expressed genes after EphB2 knock-down

In previous experiments we could show that EphB2 knock-down induced cells death in the 1p-deleted cell line IMR-32 (3.4.2.5.2). Although most cells died after siRNA treatment, a small proportion of cells remained alive. Here, we wanted to investigate which processes mediate this resistance. For this, we performed RNA sequencing of the cells 96 hours after EphB2 knock-down via three different siRNAs and compared the results to untreated cells and cells treated with a non-targeting scrambled negative control (both used as negative control as differentially expression of genes in scrambled-treated cells was not seen). The expression of each condition was estimated and the fold change in each group (control, knock-down) was calculated. After EphB2 knock-down 47 genes were upregulated (fold change >1.5) whereas only 8 genes were downregulated (fold change <-1.5, Tab. S3) indicating that the knock-down has a generally repressive effect on gene expression. However, GO term analysis did not reveal any results. Among the

differentially expressed genes after EphB2 knock-down some neuron-related genes were detected and the c-MET activator HGF (Tab. 3.11). Validation of exemplary genes (*HGF*, *EPHB2*, *LRRC4B*, *SRGAP3* and *PRAME)* has been performed via RT-PCR and compared to the RNA sequencing fold changes (Fig. 3.24).

Tab. 3.11: Differentially expressed genes in IMR-32 after EphB2 knock-down.

Gene	Fold change	Further explanation
HGF	6.19	c-MET activator
LRRC4B	5.19	synaptic formation
NAV2-AS2	2.83	inhibits cellular growth and differentiation
NAV2-AS3	2.56	inhibits cellular growth and differentiation
GDNF	2.53	neurotrophic factor
PCDHA6	1.95	neuronal maintenance
IFIT3	1.87	cell cycle arrest
PSAT1	1.83	associated with schizophrenia
SRGAP3	1.70	neuronal signaling
PRAME	-2.64	preventer of differentiation

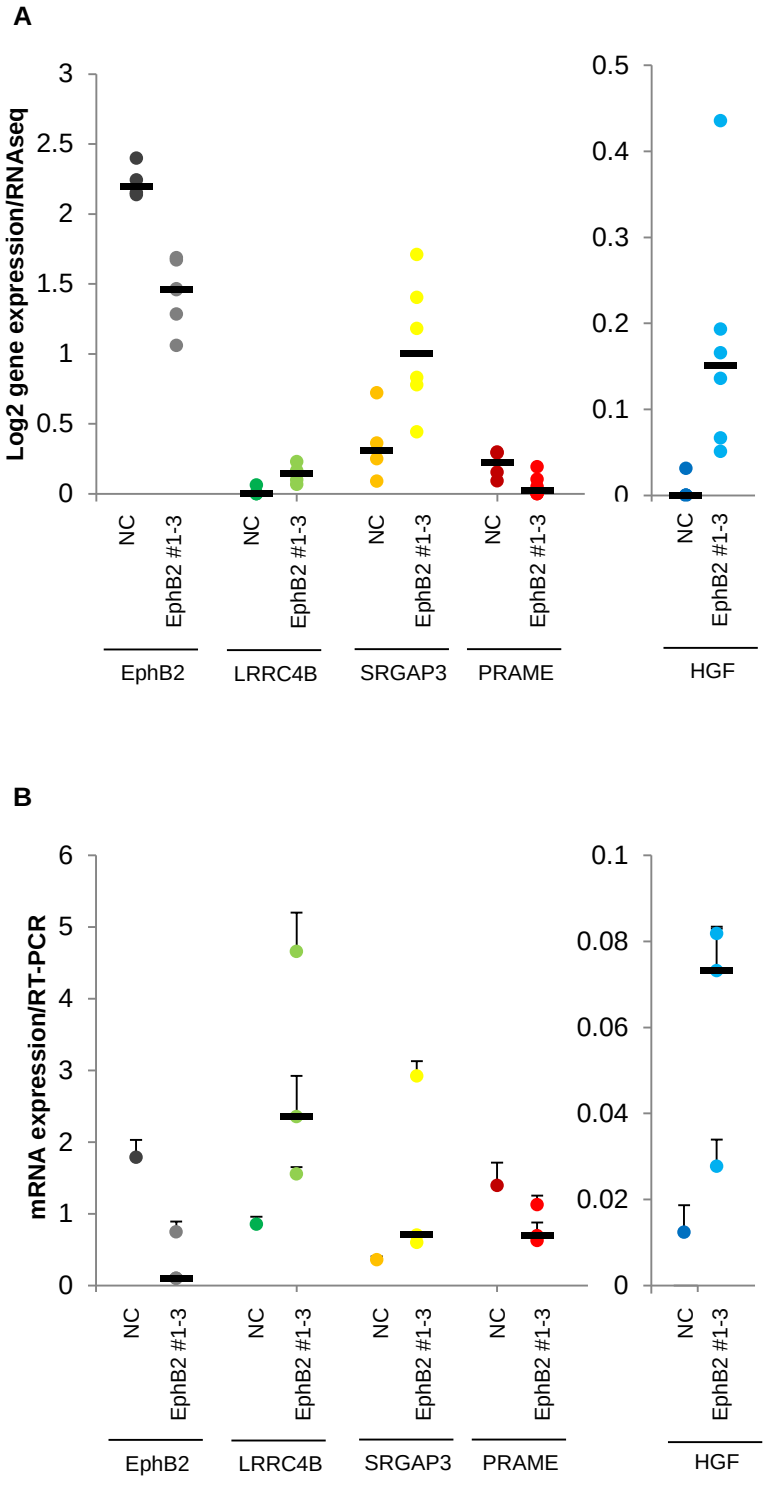

Fig. 3.24: Gene expression after EphB2 knock-down in IMR-32.

Exemplary differentially expressed genes derived from RNA sequencing data (A). Each siRNA has been performed in duplicates and compared to two untreated and two scrambled-treated approaches as negative control. Validation of these genes via RT-PCR, each point represents the mean of three results of one siRNA against EphB2 or scrambled, +SD, one exemplary result shown of at least three (B). NC = negative control, the black bar indicates the median.

3.4.2.5.5 EphB2 knock-down activates MAPK and Akt signaling pathways in 1p-deleted neuroblastoma cells

We aimed at validating the elevated HGF expression levels upon EphB2 knock-down on protein level. For this, we performed western blot analysis to measure the intracellular HGF amount and ELISA assay for extracellular levels in IMR-32. Intracellular HGF expression did not change after EphB2 knock-down. Extracellular levels of HGF were zero, both for cells treated with siRNA against EphB2 and the scrambled control. As the calculation of the protein concentration is based on a logarithmic standard curve which does not allow dealing with “0”, ELISA results are not shown here.

HGF is ligand of the c-Met receptor which activates MAPK and Akt signaling (Organ and Tsao 2011). Although there is a discrepancy between HGF RNA and protein level, we did not want to exclude the possibility of HGF-mediated c-MET activation. For this, we assessed possible activation of MAPK and Akt signaling by measuring phosphorylated p44 and p42 MAPK and phosphorylated Akt levels after EphB2 knock-down. An increase of phosphorylated p44/p42 MAPK and Akt was shown after EphB2 knock-down (Fig. 3.25). To exclude any impact of EphB2 knock-down on MAPK and Akt signaling in 1p non-deleted cell lines we performed the same experiment in TR14. We confirmed that levels of phosphorylated MAPK and Akt do not change after knock-down (Fig. S 2).

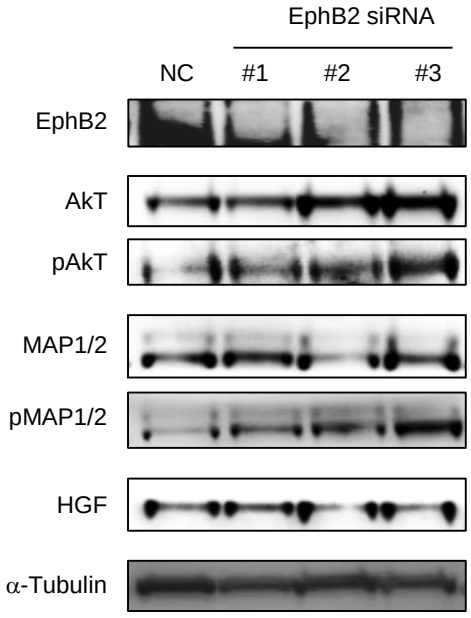

Fig. 3.25: EphB2 knock-down activates MAPK and Akt signaling.
After the 1p-deleted cell line IMR-32 was treated with three different siRNAs against EphB2, protein levels of HGF, MAPK, Akt and their phosphorylated active forms were assessed by western blot analysis. All results were compared to a non-targeting scrambled siRNA as negative control (NC).

3.4.2.5.6 MAPK inhibition in combination with EphB2 knock-down has little impact on cell confluency in 1p-deleted neuroblastoma cells

In 3.4.2.5.5 we showed that EphB2 knock-down induces MAPK activation in the 1p-deleted cell line IMR-32. Here, we wanted to test if MAPK inhibition enhances the effect of EphB2 downregulation. We knocked down EphB2 with three different siRNAs in the presence and absence of FR180204, a selective MAPK inhibitor and assessed cell confluency after 0, 6, 12, 24, 36, 48 and 72 hours. FR180204 reduced the amount of cells by ~ 5% for siRNA #1 and #2 but had no effect in addition to siRNA #3. To exclude an effect on 1p non-deleted cell lines the same experiments was performed in TR14 cells (Fig. S 3).

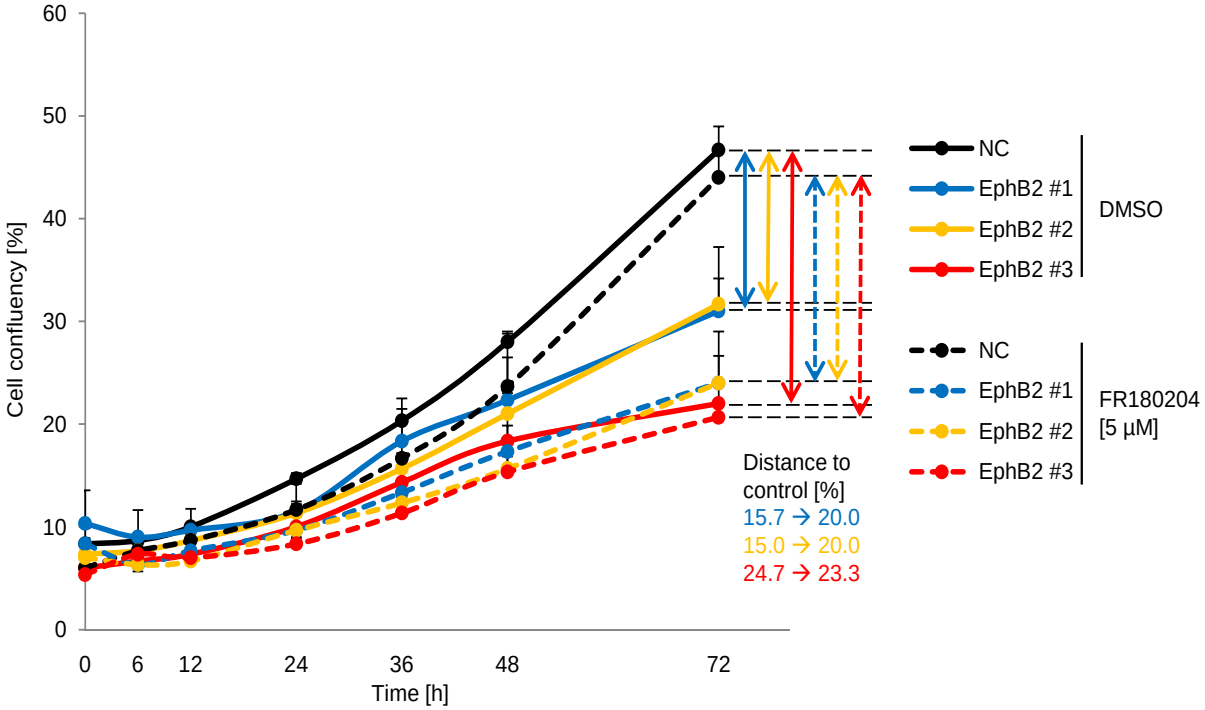

Fig. 3.26: EphB2 knock-down in combination with MAKP inhibition has little impact on cell confluency.

The 1p-deleted cell line IMR-32 was treated with three different siRNAs against EphB2 in combination with the selective MAPK inhibitor FR180204 [5 µM]. All results are compared to cells treated with DMSO, NC: negative control/non-targeting scrambled siRNA. The cell confluency was assessed after 0, 6, 12, 24, 36, 48 and 72 h. One exemplary result in triplicates, +SD.

3.4.2.5.7 EphB2 cDNA overexpression rescues 1p-deleted neuroblastoma cell lines from cell death induced by EphB2 siRNA knock-down

We hypothesized that ectopic expression of EphB2 in hemizygously deleted cells may rescue these from death upon siRNA treatment. For this, we transfected the 1p-deleted

cell line IMR32-6TR (expressing tetracycline/doxycycline-inducible repressor protein 6TR) with an inducible vector (pEXP30-EphB2) for EphB2 cDNA expression. The overexpression of EphB2 was confirmed by western blot (Fig. 3.27 A).

We treated the stable cell line with three different siRNAs against EphB2 and a non-targeting scrambled control siRNA in the absence (EphB2 cDNA Off) and presence of doxycycline (EphB2 cDNA On). After 96 hours cell confluency was assessed.

In all our experiments we could show that overexpression of EphB2 had minimal impact on the untreated and control siRNA-treated cells indicating that *EPHB2* has no tumor-promoting role in IMR-32. The knock-down-induced phenotype could be rescued by EphB2 overexpression which was significant (siRNA #3) or highly significant (siRNA #1 and #2; Fig. 3.27 B, C)

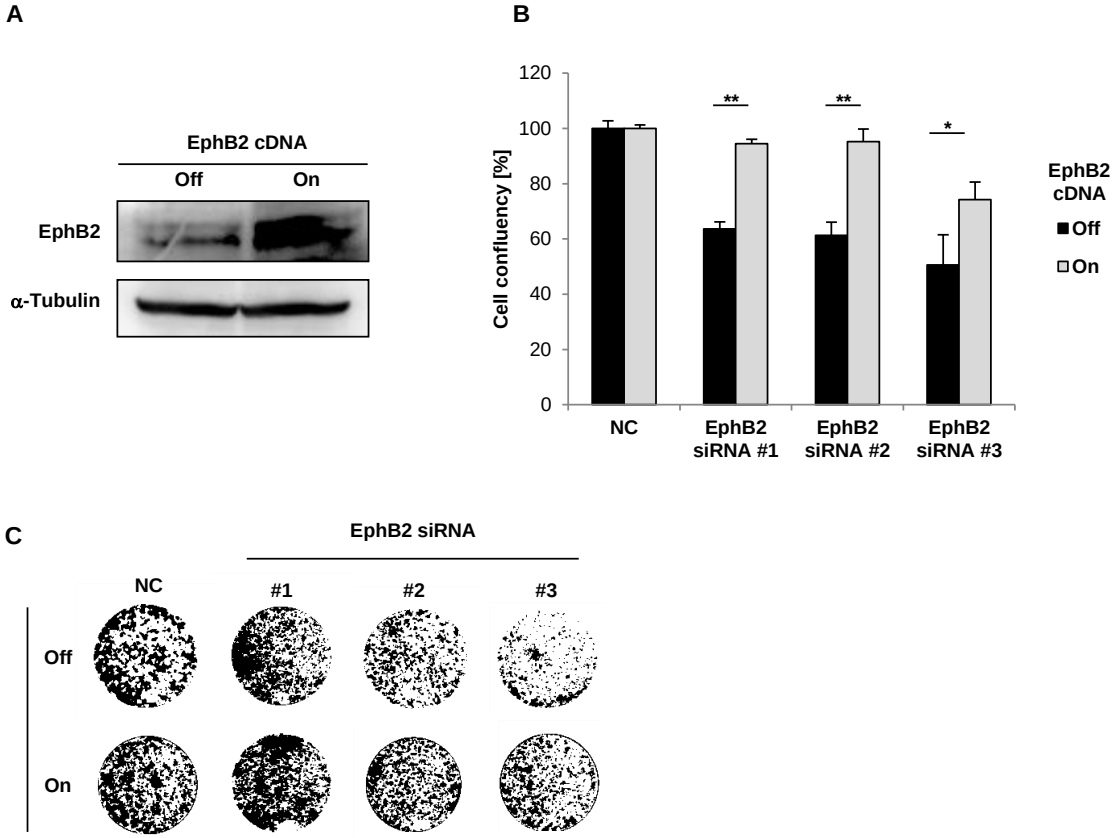

Fig. 3.27: EphB2 cDNA overexpression rescues 1p-deleted cells from cell death induced by EphB2 knock-down.

Doxycycline-inducible EphB2 overexpression clones were generated from the 1p-deleted cell line IMR32-6TR. The upregulation of EphB2 expression was confirmed by western blot (A). The cells were treated with three different siRNAs to knock-down EphB2 in the absence (EphB2 cDNA Off) and presence (EphB2 cDNA On) of doxycycline. After 96 h cells were stained with Giemsa to detect cell confluency (B, C). B and C show one representative result, all results were performed in triplicates, +SD, *p<0.05, **p<0.001.

3.4.2.5.8 shEphB2 knock-down reduces cell confluency in 1p-deleted neuroblastoma cell lines

To confirm the previously described effects of EphB2 knock-down on IMR-32 we generated stable cell lines with doxycycline-inducible shEphB2 expression. For this, we cloned the sequences of EphB2 siRNAs #2, #3 and a scrambled non-targeting sequence (Scrbl) as negative control into a pTER30+ vector and transfected these constructs into IMR32_6TR cells. However, we were not able to select single clones to raise monoclonal cell cultures and therefore all experiments were performed in polyclonal cell cultures. The knock-down efficiency was confirmed by western blot (Fig. 3.28 A) and RT-PCR (Fig. 3.28 B). The mRNA and protein levels were reduced after shEphB2 induction; however, the background leakiness of the vectors was already strong enough to generally induce level reduction.

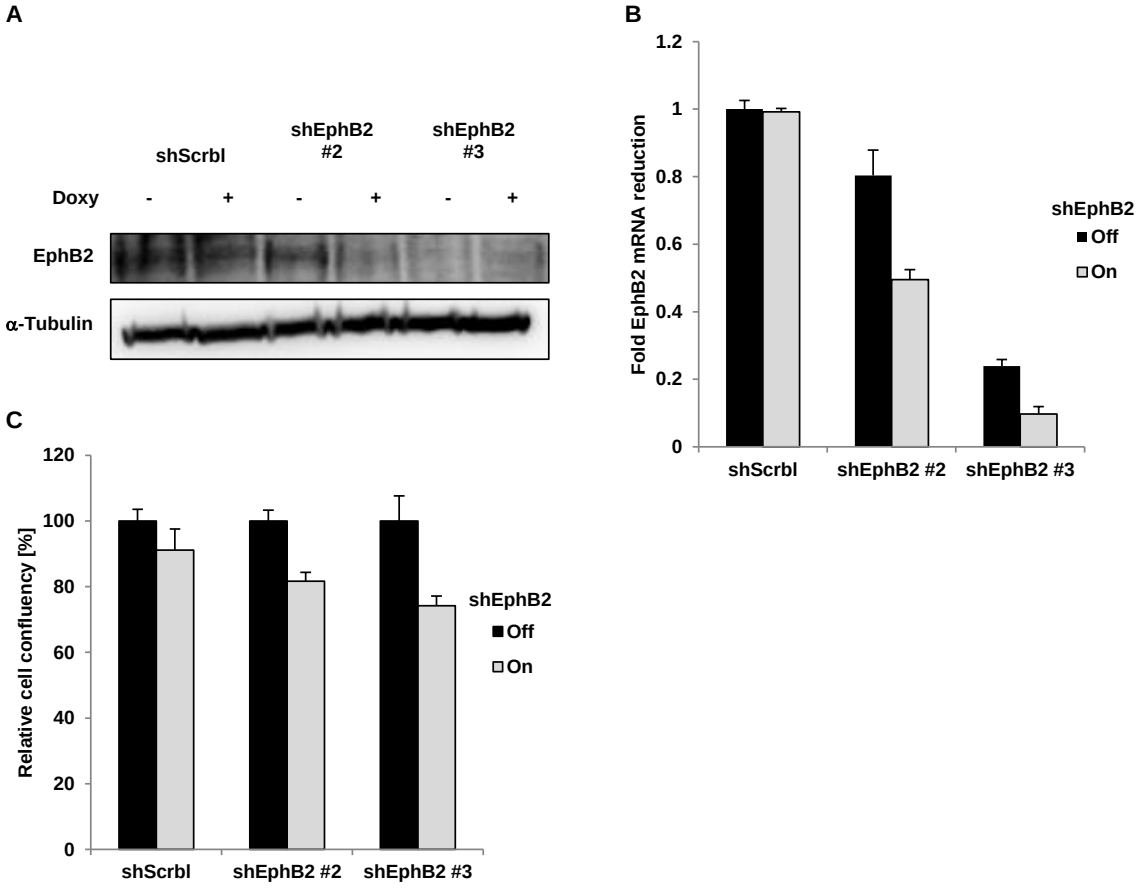

Fig. 3.28: shEphB2 overexpression reduces cell confluency in 1p-deleted cell lines.
Doxycycline-inducible shEphB2 overexpression clones were generated from the 1p-deleted cell line IMR32_6TR. The knock-down of EphB2 was confirmed by western blot (A) and RT-PCR (B) in IMR32_shEphB2 #2 and IMR32_shEphB2 #3 cells and compared to IMR32_shScrbl cells. One exemplary result performed in triplicates, +SD (B). Cell confluency was assessed 96 h after doxycycline induction with Giemsa staining (C). One representative experiment is shown; all results are in triplicates, +SD.

To assess the impact of shEphB2 on cell confluency, the cells were seeded in the presence or absence of doxycycline and after 96 stained with Giemsa. As the cell line clones behave differentially in cell culture it was not possible to seed the same amounts of cells. For this reason, we cannot compare all conditions with IMR32_shScrbl which would be necessary to determine the impact of the vector leakiness on cell survival. Here, we compared each shEphB2 On situation with the Off condition within one cell line. In IMR32_shpEphB2 #2 and IMR32_shEphB2 #3 we showed that doxycycline-induced shEphB2 expression reduced cell confluency by ~20% compared to shEphB2 Off (Fig. 3.28 C). In general, the shEphB2-expressing clones were weak in viability and showed a high amount of dead cells in the culture medium compared to their shScrbl expressing counterparts. These results indicate that the general EphB2 reduction is in the cell line clones strong and impairs cell survival. Induced shEphB2 expression further reduces the mRNA and protein levels but further impact on cell confluency is little.

3.4.2.5.9 shEphB2 induces cell cycle arrest in stable 1p-deleted neuroblastoma cell clones

The stable cell line clones IMR32_shEphB2 #2, IMR32_shEphB2 #3 and IMR32_shScrbl were seeded in the presence or absence of doxycycline. After 96 hours the cell cycle status was assessed by DAPI staining followed by FACS analysis. Doxycycline-induced shEphB2 expression induced G_2 arrest in IMR32_shEphB2 #3. In IMR32_shEphB2 #2 the presence of doxycycline had no impact on the phenotype; however, due to background leakiness of the pTER30+ vector, the distribution of cells in G_1/G_0 was in general larger compared to IMR32_shScrbl cells (Fig. 3.29).

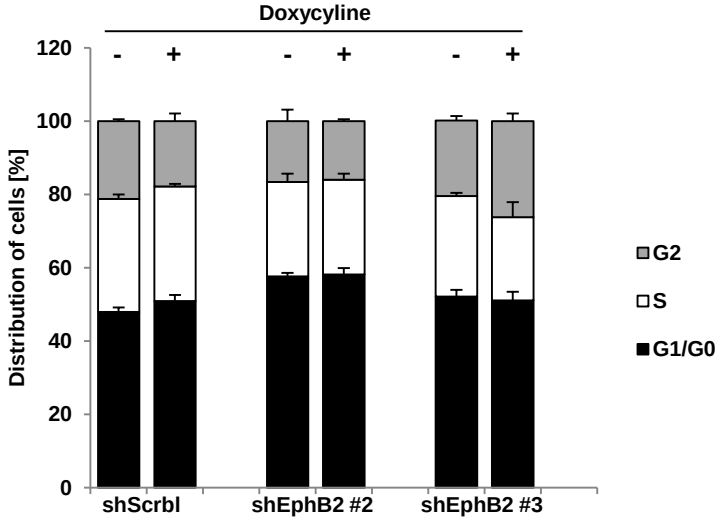

Fig. 3.29 IMR32_shEphB2 cell line clones show cell cycle arrest.

The 1p-deleted stable cell line clones IMR32_shEphB2 #2 and IMR32_shEphB2 #3 were treated with doxycycline and cell cycle phases were assessed after 96 h through DAPI staining and FACS analysis. The results were compared to IMR32_shScrbl cells expressing a non-targeting scrambled shRNA. The mean of three independent experiments is shown, + SD.

3.4.2.5.10 RNA sequencing of 1p-deleted cells with inducible shEphB2 expression reveals differentially expressed genes

To investigate which genes get differentially expressed upon shEphB2 knock-down, we performed RNA sequencing in the stable cell lines IMR32_shScrbl, IMR32_shEphB2 #2 and IMR32_shEphB2 #3.

First, we checked the different gene expression in absence (shEphB2 Off) vs presence (shEphB2 On) of doxycycline after 96 hours in IMR32_shEphB2 #2 and #3. However, we could not detect any differentially expressed genes between On and Off condition including *EPHB2* which is likely due to the already described background leakiness of the vectors (Fig. 3.30 A, 3.4.2.5.8). For this reason, further comparison of shEphB2 On was done vs IMR32_shScrbl On and Off, both used as negative control as differentially expression of genes upon shScrbl induction was not seen. The total number of significantly differentially expressed genes in shEphB2 On conditions was 127 with 55 being upregulated (fold change >1.5) and 72 being downregulated (fold change <-1.5, Tab. S4, Tab. S5). A GO term analysis revealed that genes required for neuronal development and morphogenesis were preferentially upregulated (Tab. 3.12).

Tab. 3.12: GO terms enriched after shEphB2 knock-down.

Enriched GO term (DAVID)	No of genes	%	Adjusted p value
neuron projection morphogenesis	11	18.03	1.75E-02
synapse organization	7	11.48	1.97E-02
positive regulation of neuron projection development	7	11.48	2.06E-02
positive regulation of nervous system development	9	14.75	2.20E-02
axonogenesis	9	14.75	2.21E-02
axon development	9	14.75	2.33E-02
positive regulation of multicellular organismal process	15	24.59	2.39E-02
neuron projection guidance	7	11.48	2.60E-02
cell part morphogenesis	12	19.67	2.70E-02
cell projection morphogenesis	12	19.67	2.87E-02
axon guidance	7	11.48	2.95E-02
cell morphogenesis involved in neuron differentiation	10	16.39	2.95E-02
neuron projection development	11	18.03	4.18E-02

Note: p values are Benjamini-Hochberg adjusted as implemented in the DAVID platform

GO: gene ontology, DAVID: database for annotation, visualization and integrated discovery tool.

As we hypothesized that the gene expression in presence and absence of doxycycline should be similar due to the previously described background leakiness in IMR32_shEphB2 #2 and IMR32_shEphB2 #3, we included the analysis of shEphB2 Off

conditions to verify our data. Indeed, we could show that the vast majority of differentially expressed genes compared to shScrbl-expressing cell lines was the same (Tab. S4). The total number of differentially expressed genes in shEphB2 Off (but EphB2 low) was 139, of which 104 overlapped with the 127 genes identified in shEphB2 On with similar fold changes in both conditions (Fig. 3.30 B, Tab. S5). This indicates that the background leakiness is enough to have significant impact on gene expression.

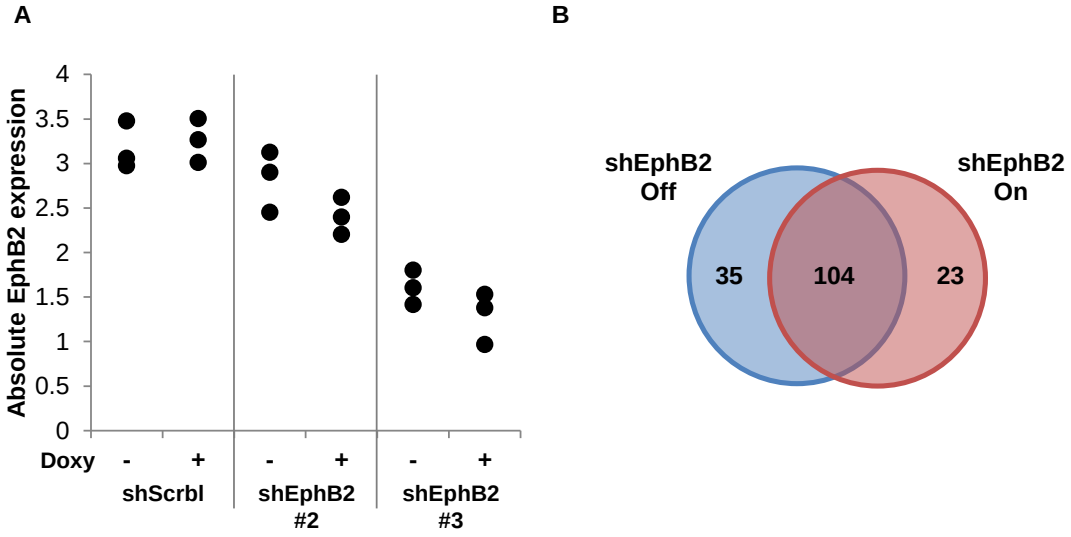

Fig. 3.30: Doxycycline-induced shEphB2 knock-down has little impact on gene expression.
The cell lines IMR32_shScrbl, IMR32_shEphB2 #2 and IMR32_shEphB2 #3 were treated with doxycycline and the gene expression was analyzed. Absolute gene expression of EphB2 in absence or presence of doxycycline (A). Venn diagram of differentially expressed genes in shEphB2 Off and shEphB2 On conditions compared shScrbl On/Off (B).

3.4.2.5.11 shEphB2 expression induces MAPK and Akt signaling in 1p-deleted neuroblastoma cell lines

In 3.4.2.5.5 we could show that knock-down of EphB2 induces MAPK and Akt signaling in the 1p-deleted cell line IMR-32. To analyze if these mechanisms also play a role in the stable cell lines IMR32_shEphB2 #2 and IMR32_shEphB2 #3 we performed western blot analysis and assessed phosphorylated MAPK and Akt levels. In both shEphB2 expressing cell lines the pMAPK and pAkt amounts where higher than in the control cell line IMR32_shScrbl (Fig. 3.31). The proteins were equally expressed in absence or presence of doxycycline indicating that the effects induced by the background leakiness of the vectors are strong enough that survival mechanisms have to get activated.

The HGF protein level remained in all conditions the same. Also we were not able to generate consistent results on an mRNA level which indicates that an alternative activation of MAPK and Akt signaling may play a role here.

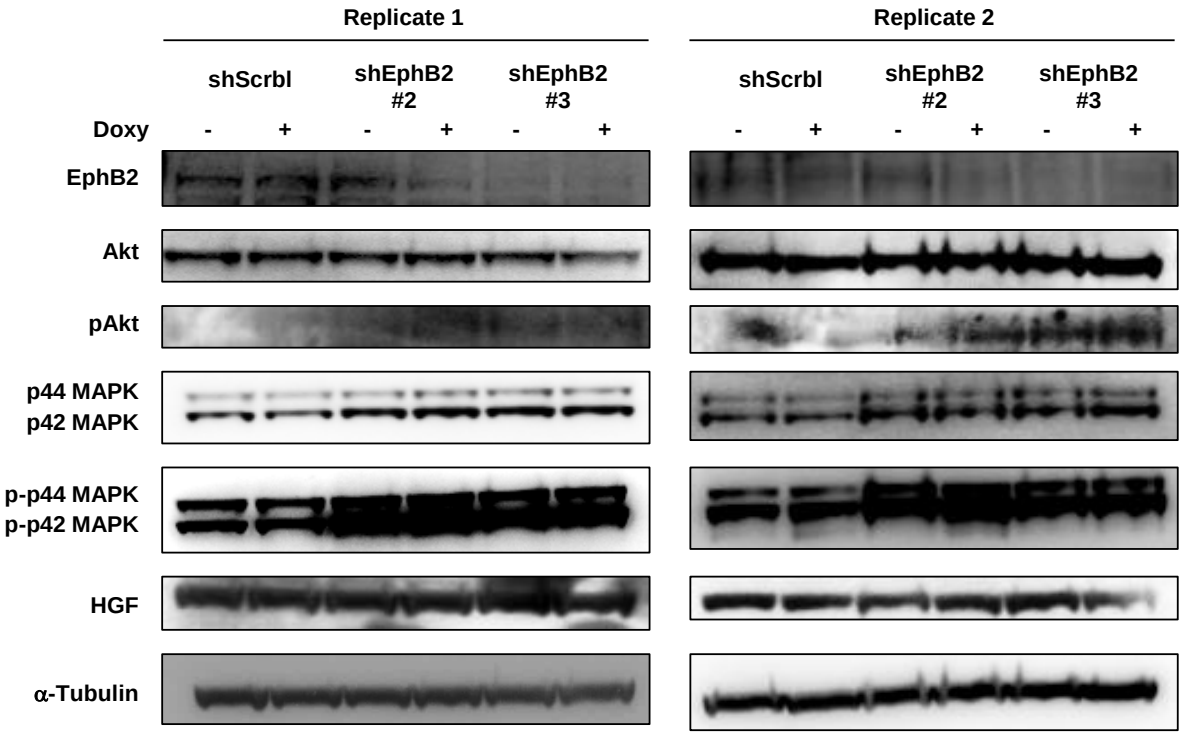

Fig. 3.31: Stable cell line clones expressing shEphB2 show induced levels of phosphorylated MAPK and Akt.

Western blot analysis in the stable cell lines IMR32_shEphB2 #2, IMR32_shEphB2 #3 and IMR32_shScrbl in the presence and absence of doxycycline. Two exemplary results from totally five, Scrbl: scrambled, p: phosphorylated.

3.4.2.6 Characterization of 1p non-deleted neuroblastoma cells after EphB2 knock-down

For all validation experiments of 1p non-deleted cell lines, TR14 has been selected.

3.4.2.6.1 EphB2 knock-down induces cell cycle arrest in 1p non-deleted cells

To analyze changes in cell cycle progression, we knocked down EphB2 with three different siRNAs and measured the DNA content after 96 hours via FACS. The distribution of cells in G_1/G_0 was higher after treatment with all three siRNAs compared to the negative control. Also the amount of cells in G_2 increased leading to a reduction of cells in S phase (Fig. 3.32).

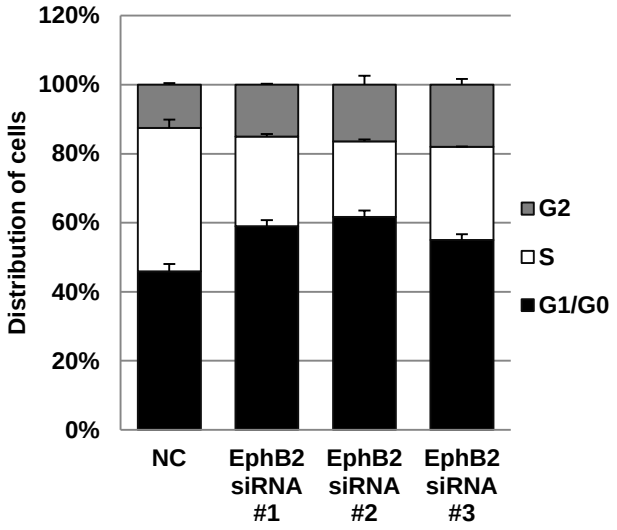

Fig. 3.32: EphB2 knock-down induces cell cycle arrest.
EphB2 was knocked down in TR14 (1p non-deleted) and after 96 h the amount of cells in G_1/G_0, S and G_2 phase was assessed via FACS. All results were compared to a non-targeting siRNA as negative control (NC), one exemplary result out of three, +SD.

3.4.2.6.2 EphB2 knock-down induces upregulation of differentiation markers in 1p non-deleted neuroblastoma cell lines

As described in 3.4.2.6.1 cell cycle arrest was observed in G_1/G_0 phase in 1p non-deleted cell lines. The 1p non-deleted cell line TR14 did not die after siRNA knock-down but showed changes in morphology (3.4.2.1). Morphologic changes, especially fiber outgrowth, in combination with G_1/G_0 arrest are strong indicators of cell differentiation of neuroblastoma cell lines (Wainwright, et al. 2001).

To investigate if EphB2 siRNA knock-down induces differentiation in 1p non-deleted cell lines we assessed the mRNA levels of genes involved in differentiation after 6, 12, 24 and 48 hours. MAP2 and NEFL were not upregulated after EphB2 knock-down whereas there is tendency for TUBB3 mRNA upregulation (Fig. 3.33).

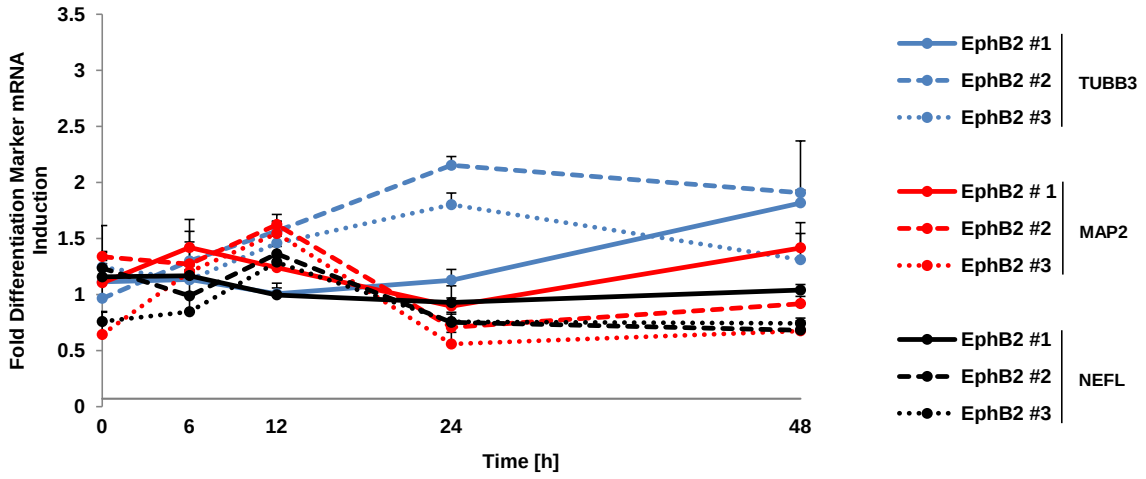

Fig. 3.33: EphB2 knock-induces upregulation of differentiation markers.
After EphB2 knock-down in TR14 cells the mRNA levels of TUBB3, MAP2 and NEFL have been analyzed after 6, 12, 24 and 48 h, all results are normalized to a non-targeting scrambled siRNA as negative control, results are performed in triplicates and the mean of three independent

3.4.2.6.3 EphB2 knock-down induces neuronal fiber outgrowth in 1p non-deleted neuroblastoma cell lines

TUBB3, also known as β-tubulin, is a protein uniquely expressed in neuronal cells and a main component of neurite fibers (Tischfield, et al. 2010). To confirm our findings in 3.4.2.6.2 and to investigate if the changes in morphology upon EphB2 knock-down are due to neurite outgrowth, we knocked down EphB2 with three different siRNAs and stained the cells after 96 hours with a fluorescence-labeled antibody against TUBB3. We could show that especially siRNA #2 and #3 inducd extended neurite fiber outgrowth in TR14 consisting of TUBB3 (Fig. 3.34)

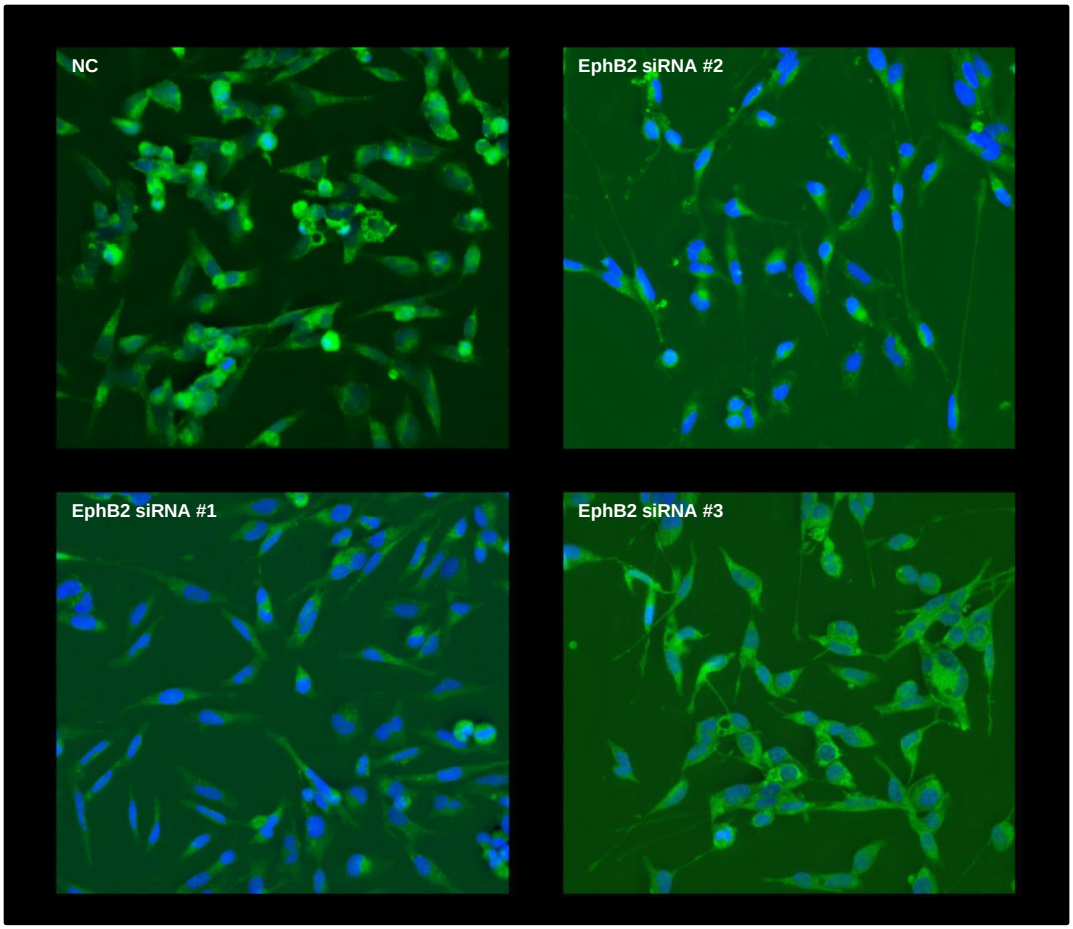

Fig. 3.34: EphB2 knock-down induces neurite outgrowth in 1p non-deleted cell lines.
In TR14 cells EphB2 was knocked down with three different siRNAs. After 96 h the cells were fixated and stained with a fluorescence labeled antibody against TUBB3, blue: DAPI, green: FITC/ TUBB3, magnification x200.

3.4.2.6.4 EphB2 knock-down does not induce senescence in 1p non-deleted neuroblastoma cell lines.

Morphologic changes in combination with G_1/G_0 have been reported as an indicator of senescence (Wainwright, et al. 2001). A characteristic of senescent cells is the secretion of β-galactosidase which could not be found in pre-senescent, quiescent or immortal cells (Dimri, et al. 1995).
We treated the 1p non-deleted cell line TR14 with three different siRNAs to knock-down EphB2. After 96 hours we added X-Gal to the cells which is a substrate of β-galactosidase. Cleavage of X-Gal results in blue dye which accumulates within the cells and can be assessed microscopically. However, we could not detect any significant changes in color compared to the non-coding siRNA negative control (Fig. 3.35).

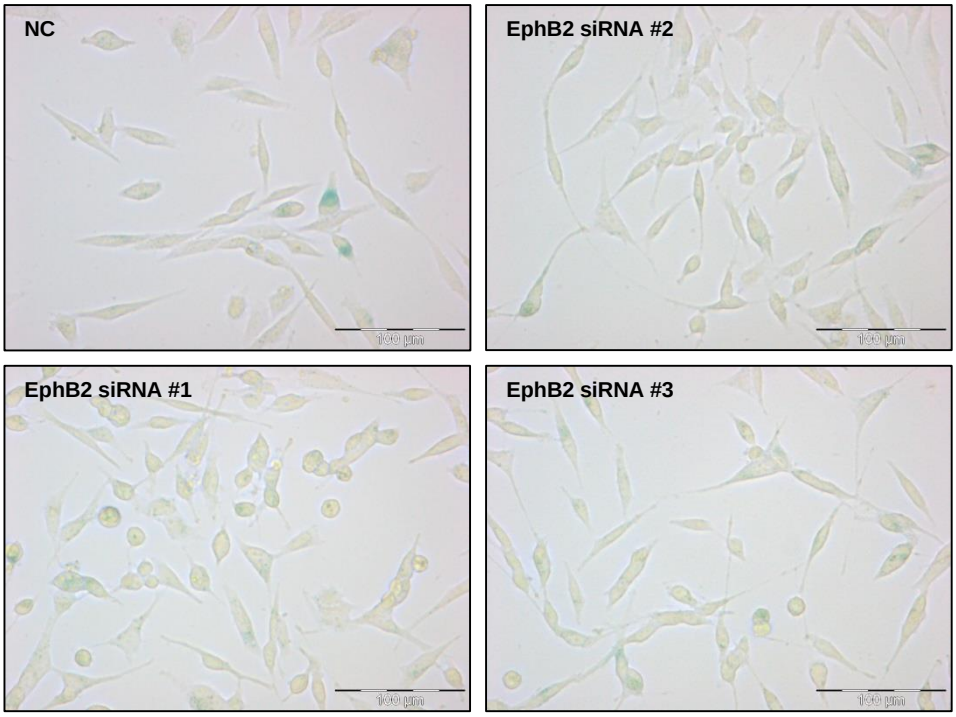

Fig. 3.35: EphB2 knock-down does not induce senescence in 1p non-deleted cells.
EphB2 was knocked down with three different siRNA in the 1p non-deleted cell line TR14. After 96 h a β-galactosidase assay was performed to detect senescence. All results are compared to a non-specific siRNA as negative control (NC), magnification x200.

3.4.2.6.5 EphB2 knock-down inhibits migration in 1p non-deleted neuroblastoma cell lines

EphB2 has been shown to be involved in cell migration in different cancer types (Farshchian, et al. 2015; Sikkema, et al. 2012; Wang, et al. 2012). To analyze if knock-down of EphB2 has an impact on 1p non-deleted neuroblastoma cell lines we performed migration assays with TR14. We seeded the cells in 24 well plates containing a silicone plug. After a confluency of 100% was achieved, the cells were treated with three different siRNAs against EphB2 and a non-targeting scrambled siRNA which served as negative control. After 24 hours the plug was removed remaining a standardized cell-free space. To assess how fast the cells enter the empty area, microscopic analysis was done after 0, 72, 144 and 160 hours. After 160 hours the exclusive zone was overgrown in the negative control whereas the cells treated with EphB2 siRNAs did not conquer the entire space (Fig. 3.36). These results indicate that EphB2 knock-down inhibits cell migration in 1p non-deleted cell lines.

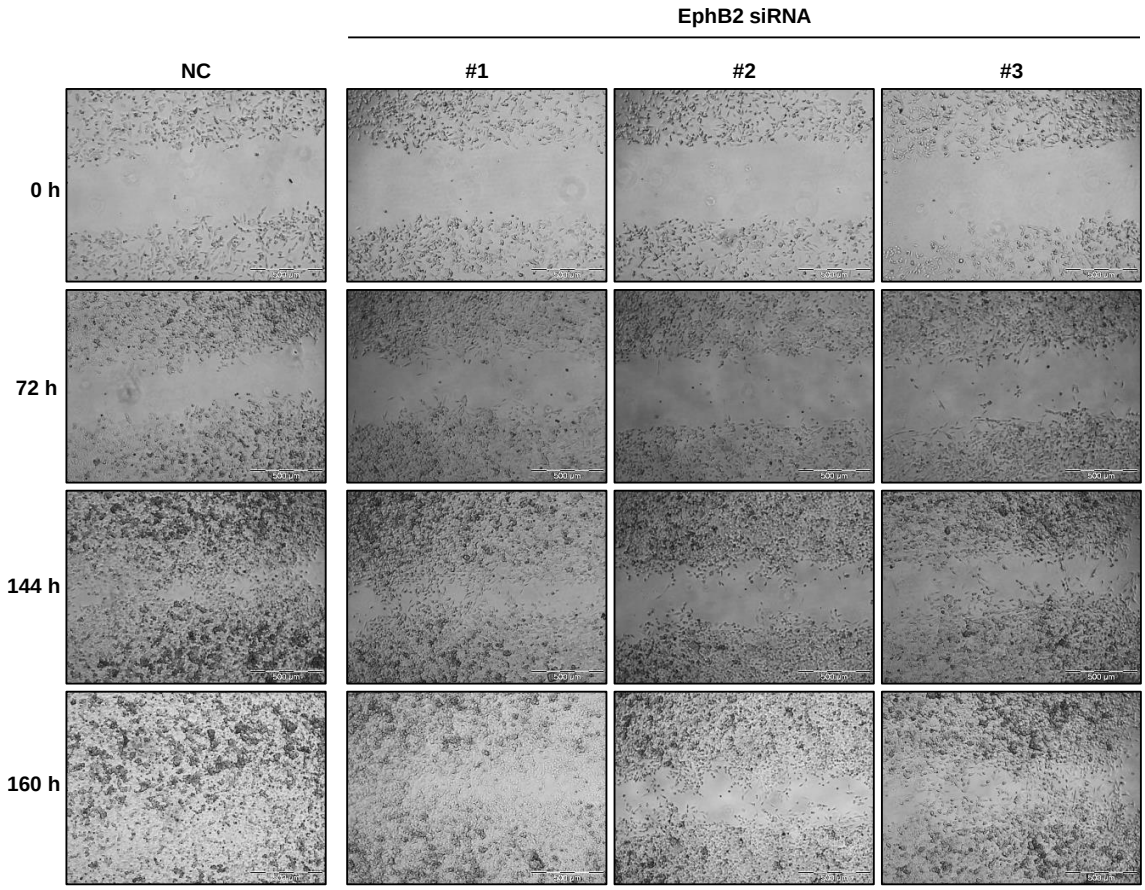

Fig. 3.36 EphB2 knock-down inhibits migration in 1p non-deleted cells.

The 1p non-deleted cell line TR14 was seeded in 24 well plates containing a silicone plug. After a cell confluency of 100% was achieved, the cells were treated with three siRNAs against EphB2 and a non-targeting scrambled siRNA as negative control (NC). After 24 h the plug was removed to leave a cell-free space. Overgrowing of the area was microscopically reported after 0, 72, 144 and 160 h. One exemplary result is shown, magnification: x20.

3.4.2.6.6 RNA sequencing of 1p non-deleted cells reveals differentially expressed genes after EphB2 knock-down

To assess differentially expressed genes in 1p non-deleted cell lines after EphB2 knock-down, we treated TR14 with three different siRNA and after 96 hours RNA sequencing was performed. The results of all three siRNAs were summarized and compared to scrambled-treated and untreated cells to calculate the fold change (both used as negative control as differentially expression of genes in scrambled-treated cells was not seen). Totally, 34 genes were differentially expressed whereas 20 were upregulated (fold change >1.5) and 14 downregulated (fold change <-1.5, Tab. S6). GO term analysis did not reveal any results (3.4.2.5.4).

We identified 8 genes that are involved in neuronal development and neuron protection (Tab. 3.13). These results indicate that general impact of EphB2 knock-down is lower than in 1p-deleted cell lines.

Tab. 3.13: Differentially expressed genes after EphB2 knock-down in TR14.

Gene	Fold change	Function
ADAMTS14	4.86	matrix protein for neurogenesis
TMEM178A	4.50	neuro-protective
PARK2	2.70	neuro-protective
RNF180	1.94	neuronal development
INSM1	1.80	neuronal differentiation
DAB1	1.64	neuronal development
AMER2	-2.24	neuronal development
ADAM21	-2.70	matrix protein for neurogenesis

4. Discussion

4.1 Do CYCLOPS genes play a role in neuroblastoma?

Cancer genomes are characterized by instability leading to the amplification of oncogenes or the deletion of tumor suppressor genes (TSGs). Often these alterations do not affect only the effector gene but also multiple surrounding genes. The loss of a TSG, which contributes to tumor initiation or progression is a “driving event”. Losses of neighboring genes that are irrelevant for tumor development are defined as “passenger events”. Elimination of TSGs is a result of selective pressure, the loss of the latter happens as collateral damage. Besides passenger genes do not contribute to the tumor itself, at least some of them are thought to be cell-essential and may be required for survival rendering hemizygously-deleted cells vulnerable to further impairment. These so-called CYCLOPS genes have been introduced firstly by Nijhawan et al. in 2012. They integrated data from copy number profiles and gene dependencies from 86 cancer lines and identified 56 CYCLOPS genes candidates. A more recent study expanded the cancer line set to 179 and identified 124 potential CYCLOPS genes. Additionally, they showed that the most enriched group of copy number-associated gene dependencies are CYCLOPS genes (Paolella, et al. 2017). However, both of the studies deal mainly with adult cancers and the role of CYCLOPS genes in neuroblastoma remains unclear. To address this issue in a pilot study, we analyzed previously assessed data from a genome-wide siRNA screen in a neuroblastoma cell line and RNA sequencing data from 573 neuroblastoma patients. We could show that genes with high dependency map preferentially to chromosome arm 1p and their expression correlates with the copy number status with hemizygously-deleted genes showing a reduced expression compared to non-deleted tumors. This information suggested that chromosome arm 1p is a promising region for the search of CYCLOPS genes in neuroblastoma.

4.2 Characterization of the 1p status in neuroblastoma cell lines

Before starting the study it was crucial to assess the 1p status in the neuroblastoma cell lines to be used as models. The copy number ratio of 1p and exact breaking points were estimated with WGS. More complex rearrangements as partial translocations or intrachromosomal insertions were detected via FISH analysis. After characterization of the 1p status in 34 neuroblastoma cell lines we selected 5 with 1p36 deletion (CHP-126, NB69, CLB.Ga, SK-N-BE(2) and IMR-32) and 5 1p non-deleted cell lines (TR14, LS, SK-N-AS, SK-N-FI, SH-SY5Y).

4.3 Candidate gene identification

In the siRNA CYCLOPS screen we identified 35 candidate genes whose knock-down reduced cell confluency in 1p-deleted but had no impact on 1p non-deleted cell lines. Interestingly, 6 of these genes were encoding for components of protein-modifying proteins: *MMEL1* (membrane metalloendopeptidase like 1), *FBXO44* (F-box protein 44), *FBXO6* (F-box protein 6), *DNAJC11* (DnaJ heat shock protein family (Hsp40) member C11), *HSPB7* (heat shock protein family B (small) member 7) and *USP48* (ubiquitin specific peptidase 48). This is in line with Nijhawan reporting that CYCLOPS candidates were enriched for protein-modifying proteins, namely spliceosomes, proteasomes and ribosomes (Nijhawan, et al. 2012). Next, we observed 13 genes required for cell cycle and cell growth to impair viability upon knock-down in both, 1p-deleted and 1p non-deleted cell lines. Examples are *CDK11B* (cyclin-dependent kinase 11A and 11B) and *CDC42* (cell division cycle 42). Furthermore, 16 neuron-related genes were identified that showed negative confluency scores after knock-down in all cell lines, e.g. the neuronal receptors *HTR6* and *HTR1D* (5-hydroxytryptamine receptors 6 and 1D) or *ATP13A2* (ATPase cation transporting 13A2), a transporter required for neuronal integrity. Even if 1p normal cells were not able to tolerate gene knock-down, 1p-deleted cells may have developed compensatory mechanisms to overcome the hemizygous loss, although further reduction could also not be compensated indicating that these genes play important roles in neuroblastoma but are not essential.

For candidate prioritization we took into account that one requirement a CYCLOPS gene has to fulfill is lower expression in deleted compared to non-deleted cells. After analyzing expression profiles of all candidates in primary tumors and in the selected cell lines we chose *AURKAIP1* (aurora kinase A interacting protein 1), *ICMT* (isoprenylcysteine carboxyl methyltransferase) and *SDF4* (stromal cell derived factor 4). Next we noticed, that the siRNA screen revealed all included genes belonging to the ephrin receptor family as CYCLOPS candidates, namely *EPHA2*, *EPHA8* and *EPHB2* (EPH receptor A2/A8/B2). Although their dependency scores were moderate they were selected due to their role for neuronal and embryonic development. Gene expression in primary tumors was for *EPHA2* and *EPHB2* lower in 1p-deleted than in 1p non-deleted cases, which fulfills the CYCLOPS requirements. However, the opposite was true for *EPHA8* and for this reason we did not include it in our validation pipeline.

4.4 Candidate gene validation

Prior to the candidate gene validation we set parameters which had to be fulfilled by a gene to be cosidered as a potential CYCLOPS gene (1.4.1.1). In particular, the impact of

gene knock-down had to be as weak as possible on 1p non-deleted cells ($1p^{norm}$ <15%), 1p-deleted cells should show a certain reduction in cell survival ($1p^{del}$ >25%) and a remarkable difference between these two values should be noticeable (distance >20).

The validation process was started with cell confluency and viability assays. We noticed that the outcome of cell growth/survival was often diverging depending on the assay platform, which can be explained with the different approaches of these methods. In contrast to cell confluency, which counts the actual number of cells, viability assays aim to address the metabolic activity. We observed that the total number of cells often did not correspond with their metabolism. Precisely, the more cells in a well the lower their metabolic activity which may be due to the lack of space and nutrition. To assess the direct survival effect of gene knock-down we refer in this discussion mainly to the cell confluency data.

4.4.1 Validation of *AURKAIP1*, *ICMT* and *SDF4*

The knock-down of AURKAIP1, ICMT and SDF4 efficiently reduced the number of 1p-deleted cells. However, the effect was also strong on 1p non-deleted cells. This indicates that 1p normal cells express a minimum amount of protein required for cell survival and no loss can be tolerated. In 1p-deleted cells alternative mechanisms may be activated to compensate the permanently reduced level but further knock-down also induces cell death. However, the concept of CYCLOPS assumes that only genes with hemizygous loss are sensitive to further down-regulation which has the great advantage that potential side effects of targeted therapy may be avoided in cells without deletion. Also treatment with the selective ICMT inhibitor revealed no correlation between cell viability and gene copy number. Hence, no further validation experiments were performed with these candidates.

4.4.2 Validation of ephrin receptor gene candidates (*EPHA2*, *EPHB2*)

It is remarkable that all Eph receptor genes we screened for were identified as potential CYCLOPS genes underlying their important role for neuroblastoma cells. In general, Eph receptors including EphB2 are essential for developing cells in embryos and are required for angiogenesis, lymphangiogenesis, palate development and, most importantly, development of the neuronal system (Kania and Klein 2016; Noren and Pasquale 2004). Eph receptors fulfill these tasks through regulation of cytoskeleton dynamics which control migration and positioning, cell-cell segregation or, depending on the context, cell-cell adhesion (Nievergall, et al. 2012). But also in developing adult cells Eph receptors play a

role, for instance in intestinal stem cells (Genander, et al. 2010; Merlos-Suarez and Batlle 2008).

The results for *EPHA2* were not promising as the knock-down effect on 1p-deleted cells was not much stronger than on 1p normal cells. In the contrary, knock-down of EphB2 reduced survival of 1p-deleted cell lines but had little impact in 1p normal cells. Taking the EphB2 expression levels together with knock-down experiments of all used cell lines, it becomes clear that sensitivity to suppression does not tightly correspond to gene expression but only the copy number status. For example, the 1p non-deleted cell line SK-N-FI had the lowest mRNA expression level but EphB2 knock-down had no impact on viability or cell confluency. The opposite is true for CLB.Ga and CHP-126 (1p-deleted) which showed relatively high EphB2 expression and were sensitive to knock-down. This indicates that cells with two transcriptional templates may mediate more flexible compensation of challenged transcript levels. Exceptional behavior was seen for the cell line LS which also died upon EphB2 knock-down although it had high EphB2 mRNA expression and no 1p-deletion. Additionally, mRNA expression analysis of two exemplary cell lines revealed that EphB2 knock-down reduced the mRNA in TR14 (1p non-deleted) to the same level as it is in IMR-32 (1p-deleted) prior knock-down. As TR14 did not die upon EphB2 knock-down it becomes clear that the cells express more of this protein than it is required for survival, whereas in IMR-32 the level is close to the minimal threshold. These findings were confirmed by ectopic expression of EphB2 in IMR-32 which strongly enhanced the protein level and saved the cells from siRNA-mediated knock-down. The largely differential cell death in 1p-deleted cells suggests that EphB2 is a cell essential gene as loss of any non-essential gene leads to compensatory mechanisms through another gene (Hughes, et al. 2000). Besides EphB2 belongs to the largest group of tyrosine kinases with five members of the B subtype and nine members of the A subtype having similar functions (Gale, et al. 1996), none of these seems to be able to replace EphB2 after knock-down.

We then wanted further dissect the phenotype seen upon EphB2 knock-down. Starting with the 1p-deleted cell line IMR-32 we observed G_1/G_0 arrest upon knock-down which is accompanied by the measured cell death. Reseeding experiments of floating cells showed, that the vast majority of cells which were not dead after our endpoint measurement died in a longer time manner or, at least, lacked regrowth ability. As the reseeding was done in the absence of siRNAs these results also indicate that knock-down of EphB2 has a long term effect. Unfortunately, our attempts to elucidate which kind of cell death occurs to the cells remained unsolved. Neither apoptosis, ferroptosis, necroptosis nor autophagy mediate cell death in IMR-32. However, it cannot be assumed that all of

the tested cell lines have the same faith. There was evidence that e.g. NB69 show apoptosis-related PARP (poly (ADP-ribose) polymerase 1*)* cleavage after knock-down whereas other cells including IMR-32 did not (data not shown).

Besides strongly reduced survival in IMR-32 after EphB2 knock-down there was still a small proportion of living cells. RNA sequencing revealed that these cells express genes which induce cell cycle arrest (*IFIT3*; interferon induced protein with tetratricopeptide repeats 3) and cell growth inhibitors as *NAV2-AS2* and *NAV2-AS3* (neuron navigator 2 antisense RNA 2 and 3) which is accompanied by the already described cell cycle arrest in G_1/G_0. Interestingly, the preventer of differentiation *PRAME* (preferentially expressed antigen in melanoma) was shown to be downregulated. This gene was described in other studies as upregulated in high-stage neuroblastomas and is associated with unfavorable outcome (Henrich, et al. 2016; Oberthuer, et al. 2004). Here, the down-regulated *PRAME* together with overexpression of the neuron-forming gene *LRRC4B* (leucine rich repeat containing 4B) indicate that differentiating processes get activated. As we could not observe any hallmarks of differentiation like neurite outgrowth or upregulation of differentiation markers it is more likely that these genes somehow contribute to cell survival. The strongest differentially expressed gene was *HGF* (hepatocyte growth factor). HGF is, so far known, the only ligand of the receptor tyrosine kinase c-MET. This surface receptor is required for normal cell development, embryo- and organogenesis and migration (Organ and Tsao 2011). Overexpression of c-MET has been observed in many cancers including neuroblastoma (Cooper 1992; Hecht, et al. 2004; International Cancer Genome Consortium PedBrain Tumor 2016). The c-MET oncogene activation happens through the establishment of a HGF/c-MET autocrine loop, overexpression of c-MET and/ or HGF or receptor binding site mutation of c-MET (Eder, et al. 2009). The downstream response of HGF/c-MET signaling axis is mediated by MAPK (mitogen activated protein kinase) and Akt pathways which promote cell proliferation, survival, differentiation or morphogenesis (Trusolino, et al. 2010). We hypothesized that the resistance of the surviving cells after EphB2 knock-down is mediated by c-MET signaling and indeed we could detect accumulation of phosphorylated MAPK and Akt, the active form of these proteins. Although the induced *HGF* expression was confirmed by RT-PCR no changes on an intracellular protein level could be assessed and no extracellular HGF was measured at all. Two possibilities may explain this discrepancy between enhanced mRNA expression and constant or no protein levels. First, there are different isotypes of HGF existing and possibly the used antibodies detect another isoform which does not activate c-MET signaling and has therefore unaltered levels (Day, et al. 1999; Mungunsukh, et al. 2014). Second, these findings may also indicate that as long as a constant level of

intracellular HGF is present no further protein production may be required. Stress-induction activates HGF expression and all proteins over a certain threshold might get secreted. That no accumulation of HGF in the extracellular medium was assessed might be evidence of immediate binding to the c-MET receptor. To poof this assumption receptor-ligand interaction/binding assays should be done in further studies.

Taken together, this data set shows that EphB2 knock-down induced cell death in the vast majority of 1p-deleted cells but surviving cells activated HGF overexpression and c-MET signaling via MAPK and Akt as a resistance mechanism. Unfortunately, our attempt to overcome the resistance with a selective MAPK inhibitor failed as further loss of cell confluency of only maximum 5% was achieved. Targeting only one of these resistance pathways may be compensated by boosting the other one. More promising results may be achieved by inhibiting both, MAKP and Akt signaling in combination with EphB2 knock-down.

To confirm our findings on phenotypic changes upon EphB2 knock-down we generated stable cell lines with inducible shEphB2 expression. The general EphB2 expression is in IMR-32 on such a low level that the background leakiness of the vector was enough to have impact on survival and induce cell cycle arrest in G_1/G_0. Doxycycline-induced shEphB2 expression further reduced EphB2 but the effect on phenotypes was minimal. For instance, only 20% of loss of cell confluency could be achieved upon doxycycline induction but already the general vitality of the clones was weak compared to their counterparts carrying a control vector. The shEphB2 cells were growing slower and showed a high amount of detached cells in the medium. Also the levels of phosphorylated MAKP and Akt were enhanced but did not get further upregulated in the presence of doxycycline. However, in contrast to transient knock-down in the parental cell line IMR-32, we could not detect any upregulation of HGF and corresponding c-MET signaling. Whereas the HGF-mediated resistance in IMR-32 seems to be a fast response to EphB2 knock-down, the long term survival mechanism in a permanently EphB2-lacking situation as it is in the shEphB2 clones may be HGF-independent. Hence, alternative mechanisms may activate MAPK and Akt signaling to mediate survival.

Next we noticed that due to the construct leakiness differentially expressed genes were to a vast majority the same in the clones, no matter if vector expression was induced or not. Gene enrichment analysis revealed that many of the upregulated genes are involved in neuronal development, e.g. *SEMA5A* (semaphorin 5A), *RELN* (reelin) or *ROBO2* (roundabout guidance receptor 2). Again, it seems rather unlikely that induction of these genes promotes neuro-differentiation in EphB2-reduced stress conditions but possibly their upregulation contributes to cell survival. SEMA5A is also known to be involved in

MAPK and Akt signaling. Many more players of these pathways were also identified to be upregulated, such as the interleukin receptors IL13RA1 and IL1RAPL1 or BMP7 (bone morphogenic protein 7) strengthening our hypothesis of HGF-independent pathway activation.

In summary, the EphB2 expression in the 1p-deleted cell line IMR-32 is so low that even the background leakiness of an shRNA plasmid was enough to induce the described phenotypes and had a strong impact on gene expression. Therefore, the shEphB2 clones are less viable than cells expressing a control shRNA. Doxycycline induction led to further EphB2 downregulation but this did not influence the already persisting phenotype. The results further indicate that permanent EphB2 downregulation in the clones led to a selection of knock-down resistant cells which compensate the protein loss with enhanced MAPK and Akt signaling.

As described previously, knock-down of EphB2 had no impact on cell survival in 1p non-deleted cells. We also found no evidence for activation of MAPK and Akt signaling after EphB2 knock-down indicating that no survival mechanisms employing this pathway are required. Supporting these findings, no effects could be assessed by combination of EphB2 knock-down and inhibition of MAPK by FR180204. Nevertheless, other phenotypes could be observed including morphological changes. All 1p non-deleted cells showed fiber outgrowth und cell body lengthening (again excluding LS) which was not seen for 1p-deleted cell lines (except SK-N-BE(2)). In our exemplary cell line TR14, we also measured cell cycle arrest in G_1/G_0. Neurite outgrowth and cell cycle arrest are indicators of senescence or differentiation (Childs, et al. 2014; Myster and Duronio 2000). We excluded the first but detected the upregulation of *TUBB3* (tubulin beta 3 class III). TUBB3 is a part of the cytoskeleton and uniquely expressed in neurons. We showed that the outgrown fibers upon EphB2 knock-down contained TUBB3, which confirmed differentiation. Generally, these findings are in accordance with the known impact of EphB2 on the cytoskeleton and axon guidance (Kania and Klein 2016).

Another cause for cell cycle arrest and morphologic changes is cell migration. Cytoskeletal contractility and elongated cell bodies have been described in migrating cells in other entities (Grinnell 2003; Thiery 2002). It is also well know that ephrin receptors including EphB2 are regulators of cell movement (Nievergall, et al. 2012; Noren and Pasquale 2004). EphB2 knock-down in 1p non-deleted TR14 inhibited migration and general motility was slowed down. Together with cell differentiation after EphB2 knock-down this points to an oncogenic role of this gene in TR14. In fact, deregulated EphB2 has been observed in many tumors with controversy functions. In most studies, EphB2

has been identified as a potential TSG but there are also cases where oncogenic functions have been described (Batlle, et al. 2005; Farshchian, et al. 2015; Husa, et al. 2016; Huusko, et al. 2004). However, in contrast to this hypothesis is the fact that 1p-deleted cell lines and tumors do not show significant upregulation of EphB2 to gain its oncogenic benefits. Additionally, in the previously mentioned cDNA overexpression experiments in IMR-32 the ectopic expression of EphB2 alone did not influence cell growth, which supports the theory that EphB2 has no tumor-driving function in neuroblastoma.

In summary, knock-down of EphB2 had a small impact on the 1p non-deleted cell line TR14 as cell growth and survival did not get affected and only a few genes were differentially expressed. Differentiation and inhibited cell motility upon EphB2 knock-down indicate that EphB2 may support tumor maintenance in TR14.

4.5 Conclusion and perspective

When Nijhawan et al. introduced their concept they proposed which requirements a CYCLOPS gene has to fulfill. First, the gene has to be essential for general cell or cell lineage-dependent survival. Second, the gene has to be hemizygously deleted in tumors, mainly as a collateral damage in the turn of selection pressure-driven loss of tumor suppressor genes. And third, the expression ratio of a CYCLOPS gene strongly correlates with its copy number. In other words, cells with a deletion of that gene have to have a reduced expression and corresponding protein level compared to cells with both copies. This means that the latter express more protein than required for viability (Nijhawan, et al. 2012).

In this study we showed that among all selected CYCLOPS gene candidates EphB2 was the most promising one. It is deleted in ~35% of all neuroblastoma tumors and its overall expression is reduced in these cases. We further showed that knock-down of EphB2 in 1p-deleted cell lines led to cell death, whereas 1p non-deleted cell lines survived. This suggests on one hand that the non-deleted cell lines express more protein than required for survival; on the other hand it becomes clear that EphB2 is an essential gene in neuroblastoma cells. Interestingly, none of its 13 tyrosine kinase family members could replace the loss besides all of them have similar functions.

Although we proved that 1p-deleted cells die upon EphB2 knock-down we were not able to elucidate the cell death mechanism. We plan to perform time line RNA sequencing to address this question.

Even if the majority of the 1p-deleted cells after knock-down died there was still a small proportion of survivors. We uncovered that the resistance may be due overexpression of

HGF and activation of c-MET signaling which might be mediated through MAKP and Akt pathways. Unfortunately, our attempts to impair this resistance by inhibiting MAPK had only moderate effect. In future experiments we will inhibit MAPK and Akt signaling in combination with EphB2 knock-down to avoid that one resistance pathway can compensate the inhibited other.

As usual for validation series we generated stable cell lines expressing shEphB2 under the control of a doxycycline inducible vector. The background leakiness of the plasmid was strong enough to disrupt the low EphB2 level and induce the phenotypes we also showed in the siRNA experiments. Further EphB2 knock-down through induced vector expression did not have an additional impact on phenotypes. Also differential gene expression with and without doxycycline was almost the same compared to cell lines expressing a control non-targeting shRNA. Nevertheless, these cloning issues should not be regarded as failure as the observed effects proof that the 1p-deleted cell line IMR-32 expresses a required minimum of EphB2 for survival and even the moderate depletion is enough to break the sensible equilibrium. These findings also indicate that EphB2 knock-down resistant cells have been selected whose resistance was mediated by upregulation of MAPK and Akt signaling. In contrast to transient knock-down in the parental IMR-32 cells, MAPK and Akt activation was not induced by HGF/c-Met. Possibly, there may be an alternative way to activate these resistance pathways in shEphB2 clones.

Still, to avoid interference with background leakiness more sophisticated methods can be used as the knock-out approach via CRISPR/Cas.

This study used TR14 as a control cell line for 1p non-deleted cells. Here, knock-down of EphB2 did not influence survival and the impact on global gene expression was low. Morphologic changes were observed and we identified differentiation to be the driving force behind this process. We also showed that EphB2 knock-down restricts cell motility in TR14. This reduced migration in combination with differentiation points to an oncogenic role of *EPHB2* in 1p non-deleted cells. This is not in conflict with the CYCLOPS concept as long as the gene does not have tumor-driving functions in deleted cells. However, as 1p-deleted cells do not show upregulation of EphB2 and ectopic expression had no influence on cell growth, it seems unlikely that only 1p non-deleted cells may be dependent on *EPHB2* as an oncogene. To avoid the problem of genes with bipolar functions future CYCLOPS studies should also include non-malignant cells for control experiments.

As recurrent somatic mutations are rare in neuroblastoma but 1p-deletion is seen in ~35% of cases, this study might open a new therapeutic window which may be beneficial for a large patient group. We showed that *EPHB2* is a promising CYCLOPS candidate as it fulfills all requirements. Due to little effect on 1p non-deleted cells, common side effects of potential targeted therapy addressing EphB2 may be avoided or reduced. If *EPHB2* is also a CYCLOPS gene in other 1p-deleted entities remains to be clarified, but this approach may be regarded as a proof-of-principle for these cancer types.

5. References

Adhikary, S., and M. Eilers
2005 Transcriptional regulation and transformation by Myc proteins. Nat Rev Mol Cell Biol 6(8):635-45.

Alaminos, M., et al.
2004 Clustering of gene hypermethylation associated with clinical risk groups in neuroblastoma. J Natl Cancer Inst 96(16):1208-19.

Alimonti, A., et al.
2010 Subtle variations in Pten dose determine cancer susceptibility. Nat Genet 42(5):454-8.

Anderson, M. W., et al.
1992 Role of proto-oncogene activation in carcinogenesis. Environ Health Perspect 98:13-24.

Balmain, A.
1985 Transforming ras oncogenes and multistage carcinogenesis. Br J Cancer 51(1):1-7.

Batlle, E., et al.
2005 EphB receptor activity suppresses colorectal cancer progression. Nature 435(7045):1126-30.

Bauer, A., et al.
2001 Smallest region of overlapping deletion in 1p36 in human neuroblastoma: a 1 Mbp cosmid and PAC contig. Genes Chromosomes Cancer 31(3):228-39.

Berger, A. H., A. G. Knudson, and P. P. Pandolfi
2011 A continuum model for tumour suppression. Nature 476(7359):163-9.

Berthold F, Hero B, Jobke A, Horz S, Boos J, Bretz R, Burdach S, Claviez A, Henze G, Klingebiel T, Kremens B, Kühl J, Schwabe D
1998 Sind Spontanregressionen beim Neuroblastom verspätete embryofetale Involutionen? Heim ME, Schwarz R (eds). Spontanremissionen in der Onkologie. Schattauer: Stuttgart New York:**84-94**.

Berthold, F., and B. Hero
2000 Neuroblastoma: current drug therapy recommendations as part of the total treatment approach. Drugs 59(6):1261-77.

Biedler, J. L., L. Helson, and B. A. Spengler
1973 Morphology and growth, tumorigenicity, and cytogenetics of human neuroblastoma cells in continuous culture. Cancer Res 33(11):2643-52.

Biedler, J. L., et al.
1978 Multiple neurotransmitter synthesis by human neuroblastoma cell lines and clones. Cancer Res 38(11 Pt 1):3751-7.

Biedler, J. L., and B. A. Spengler
1976 A novel chromosome abnormality in human neuroblastoma and antifolate-resistant Chinese hamster cell lives in culture. J Natl Cancer Inst 57(3):683-95.

Bown, N.
2001 Neuroblastoma tumour genetics: clinical and biological aspects. J Clin Pathol 54(12):897-910.

Bown, N., et al.
1999 Gain of chromosome arm 17q and adverse outcome in patients with neuroblastoma. N Engl J Med 340(25):1954-61.

Bown, N., et al.
2001 17q gain in neuroblastoma predicts adverse clinical outcome. U.K. Cancer Cytogenetics Group and the U.K. Children's Cancer Study Group. Med Pediatr Oncol 36(1):14-9.

Boyd, J. A., and J. C. Barrett
1990 Tumor suppressor genes: possible functions in the negative regulation of cell proliferation. Mol Carcinog 3(6):325-9.
Boyer, L. A., et al.
2005 Core transcriptional regulatory circuitry in human embryonic stem cells. Cell 122(6):947-56.
Brison, O.
1993 Gene amplification and tumor progression. Biochim Biophys Acta 1155(1):25-41.
Brodeur, G. M., et al.
1988 International criteria for diagnosis, staging and response to treatment in patients with neuroblastoma. Prog Clin Biol Res 271:509-24.
Brodeur, G. M., et al.
1984 Amplification of N-myc in untreated human neuroblastomas correlates with advanced disease stage. Science 224(4653):1121-4.
Brodeur, G. M., G. Sekhon, and M. N. Goldstein
1977 Chromosomal aberrations in human neuroblastomas. Cancer 40(5):2256-63.
Caron, H., et al.
2001 Chromosome bands 1p35-36 contain two distinct neuroblastoma tumor suppressor loci, one of which is imprinted. Genes Chromosomes Cancer 30(2):168-74.
Caron, H., et al.
1994 Chromosome 1p allelic loss in neuroblastoma: prognosis, genomic imprinting and 1;17 translocations. Prog Clin Biol Res 385:35-42.
Cavenee, W. K., et al.
1983 Expression of recessive alleles by chromosomal mechanisms in retinoblastoma. Nature 305(5937):779-84.
Chase, A., and N. C. Cross
2011 Aberrations of EZH2 in cancer. Clin Cancer Res 17(9):2613-8.
Chayka, O., et al.
2015 Identification and pharmacological inactivation of the MYCN gene network as a therapeutic strategy for neuroblastic tumor cells. J Biol Chem 290(4):2198-212.
Chen, Z., et al.
2005 Crucial role of p53-dependent cellular senescence in suppression of Pten-deficient tumorigenesis. Nature 436(7051):725-30.
Cheung, N. K., and M. A. Dyer
2013 Neuroblastoma: developmental biology, cancer genomics and immunotherapy. Nat Rev Cancer 13(6):397-411.
Childs, B. G., et al.
2014 Senescence and apoptosis: dueling or complementary cell fates? EMBO Rep 15(11):1139-53.
Cohn, S. L., et al.
1990 Prolonged N-myc protein half-life in a neuroblastoma cell line lacking N-myc amplification. Oncogene 5(12):1821-7.
Combaret, V., et al.
1995 Sensitive detection of numerical and structural aberrations of chromosome 1 in neuroblastoma by interphase fluorescence in situ hybridization. Comparison with restriction fragment length polymorphism and conventional cytogenetic analyses. Int J Cancer 61(2):185-91.
Cooper, C. S.
1992 The met oncogene: from detection by transfection to transmembrane receptor for hepatocyte growth factor. Oncogene 7(1):3-7.

Cowell, J. K., and H. T. Rupniak
1983 Chromosome analysis of human neuroblastoma cell line TR14 showing double minutes and an aberration involving chromosome 1. Cancer Genet Cytogenet 9(3):273-80.
Croce, Carlo M.
2008 Oncogenes and Cancer. The New England Journal of Medicine 358:502-511.
D'Angio, G. J., A. E. Evans, and C. E. Koop
1971 Special pattern of widespread neuroblastoma with a favourable prognosis. Lancet 1(7708):1046-9.
Day, R. M., et al.
1999 Differential signaling by alternative HGF isoforms through c-Met: activation of both MAP kinase and PI 3-kinase pathways is insufficient for mitogenesis. Oncogene 18(22):3399-406.
De Brouwer, S., et al.
2010 Meta-analysis of neuroblastomas reveals a skewed ALK mutation spectrum in tumors with MYCN amplification. Clin Cancer Res 16(17):4353-62.
Deininger, P.
1999 Genetic instability in cancer: caretaker and gatekeeper genes. Ochsner J 1(4):206-9.
Dimri, G. P., et al.
1995 A biomarker that identifies senescent human cells in culture and in aging skin in vivo. Proc Natl Acad Sci U S A 92(20):9363-7.
Donti, E., et al.
1988 Cytogenetic and molecular study of two human neuroblastoma cell lines. Cancer Genet Cytogenet 30(2):225-31.
Durinck, K., and F. Speleman
2018 Epigenetic regulation of neuroblastoma development. Cell Tissue Res 372(2):309-324.
Eder, J. P., et al.
2009 Novel therapeutic inhibitors of the c-Met signaling pathway in cancer. Clin Cancer Res 15(7):2207-14.
Ejeskar, K., et al.
2001 Fine mapping of a tumour suppressor candidate gene region in 1p36.2-3, commonly deleted in neuroblastomas and germ cell tumours. Med Pediatr Oncol 36(1):61-6.
El-Badry, O. M., et al.
1989 Autonomous growth of a human neuroblastoma cell line is mediated by insulin-like growth factor II. J Clin Invest 84(3):829-39.
Farshchian, M., et al.
2015 EphB2 Promotes Progression of Cutaneous Squamous Cell Carcinoma. J Invest Dermatol 135(7):1882-1892.
Fernandez-Medarde, A., and E. Santos
2011 Ras in cancer and developmental diseases. Genes Cancer 2(3):344-58.
Fitzgerald, P. H., A. Adams, and F. W. Gunz
1963 Chronic granulocytic leukemia and the Philadelphia chromosome. Blood 21:183-96.
Fong, C. T., et al.
1989 Loss of heterozygosity for the short arm of chromosome 1 in human neuroblastomas: correlation with N-myc amplification. Proc Natl Acad Sci U S A 86(10):3753-7.
Fowler, T., et al.
2014 Regulation of MYC expression and differential JQ1 sensitivity in cancer cells. PLoS One 9(1):e87003.

Frohling, S., and H. Dohner
2008 Chromosomal abnormalities in cancer. N Engl J Med 359(7):722-34.
Gale, N. W., et al.
1996 Eph receptors and ligands comprise two major specificity subclasses and are reciprocally compartmentalized during embryogenesis. Neuron 17(1):9-19.
Gauthier, M. L., et al.
2007 Abrogated response to cellular stress identifies DCIS associated with subsequent tumor events and defines basal-like breast tumors. Cancer Cell 12(5):479-91.
Genander, M., J. Holmberg, and J. Frisen
2010 Ephrins negatively regulate cell proliferation in the epidermis and hair follicle. Stem Cells 28(7):1196-205.
Grinnell, F.
2003 Fibroblast biology in three-dimensional collagen matrices. Trends Cell Biol 13(5):264-9.
Guo, C., et al.
2000 Deletion of 11q23 is a frequent event in the evolution of MYCN single-copy high-risk neuroblastomas. Med Pediatr Oncol 35(6):544-6.
Hanahan, D., and R. A. Weinberg
2011 Hallmarks of cancer: the next generation. Cell 144(5):646-74.
Hayashi, Y., et al.
1989 Cytogenetic findings and prognosis in neuroblastoma with emphasis on marker chromosome 1. Cancer 63(1):126-32.
Hecht, M., et al.
2004 Hepatocyte growth factor/c-Met signaling promotes the progression of experimental human neuroblastomas. Cancer Res 64(17):6109-18.
Heisterkamp, N., et al.
1985 Structural organization of the bcr gene and its role in the Ph' translocation. Nature 315(6022):758-61.
Henrich, K. O., et al.
2016 Integrative Genome-Scale Analysis Identifies Epigenetic Mechanisms of Transcriptional Deregulation in Unfavorable Neuroblastomas. Cancer Res 76(18):5523-37.
Henrich, K. O., M. Schwab, and F. Westermann
2012 1p36 tumor suppression--a matter of dosage? Cancer Res 72(23):6079-88.
Hero, B., et al.
2008 Localized infant neuroblastomas often show spontaneous regression: results of the prospective trials NB95-S and NB97. J Clin Oncol 26(9):1504-10.
Hnisz, D., et al.
2013 Super-enhancers in the control of cell identity and disease. Cell 155(4):934-47.
Ho, N., et al.
2018 Delineation of the frequency and boundary of chromosomal copy number variations in paediatric neuroblastoma. Cell Cycle:1-18.
Honorio, S., et al.
2003 Detection of RASSF1A aberrant promoter hypermethylation in sputum from chronic smokers and ductal carcinoma in situ from breast cancer patients. Oncogene 22(1):147-50.
Howlader N, Noone AM, Krapcho M, Miller D, Bishop K, Kosary CL, Yu M, Ruhl J, Tatalovich Z, Mariotto A, Lewis DR, Chen HS, Feuer EJ, Cronin KA (eds)
2011 SEER Cancer Statistics Review, 1975-2008, Based on November 2010 SEER Data Submission. Bethasda, MD: National Cancer Institute.

Hubaux, R., et al.
2012 Arsenic, asbestos and radon: emerging players in lung tumorigenesis. Environ Health 11:89.
Hughes, T. R., et al.
2000 Functional discovery via a compendium of expression profiles. Cell 102(1):109-26.
Husa, A. M., et al.
2016 EPH/ephrin profile and EPHB2 expression predicts patient survival in breast cancer. Oncotarget 7(16):21362-80.
Huusko, P., et al.
2004 Nonsense-mediated decay microarray analysis identifies mutations of EPHB2 in human prostate cancer. Nat Genet 36(9):979-83.
International Cancer Genome Consortium PedBrain Tumor, Project
2016 Recurrent MET fusion genes represent a drug target in pediatric glioblastoma. Nat Med 22(11):1314-1320.
Janoueix-Lerosey, I., et al.
2009 Overall genomic pattern is a predictor of outcome in neuroblastoma. J Clin Oncol 27(7):1026-33.
Kaneko, Y., et al.
1987 Different karyotypic patterns in early and advanced stage neuroblastomas. Cancer Res 47(1):311-8.
Kania, A., and R. Klein
2016 Mechanisms of ephrin-Eph signalling in development, physiology and disease. Nat Rev Mol Cell Biol 17(4):240-56.
Kazanets, A., et al.
2016 Epigenetic silencing of tumor suppressor genes: Paradigms, puzzles, and potential. Biochim Biophys Acta 1865(2):275-88.
Keshelava, N., et al.
1998 Drug resistance patterns of human neuroblastoma cell lines derived from patients at different phases of therapy. Cancer Res 58(23):5396-405.
Kinzler, K. W., and B. Vogelstein
1997 Cancer-susceptibility genes. Gatekeepers and caretakers. Nature 386(6627):761, 763.
Knudson, A. G., Jr.
1971 Mutation and cancer: statistical study of retinoblastoma. Proc Natl Acad Sci U S A 68(4):820-3.
Korja, M., et al.
2009 Absence of polysialylated NCAM is an unfavorable prognostic phenotype for advanced stage neuroblastoma. BMC Cancer 9:57.
Kornberg, R. D., and Y. Lorch
1999 Twenty-five years of the nucleosome, fundamental particle of the eukaryote chromosome. Cell 98(3):285-94.
Kouzarides, T.
2007 Chromatin modifications and their function. Cell 128(4):693-705.
Kumar, M. S., et al.
2009 Dicer1 functions as a haploinsufficient tumor suppressor. Genes Dev 23(23):2700-4.
Lambertz, I., et al.
2010 Monoallelic but not biallelic loss of Dicer1 promotes tumorigenesis in vivo. Cell Death Differ 17(4):633-41.
Lieber, M. R.
1998 Warner-Lambert/Parke-Davis Award Lecture. Pathological and physiological double-strand breaks: roles in cancer, aging, and the immune system. Am J Pathol 153(5):1323-32.

Lister, R., et al.
2009 Human DNA methylomes at base resolution show widespread epigenomic differences. Nature 462(7271):315-22.
Liu, L., et al.
2002 Frequent hypermethylation of the RASSF1A gene in prostate cancer. Oncogene 21(44):6835-40.
Lo, K. W., et al.
2001 High frequency of promoter hypermethylation of RASSF1A in nasopharyngeal carcinoma. Cancer Res 61(10):3877-81.
Lochmann, T. L., et al.
2018 Targeted inhibition of histone H3K27 demethylation is effective in high-risk neuroblastoma. Sci Transl Med 10(441).
Loeb, L. A.
2001 A mutator phenotype in cancer. Cancer Res 61(8):3230-9.
London, W. B., et al.
2005 Evidence for an age cutoff greater than 365 days for neuroblastoma risk group stratification in the Children's Oncology Group. J Clin Oncol 23(27):6459-65.
Luger, K., and T. J. Richmond
1998 The histone tails of the nucleosome. Curr Opin Genet Dev 8(2):140-6.
Mandriota, S. J., et al.
2015 Ataxia-telangiectasia mutated (ATM) silencing promotes neuroblastoma progression through a MYCN independent mechanism. Oncotarget 6(21):18558-76.
Marini, P., et al.
1999 SiMa, a new neuroblastoma cell line combining poor prognostic cytogenetic markers with high adrenergic differentiation. Cancer Genet Cytogenet 112(2):161-4.
Maris, J. M.
2010 Recent advances in neuroblastoma. N Engl J Med 362(23):2202-11.
Maris, J. M., et al.
2007 Neuroblastoma. Lancet 369(9579):2106-20.
Maris, J. M., et al.
2000 Loss of heterozygosity at 1p36 independently predicts for disease progression but not decreased overall survival probability in neuroblastoma patients: a Children's Cancer Group study. J Clin Oncol 18(9):1888-99.
Mayol, G., et al.
2012 DNA hypomethylation affects cancer-related biological functions and genes relevant in neuroblastoma pathogenesis. PLoS One 7(11):e48401.
Mena, M. A., et al.
1989 Biochemical properties of monoamine-rich human neuroblastoma cells. Brain Res 486(2):286-96.
Merlos-Suarez, A., and E. Batlle
2008 Eph-ephrin signalling in adult tissues and cancer. Curr Opin Cell Biol 20(2):194-200.
Michaelis, M., et al.
2011 Adaptation of cancer cells from different entities to the MDM2 inhibitor nutlin-3 results in the emergence of p53-mutated multi-drug-resistant cancer cells. Cell Death Dis 2:e243.
Michels, E., et al.
2008 CADM1 is a strong neuroblastoma candidate gene that maps within a 3.72 Mb critical region of loss on 11q23. BMC Cancer 8:173.
Michor, F., Y. Iwasa, and M. A. Nowak
2004 Dynamics of cancer progression. Nat Rev Cancer 4(3):197-205.

Mills, K. D., D. O. Ferguson, and F. W. Alt
2003 The role of DNA breaks in genomic instability and tumorigenesis. Immunol Rev 194:77-95.
Mitelman, F., B. Johansson, and F. Mertens
2007 The impact of translocations and gene fusions on cancer causation. Nat Rev Cancer 7(4):233-45.
Mlakar, V., et al.
2017 11q deletion in neuroblastoma: a review of biological and clinical implications. Mol Cancer 16(1):114.
Molenaar, J. J., et al.
2012 Sequencing of neuroblastoma identifies chromothripsis and defects in neuritogenesis genes. Nature 483(7391):589-93.
Molenaar, J. J., et al.
2003 Rearrangements and increased expression of cyclin D1 (CCND1) in neuroblastoma. Genes Chromosomes Cancer 36(3):242-9.
Morris, L. G., and T. A. Chan
2015 Therapeutic targeting of tumor suppressor genes. Cancer 121(9):1357-68.
Mungunsukh, O., E. A. McCart, and R. M. Day
2014 Hepatocyte Growth Factor Isoforms in Tissue Repair, Cancer, and Fibrotic Remodeling. Biomedicines 2(4):301-326.
Myster, D. L., and R. J. Duronio
2000 To differentiate or not to differentiate? Curr Biol 10(8):R302-4.
Nievergall, E., M. Lackmann, and P. W. Janes
2012 Eph-dependent cell-cell adhesion and segregation in development and cancer. Cell Mol Life Sci 69(11):1813-42.
Nijhawan, D., et al.
2012 Cancer vulnerabilities unveiled by genomic loss. Cell 150(4):842-54.
Noren, N. K., and E. B. Pasquale
2004 Eph receptor-ephrin bidirectional signals that target Ras and Rho proteins. Cell Signal 16(6):655-66.
Oberthuer, A., et al.
2004 The tumor-associated antigen PRAME is universally expressed in high-stage neuroblastoma and associated with poor outcome. Clin Cancer Res 10(13):4307-13.
Oberthuer, A., et al.
2015 Revised risk estimation and treatment stratification of low- and intermediate-risk neuroblastoma patients by integrating clinical and molecular prognostic markers. Clin Cancer Res 21(8):1904-15.
Ohira, M., et al.
2000 Identification and characterization of a 500-kb homozygously deleted region at 1p36.2-p36.3 in a neuroblastoma cell line. Oncogene 19(37):4302-7.
Organ, S. L., and M. S. Tsao
2011 An overview of the c-MET signaling pathway. Ther Adv Med Oncol 3(1 Suppl):S7-S19.
Paolella, B. R., et al.
2017 Copy-number and gene dependency analysis reveals partial copy loss of wild-type SF3B1 as a novel cancer vulnerability. Elife 6.
Pearce, N., et al.
2015 IARC monographs: 40 years of evaluating carcinogenic hazards to humans. Environ Health Perspect 123(6):507-14.
Peifer, M., et al.
2015 Telomerase activation by genomic rearrangements in high-risk neuroblastoma. Nature 526(7575):700-4.

Pietsch, T., et al.
1988 Characterization of a continuous cell line (MHH-NB-11) derived from advanced neuroblastoma. Anticancer Res 8(6):1329-33.
Plantaz, D., et al.
1997 Gain of chromosome 17 is the most frequent abnormality detected in neuroblastoma by comparative genomic hybridization. Am J Pathol 150(1):81-9.
Plantaz, D., et al.
2001 Comparative genomic hybridization (CGH) analysis of stage 4 neuroblastoma reveals high frequency of 11q deletion in tumors lacking MYCN amplification. Int J Cancer 91(5):680-6.
Pott, S., and J. D. Lieb
2015 What are super-enhancers? Nat Genet 47(1):8-12.
Pugh, T. J., et al.
2013 The genetic landscape of high-risk neuroblastoma. Nat Genet 45(3):279-84.
Quon, K. C., and A. Berns
2001 Haplo-insufficiency? Let me count the ways. Genes Dev 15(22):2917-21.
Reynolds, C. P., et al.
1986 Characterization of human neuroblastoma cell lines established before and after therapy. J Natl Cancer Inst 76(3):375-87.
Robinson, M. D., and A. Oshlack
2010 A scaling normalization method for differential expression analysis of RNA-seq data. Genome Biol 11(3):R25.
Ross, R. A., B. A. Spengler, and J. L. Biedler
1983 Coordinate morphological and biochemical interconversion of human neuroblastoma cells. J Natl Cancer Inst 71(4):741-7.
Rudolph, G., et al.
1991 Cytogenetic and molecular characterization of a newly established neuroblastoma cell line LS. Hum Genet 86(6):562-6.
Saint-Andre, V., et al.
2016 Models of human core transcriptional regulatory circuitries. Genome Res 26(3):385-96.
Sambrook J, Russel D
2002 Molecular cloning, a laboratory manual: CSHL press.
Savelyeva, L., R. Corvi, and M. Schwab
1994 Translocation involving 1p and 17q is a recurrent genetic alteration of human neuroblastoma cells. Am J Hum Genet 55(2):334-40.
Schlesinger, H. R., et al.
1976 Establishment and characterization of human neuroblastoma cell lines. Cancer Res 36(9 pt.1):3094-100.
Schwab, M., et al.
1983 Amplified DNA with limited homology to myc cellular oncogene is shared by human neuroblastoma cell lines and a neuroblastoma tumour. Nature 305(5931):245-8.
Schwab, M., C. Praml, and L. C. Amler
1996 Genomic instability in 1p and human malignancies. Genes Chromosomes Cancer 16(4):211-29.
Seeger, R. C., et al.
1985 Association of multiple copies of the N-myc oncogene with rapid progression of neuroblastomas. N Engl J Med 313(18):1111-6.
Seeger, R. C., et al.
1982 Definition of a Thy-1 determinant on human neuroblastoma, glioma, sarcoma, and teratoma cells with a monoclonal antibody. J Immunol 128(2):983-9.

Seeger, R. C., et al.
1977 Morphology, growth, chromosomal pattern and fibrinolytic activity of two new human neuroblastoma cell lines. Cancer Res 37(5):1364-71.
Sikkema, A. H., et al.
2012 EphB2 activity plays a pivotal role in pediatric medulloblastoma cell adhesion and invasion. Neuro Oncol 14(9):1125-35.
Slamon, D. J., et al.
1987 Human breast cancer: correlation of relapse and survival with amplification of the HER-2/neu oncogene. Science 235(4785):177-82.
Solimini, N. L., J. Luo, and S. J. Elledge
2007 Non-oncogene addiction and the stress phenotype of cancer cells. Cell 130(6):986-8.
Solimini, N. L., et al.
2012 Recurrent hemizygous deletions in cancers may optimize proliferative potential. Science 337(6090):104-9.
Stambolic, V., et al.
1998 Negative regulation of PKB/Akt-dependent cell survival by the tumor suppressor PTEN. Cell 95(1):29-39.
Strahl, B. D., and C. D. Allis
2000 The language of covalent histone modifications. Nature 403(6765):41-5.
Sugimoto, T., et al.
1984 Determination of cell surface membrane antigens common to both human neuroblastoma and leukemia-lymphoma cell lines by a panel of 38 monoclonal antibodies. J Natl Cancer Inst 73(1):51-7.
Takeda, O., et al.
1994 There may be two tumor suppressor genes on chromosome arm 1p closely associated with biologically distinct subtypes of neuroblastoma. Genes Chromosomes Cancer 10(1):30-9.
Teitz, T., et al.
2000 Caspase 8 is deleted or silenced preferentially in childhood neuroblastomas with amplification of MYCN. Nat Med 6(5):529-35.
Thiery, J. P.
2002 Epithelial-mesenchymal transitions in tumour progression. Nat Rev Cancer 2(6):442-54.
Tischfield, M. A., et al.
2010 Human TUBB3 mutations perturb microtubule dynamics, kinesin interactions, and axon guidance. Cell 140(1):74-87.
Trusolino, L., A. Bertotti, and P. M. Comoglio
2010 MET signalling: principles and functions in development, organ regeneration and cancer. Nat Rev Mol Cell Biol 11(12):834-48.
Tsherniak, A., et al.
2017 Defining a Cancer Dependency Map. Cell 170(3):564-576 e16.
Tumilowicz, J. J., et al.
1970 Definition of a continuous human cell line derived from neuroblastoma. Cancer Res 30(8):2110-8.
van Groningen, T., et al.
2017 Neuroblastoma is composed of two super-enhancer-associated differentiation states. Nat Genet 49(8):1261-1266.
Van Roy, N., et al.
1994 1;17 translocations and other chromosome 17 rearrangements in human primary neuroblastoma tumors and cell lines. Genes Chromosomes Cancer 10(2):103-14.

Van Roy, N., et al.
2006 Translocation-excision-deletion-amplification mechanism leading to nonsyntenic coamplification of MYC and ATBF1. Genes Chromosomes Cancer 45(2):107-17.
Vandepoele, K., et al.
2005 A novel gene family NBPF: intricate structure generated by gene duplications during primate evolution. Mol Biol Evol 22(11):2265-74.
Vandesompele, J., et al.
2005 Unequivocal delineation of clinicogenetic subgroups and development of a new model for improved outcome prediction in neuroblastoma. J Clin Oncol 23(10):2280-99.
Vandesompele, J., et al.
2001 Multicentre analysis of patterns of DNA gains and losses in 204 neuroblastoma tumors: how many genetic subgroups are there? Med Pediatr Oncol 36(1):5-10.
Vogelstein, B., and K. W. Kinzler
1993 The multistep nature of cancer. Trends Genet 9(4):138-41.
—
2004 Cancer genes and the pathways they control. Nat Med 10(8):789-99.
Wada, R. K., et al.
1993 Human neuroblastoma cell lines that express N-myc without gene amplification. Cancer 72(11):3346-54.
Wainwright, L. J., A. Lasorella, and A. Iavarone
2001 Distinct mechanisms of cell cycle arrest control the decision between differentiation and senescence in human neuroblastoma cells. Proc Natl Acad Sci U S A 98(16):9396-400.
Wallis, William H. Kruskal and W. Allen
1952 Use of Ranks in One-Criterion Variance Analysis Journal of the American Statistical Association 47(260):583-621.
Wang, S. D., et al.
2012 EphB2 receptor controls proliferation/migration dichotomy of glioblastoma by interacting with focal adhesion kinase. Oncogene 31(50):5132-43.
Wang, X., H. Huang, and K. H. Young
2015 The PTEN tumor suppressor gene and its role in lymphoma pathogenesis. Aging (Albany NY) 7(12):1032-49.
Weinberg, R. A.
1989 Oncogenes, antioncogenes, and the molecular bases of multistep carcinogenesis. Cancer Res 49(14):3713-21.
Westermann, F., and M. Schwab
2002 Genetic parameters of neuroblastomas. Cancer Lett 184(2):127-47.
White, P. S., et al.
2005 Definition and characterization of a region of 1p36.3 consistently deleted in neuroblastoma. Oncogene 24(16):2684-94.
Wong, M., et al.
2017 The Histone Methyltransferase DOT1L Promotes Neuroblastoma by Regulating Gene Transcription. Cancer Res 77(9):2522-2533.
Yamaguchi, Y., et al.
2014 Novel 1p tumour suppressor Dnmt1-associated protein 1 regulates MYCN/ataxia telangiectasia mutated/p53 pathway. Eur J Cancer 50(8):1555-65.
Yan, P. S., et al.
2006 Mapping geographic zones of cancer risk with epigenetic biomarkers in normal breast tissue. Clin Cancer Res 12(22):6626-36.

Zhu, S., et al.
2007 MicroRNA-21 targets the tumor suppressor gene tropomyosin 1 (TPM1). J Biol Chem 282(19):14328-36.
Zhu, S., et al.
2008 MicroRNA-21 targets tumor suppressor genes in invasion and metastasis. Cell Res 18(3):350-9.
zur Hausen, H.
1977 Human papillomaviruses and their possible role in squamous cell carcinomas. Curr Top Microbiol Immunol 78:1-30.

6. Appendix

6.1 Supplementary data

Tab. S 1: siRNA IDs used in the CYCLOPS screen

Gene	siRNA ID	Gene	siRNA ID	Gene	siRNA ID	Gene	siRNA ID
ACAP3	s42080	AOF2	s617	CA6	s2259	CLCNKA	s3150
ACAP3	s42081	AOF2	s618	CA6	s2260	CLCNKA	s3151
ACAP3	s42082	AOF2	s619	CA6	s2261	CLCNKA	s3152
ACOT7	s22346	ARID1A	s15784	CALML6	s46468	CLCNKB	s3153
ACOT7	s22347	ARID1A	s15785	CALML6	s46469	CLCNKB	s3154
ACOT7	s22348	ARID1A	s15786	CALML6	s46470	CLCNKB	s3155
ACTL8	s37650	ASAP3	s31085	CAMK2N1	s30876	CLDN19	s45293
ACTL8	s37651	ASAP3	s31086	CAMK2N1	s30877	CLDN19	s229812
ACTL8	s37652	ASAP3	s31087	CAMK2N1	s30878	CLDN19	s229813
ACTRT2	s44321	ATAD3A	s30447	CAPZB	s2401	CLIC4	s24778
ACTRT2	s44322	ATAD3A	s30448	CAPZB	s2402	CLIC4	s24779
ACTRT2	s195731	ATAD3A	s195276	CAPZB	s2403	CLIC4	s24780
ADC	s41476	ATAD3B	s38233	CASP9	s2428	CLSTN1	s22583
ADC	s41477	ATAD3B	s38234	CASP9	s2429	CLSTN1	s22584
ADC	s41478	ATAD3B	s195445	CASP9	s2430	CLSTN1	s22585
AGMAT	s379	ATAD3C	s47592	CASZ1	s29704	CMPK1	s28582
AGMAT	s380	ATAD3C	s47593	CASZ1	s29705	CMPK1	s28584
AGMAT	s381	ATAD3C	s47594	CASZ1	s29706	CMPK1	s230118
AJAP1	s31811	ATP13A2	s23742	CATSPER4	s51801	CNKSR1	s20036
AJAP1	s31812	ATP13A2	s23743	CATSPER4	s51802	CNKSR1	s20037
AJAP1	s31813	ATP13A2	s23744	CATSPER4	s51803	CNKSR1	s20038
AK2	s1209	ATP6V0B	s623	CDA	s2729	CNR2	s3263
AK2	s1211	ATP6V0B	s624	CDA	s2731	CNR2	s3264
AK2	s1210	ATP6V0B	s625	CDA	s2730	CNR2	s3265
AKR1A1	s20197	ATPAF1	s34869	CDC20	s2747	COL16A1	s3356
AKR1A1	s20198	ATPAF1	s34870	CDC20	s2748	COL16A1	s3357
AKR1A1	s20199	ATPAF1	s34871	CDC20	s2749	COL16A1	s3358
AKR7A2	s16331	AURKAIP1	s29953	CDC42	s2765	COL9A2	s3332
AKR7A2	s16332	AURKAIP1	s29954	CDC42	s2766	COL9A2	s3333
AKR7A2	s16333	AURKAIP1	s195269	CDC42	s2767	COL9A2	s3334
AKR7A3	s22751	B3GALT6	s43087	CDK11A	s229390	CPSF3L	s29893
AKR7A3	s22752	B3GALT6	s43088	CDK11A	s229391	CPSF3L	s29894
AKR7A3	s22753	B3GALT6	s43089	CDK11A	s229392	CPSF3L	s29895
AKR7L	s48347	B4GALT2	s85	CDK11B	s2732	CSF3R	s3609
AKR7L	s48348	B4GALT2	s86	CDK11B	s2733	CSF3R	s3610
AKR7L	s48349	B4GALT2	s87	CDK11B	s2734	CSF3R	s3611
ALDH4A1	s16484	BAI2	s1873	CELA2B	s27288	CTPS	s3731
ALDH4A1	s16483	BAI2	s1874	CELA2B	s27289	CTPS	s3732
ALDH4A1	s16485	BAI2	s1875	CELA2B	s27290	CTPS1	s229529
ALPL	s1296	BEST4	s49003	CHD5	s24987	CTRC	s22340
ALPL	s1297	BEST4	s49004	CHD5	s24988	CTRC	s22341
ALPL	s1298	BEST4	s49005	CHD5	s24989	CTRC	s22342
ANGPTL7	s19931	BMP8B	s2038	CLCN6	s3144	CYP4A11	s3852
ANGPTL7	s19932	BMP8B	s2039	CLCN6	s3145	CYP4A11	s3853
ANGPTL7	s19933	BMP8B	s2040	CLCN6	s3146	CYP4A11	s3854

The table continuous on the next page

CYP4A22	s49696	EIF3I	s16510	FGR	s5185	GUCA2A	s6340
CYP4A22	s49697	EIF3I	s16511	FGR	s5186	GUCA2A	s6341
CYP4A22	s49698	EIF3I	s16512	FGR	s5187	GUCA2A	s6342
CYP4B1	s3855	EIF4G3	s16519	FHL3	s5200	GUCA2B	s6343
CYP4B1	s3856	EIF4G3	s16520	FHL3	s5201	GUCA2B	s6344
CYP4B1	s3857	EIF4G3	s16521	FHL3	s194411	GUCA2B	s194480
CYP4X1	s48973	ELA3A	s19727	FOXD2	s5251	H6PD	s18368
CYP4X1	s48974	ELA3A	s19728	FOXD2	s5252	H6PD	s18369
CYP4X1	s48975	ELA3A	s19729	FOXD2	s5253	H6PD	s18370
CYP4Z1	s47162	ELOVL1	s34992	GABRD	s5497	HCRTR1	s6485
CYP4Z1	s47163	ELOVL1	s34993	GABRD	s5498	HCRTR1	s6486
CYP4Z1	s47164	ELOVL1	s34994	GABRD	s5499	HCRTR1	s194519
DDI2	s38861	ENO1	s4680	GALE	s5533	HDAC1	s73
DDI2	s38862	ENO1	s4681	GALE	s5534	HDAC1	s74
DDI2	s38863	ENO1	s4682	GALE	s5535	HDAC1	s75
DDOST	s3998	EPHA10	s200588	GJA4	s5763	HECTD3	s36019
DDOST	s3999	EPHA10	s229806	GJA4	s5764	HECTD3	s36020
DDOST	s4000	EPHA10	s229807	GJA4	s5765	HECTD3	s36021
DFFA	s4056	EPHA2	s4564	GJA9	s37475	HES2	s29273
DFFA	s4058	EPHA2	s4565	GJA9	s37476	HES2	s29274
DFFA	s4057	EPHA2	s4566	GJA9	s37477	HES2	s29275
DFFB	s4059	EPHA8	s4734	GJB3	s5778	HES3	s52903
DFFB	s4060	EPHA8	s4735	GJB3	s5779	HES3	s196361
DFFB	s4061	EPHA8	s4736	GJB3	s5780	HES3	s196362
DHDDS	s36696	EPHB2	s4740	GJB4	s43184	HES4	s33732
DHDDS	s36697	EPHB2	s4741	GJB4	s43185	HES4	s195322
DHDDS	s36698	EPHB2	s4742	GJB4	s43186	HES4	s195323
DHRS3	s17688	ERMAP	s41566	GJB5	s5781	HES5	s52196
DHRS3	s17689	ERMAP	s41564	GJB5	s5782	HES5	s52197
DHRS3	s17690	ERMAP	s41565	GJB5	s5783	HES5	s52198
DMAP1	s31789	ESPN	s38139	GMEB1	s21020	HEYL	s25473
DMAP1	s31790	ESPN	s38140	GMEB1	s21021	HEYL	s25474
DMAP1	s31791	ESPN	s38141	GMEB1	s21022	HEYL	s25475
DMBX1	s43160	EXTL1	s4895	GNB1	s5901	HIVEP3	s33958
DMBX1	s43161	EXTL1	s4896	GNB1	s5902	HIVEP3	s33959
DMBX1	s43162	EXTL1	s4897	GNB1	s5903	HIVEP3	s33960
DNAJC11	s31371	EYA3	s4910	GNL2	s26649	HMGCL	s6658
DNAJC11	s31372	EYA3	s4911	GNL2	s26650	HMGCL	s6659
DNAJC11	s31373	EYA3	s4912	GNL2	s26651	HMGCL	s6660
DNAJC16	s23602	FAAH	s4961	GPN2	s29330	HMGN2	s6657
DNAJC16	s23603	FAAH	s4962	GPN2	s29331	HMGN2	s194528
DNAJC16	s23604	FAAH	s4963	GPN2	s195247	HMGN2	s194529
DNAJC8	s22442	FABP3	s4973	GPR153	s51868	HNRNPCL1	s50974
DNAJC8	s22443	FABP3	s4974	GPR153	s51869	HNRNPCL1	s50975
DNAJC8	s22444	FABP3	s4975	GPR153	s196200	HNRNPCL1	s50976
DNALI1	s15359	FBLIM1	s29380	GPR157	s36865	HNRNPR	s19979
DNALI1	s15360	FBLIM1	s195248	GPR157	s36866	HNRNPR	s19980
DNALI1	s15361	FBLIM1	s195249	GPR157	s195393	HNRNPR	s19981
DVL1	s4393	FBXO44	s41168	GPR3	s5998	HPCA	s6782
DVL1	s4394	FBXO44	s41169	GPR3	s5999	HPCA	s6783
DVL1	s4395	FBXO44	s41170	GPR3	s6000	HPCA	s6784
EFHD2	s35692	FBXO6	s25337	GRHL3	s33752	HPCAL4	s28144
EFHD2	s35693	FBXO6	s25338	GRHL3	s33753	HPCAL4	s28145
EFHD2	s35694	FBXO6	s25339	GRHL3	s33754	HPCAL4	s28146
EIF2B3	s16995	FCN3	s16269	GRIK3	s6158	HPDL	s39502
EIF2B3	s16993	FCN3	s16270	GRIK3	s6159	HPDL	s39503
EIF2B3	s16994	FCN3	s16271	GRIK3	s6160	HPDL	s39504

The table continuous on the next page

HSPB7	s25870	LDLRAD2	s53706	MPL	s8934	PABPC4	s16693
HSPB7	s25871	LDLRAD2	s53707	MPL	s8935	PABPC4	s16694
HSPB7	s25872	LDLRAD2	s196457	MPL	s8936	PABPC4	s16695
HSPG2	s7014	LEPRE1	s34536	MTF1	s9027	PADI1	s26757
HSPG2	s7015	LEPRE1	s34537	MTF1	s9028	PADI1	s26758
HSPG2	s7016	LEPRE1	s34538	MTF1	s9029	PADI1	s26759
HTR1D	s7034	LIN28A	s36195	MTHFR	s9035	PADI2	s22187
HTR1D	s7032	LIN28A	s36196	MTHFR	s9036	PADI2	s22188
HTR1D	s7033	LIN28A	s36197	MTHFR	s9037	PADI2	s22189
HTR6	s7059	LRRC47	s33094	MUTYH	s9090	PADI3	s28546
HTR6	s7060	LRRC47	s33095	MUTYH	s9091	PADI3	s28547
HTR6	s7061	LRRC47	s33096	MUTYH	s9092	PADI3	s28548
ICMT	s23871	LYPLA2	s22298	MYCBP	s25391	PADI4	s24119
ICMT	s23872	LYPLA2	s22299	MYCBP	s25392	PADI4	s24120
ICMT	s23873	LYPLA2	s22300	MYCBP	s25393	PADI4	s24121
IL22RA1	s33943	MACF1	s23937	MYOM3	s43156	PAFAH2	s10004
IL22RA1	s33944	MACF1	s23938	MYOM3	s43157	PAFAH2	s10005
IL22RA1	s33945	MACF1	s23939	MYOM3	s43158	PAFAH2	s10006
INPP5B	s7456	MAN1C1	s32754	NADK	s35239	PANK4	s30500
INPP5B	s7457	MAN1C1	s32755	NADK	s35240	PANK4	s30501
INPP5B	s7458	MAN1C1	s32756	NADK	s35241	PANK4	s30502
IPO13	s18608	MAP3K6	s17288	NASP	s9280	PAQR7	s46503
IPO13	s18609	MAP3K6	s17289	NASP	s9281	PAQR7	s46504
IPO13	s18610	MAP3K6	s17290	NASP	s9282	PAQR7	s46505
IPP	s7489	MASP2	s21119	NDUFS5	s9397	PARK7	s22304
IPP	s7490	MASP2	s195063	NDUFS5	s9398	PARK7	s22306
IPP	s7491	MASP2	s195064	NDUFS5	s9399	PARK7	s230250
KCNAB2	s16177	MAST2	s42	NECAP2	s31305	PAX7	s10070
KCNAB2	s16178	MAST2	s43	NECAP2	s31306	PAX7	s10071
KCNAB2	s16179	MAST2	s44	NECAP2	s31307	PAX7	s10072
KCNQ4	s17443	MATN1	s8529	NMNAT1	s34981	PDIK1L	s45286
KCNQ4	s17444	MATN1	s8530	NMNAT1	s34982	PDIK1L	s45287
KCNQ4	s17445	MATN1	s8531	NMNAT1	s34980	PDIK1L	s45288
KHDRBS1	s20951	MECR	s27434	NPPA	s9679	PEF1	s54735
KHDRBS1	s20952	MECR	s27435	NPPA	s9680	PEF1	s54736
KHDRBS1	s20953	MECR	s27436	NPPA	s9681	PEF1	s54737
KIF17	s33352	MED8	s41409	NPPB	s9682	PEX14	s10324
KIF17	s33353	MED8	s41410	NPPB	s9683	PEX14	s10325
KIF17	s33354	MED8	s41411	NPPB	s194662	PEX14	s10326
KIF1B	s23022	MEGF6	s4528	NR0B2	s15996	PGD	s10394
KIF1B	s23023	MEGF6	s4529	NR0B2	s15997	PGD	s10395
KIF1B	s23024	MEGF6	s4530	NR0B2	s15998	PGD	s224256
KIF2C	s21663	MFN2	s19260	NSUN4	s51859	PHC2	s4474
KIF2C	s21664	MFN2	s19261	NSUN4	s51860	PHC2	s4475
KIF2C	s21665	MFN2	s19262	NSUN4	s51861	PHC2	s4476
KLF17	s43260	MFSD2	s39564	NT5C1A	s39183	PIK3CD	s10529
KLF17	s43261	MFSD2	s39565	NT5C1A	s39184	PIK3CD	s10530
KLF17	s43262	MFSD2	s39566	NT5C1A	s39185	PIK3CD	s10531
KLHL17	s50531	MKNK1	s16319	NUDC	s21071	PIK3R3	s16151
KLHL17	s50532	MKNK1	s16321	NUDC	s21072	PIK3R3	s229780
KLHL17	s50533	MKNK1	s16320	NUDC	s21073	PIK3R3	s229781
KPNA6	s24241	MMEL1	s35722	OPRD1	s9862	PINK1	s35166
KPNA6	s24242	MMEL1	s35723	OPRD1	s9863	PINK1	s35167
KPNA6	s24243	MMEL1	s35724	OPRD1	s9864	PINK1	s35168
LCK	s8106	MMP23B	s16172	OXCT2	s34373	PLA2G2A	s10589
LCK	s8107	MMP23B	s16173	OXCT2	s34374	PLA2G2A	s10590
LCK	s8108	MMP23B	s194938	OXCT2	s34375	PLA2G2A	s10591

The table continuous on the next page

PLA2G2D	s25361	PSMB2	s481	SCMH1	s22742	SNRNP40	s18011
PLA2G2D	s25362	PSMB2	s483	SCMH1	s22743	SNRNP40	s18012
PLA2G2D	s25363	PSMB2	s482	SCMH1	s22744	SNRNP40	s18013
PLA2G2E	s26914	PTAFR	s11431	SCNN1D	s12549	SPATA21	s51633
PLA2G2E	s26915	PTAFR	s11432	SCNN1D	s194785	SPATA21	s51634
PLA2G2E	s26916	PTAFR	s11433	SCNN1D	s194786	SPATA21	s51635
PLA2G2F	s34798	PTCH2	s16444	SDF4	s27560	SPEN	s22829
PLA2G2F	s34799	PTCH2	s16445	SDF4	s27561	SPEN	s22830
PLA2G2F	s34800	PTCH2	s16446	SDF4	s27562	SPEN	s22831
PLA2G5	s10595	PTP4A2	s581	SDHB	s12653	SPSB1	s37008
PLA2G5	s10596	PTP4A2	s582	SDHB	s12654	SPSB1	s37009
PLA2G5	s10597	PTP4A2	s583	SDHB	s12655	SPSB1	s37010
PLCH2	s18563	PTPRF	s11546	SF3A3	s21534	SRM	s13430
PLCH2	s18564	PTPRF	s11547	SF3A3	s21535	SRM	s13431
PLCH2	s18565	PTPRF	s11548	SF3A3	s21536	SRM	s13432
PLEKHM2	s23280	PTPRU	s19598	SFPQ	s12710	SRRM1	s20018
PLEKHM2	s23281	PTPRU	s19599	SFPQ	s12711	SRRM1	s20019
PLEKHM2	s23282	PTPRU	s19600	SFPQ	s12712	SRRM1	s20020
PLK3	s3245	PUM1	s18680	SFRS4	s12734	SSU72	s26487
PLK3	s3246	PUM1	s18681	SFRS4	s12735	SSU72	s26488
PLK3	s3247	PUM1	s18682	SFRS4	s12736	SSU72	s26489
PLOD1	s412	RAB42	s41781	SKI	s12880	ST3GAL3	s12853
PLOD1	s413	RAB42	s41782	SKI	s12881	ST3GAL3	s12854
PLOD1	s414	RAB42	s41783	SKI	s12882	ST3GAL3	s12855
POMGNT1	s31106	RAD54L	s16012	SLC25A33	s38789	STK40	s38326
POMGNT1	s31107	RAD54L	s16013	SLC25A33	s38790	STK40	s38327
POMGNT1	s31108	RAD54L	s16014	SLC25A33	s38791	STK40	s38328
POU3F1	s10853	RBP7	s41993	SLC25A34	s49744	STX12	s24307
POU3F1	s10854	RBP7	s41994	SLC25A34	s49745	STX12	s24308
POU3F1	s10855	RBP7	s41995	SLC25A34	s49746	STX12	s24309
PPCS	s36168	RHBDL2	s29788	SLC2A1	s12925	SYTL1	s39754
PPCS	s36169	RHBDL2	s29789	SLC2A1	s12926	SYTL1	s39755
PPCS	s36170	RHBDL2	s29790	SLC2A1	s12927	SYTL1	s39756
PPIE	s20445	RHCE	s12013	SLC2A5	s12937	TAL1	s13769
PPIE	s20446	RHCE	s12014	SLC2A5	s12938	TAL1	s13770
PPIE	s20447	RHCE	s12015	SLC2A5	s229610	TAL1	s13771
PPIH	s20485	RHD	s12016	SLC2A7	s45929	TARDBP	s23829
PPIH	s20486	RHD	s12017	SLC2A7	s45930	TARDBP	s23830
PPIH	s223120	RHD	s12018	SLC2A7	s45931	TARDBP	s23831
PPP1R8	s10954	RLF	s12043	SLC30A2	s15332	TCEA3	s13853
PPP1R8	s10955	RLF	s12044	SLC30A2	s15333	TCEA3	s13854
PPP1R8	s10956	RLF	s12045	SLC30A2	s15334	TCEA3	s13855
PPT1	s11017	RPA2	s12130	SLC5A9	s47170	TCEB3	s13859
PPT1	s11018	RPA2	s12131	SLC5A9	s47171	TCEB3	s13860
PPT1	s11019	RPA2	s12132	SLC5A9	s47172	TCEB3	s13861
PRDM16	s34346	RPS6KA1	s12273	SLC6A9	s12991	TEKT2	s26075
PRDM16	s34347	RPS6KA1	s12274	SLC6A9	s12992	TEKT2	s26076
PRDM16	s34348	RPS6KA1	s12275	SLC6A9	s12993	TEKT2	s26077
PRDM2	s15357	RRAGC	s34474	SLC9A1	s13021	TESK2	s20378
PRDM2	s229620	RRAGC	s34475	SLC9A1	s13022	TESK2	s20379
PRDM2	s229621	RRAGC	s34476	SLC9A1	s13023	TESK2	s20380
PRDX1	s10007	RSC1A1	s12369	SMAP2	s34842	TFAP2E	s50547
PRDX1	s10009	RSC1A1	s12370	SMAP2	s34843	TFAP2E	s50548
PRDX1	s224164	RSC1A1	s12371	SMAP2	s34844	TFAP2E	s50549
PRKCZ	s11128	RUNX3	s2467	SMPDL3B	s26099	THAP3	s40333
PRKCZ	s11129	RUNX3	s2468	SMPDL3B	s26100	THAP3	s40334
PRKCZ	s11130	RUNX3	s2469	SMPDL3B	s26101	THAP3	s40335

The table continuous on the next page

THRAP3	s19359	TRIM62	s30482	USP48	s38642	ZMPSTE24	s20065
THRAP3	s19360	TRIM62	s30483	USP48	s38643	ZMPSTE24	s20066
THRAP3	s19361	TRIM62	s30484	USP48	s38644	ZMPSTE24	s20067
TIE1	s14140	TRIM63	s39302	UTP11L	s27479	ZMYM6	s17593
TIE1	s14141	TRIM63	s39303	UTP11L	s27480	ZMYM6	s17594
TIE1	s14142	TRIM63	s39304	UTP11L	s27481	ZMYM6	s17595
TINAGL1	s34486	TRIT1	s29468	UTS2	s21447	ZMYND12	s38660
TINAGL1	s34487	TRIT1	s29469	UTS2	s21448	ZMYND12	s38661
TINAGL1	s34488	TRIT1	s29470	UTS2	s21449	ZMYND12	s38662
TNFRSF14	s16699	TRNAU1AP	s29835	VWA1	s35040	ZNF436	s37407
TNFRSF14	s16700	TRNAU1AP	s29836	VWA1	s35041	ZNF436	s37408
TNFRSF14	s16701	TRNAU1AP	s29837	VWA1	s195357	ZNF436	s37409
TNFRSF18	s194959	TSSK3	s37745	WDTC1	s22890	ZNF593	s27294
TNFRSF18	s194960	TSSK3	s37746	WDTC1	s22891	ZNF593	s27295
TNFRSF18	s453358	TSSK3	s37747	WDTC1	s22892	ZNF593	s195205
TNFRSF1B	s14268	TTLL10	s48504	YARS	s442	ZNF683	s48848
TNFRSF1B	s14269	TTLL10	s48505	YARS	s443	ZNF683	s48849
TNFRSF1B	s14270	TTLL10	s48506	YARS	s444	ZNF683	s48850
TNFRSF25	s231644	UBE2J2	s42189	YBX1	s9731	ZNF684	s43169
TNFRSF25	s444243	UBE2J2	s42190	YBX1	s9732	ZNF684	s43170
TNFRSF25	s500476	UBE2J2	s42191	YBX1	s9733	ZNF684	s43171
TNFRSF4	s14529	UBE4B	s555	ZBTB17	s15210	ZNF691	s27316
TNFRSF4	s14530	UBE4B	s556	ZBTB17	s15211	ZNF691	s27317
TNFRSF4	s14531	UBE4B	s554	ZBTB17	s15212	ZNF691	s27318
TNFRSF8	s2630	UBR4	s23626	ZBTB40	s19248	ZSCAN20	s15066
TNFRSF8	s2631	UBR4	s23627	ZBTB40	s19249	ZSCAN20	s15067
TNFRSF8	s2632	UBR4	s23628	ZBTB40	s19250	ZSCAN20	s15068
TNFRSF9	s7386	UQCRH	s14708	ZBTB48	s6566		
TNFRSF9	s7387	UQCRH	s14709	ZBTB48	s6567		
TNFRSF9	s7388	UQCRH	s14710	ZBTB48	s6568		
TP73	s14319	UROD	s14711	ZDHHC18	s38706		
TP73	s14320	UROD	s14712	ZDHHC18	s38707		
TP73	s14321	UROD	s14713	ZDHHC18	s38708		

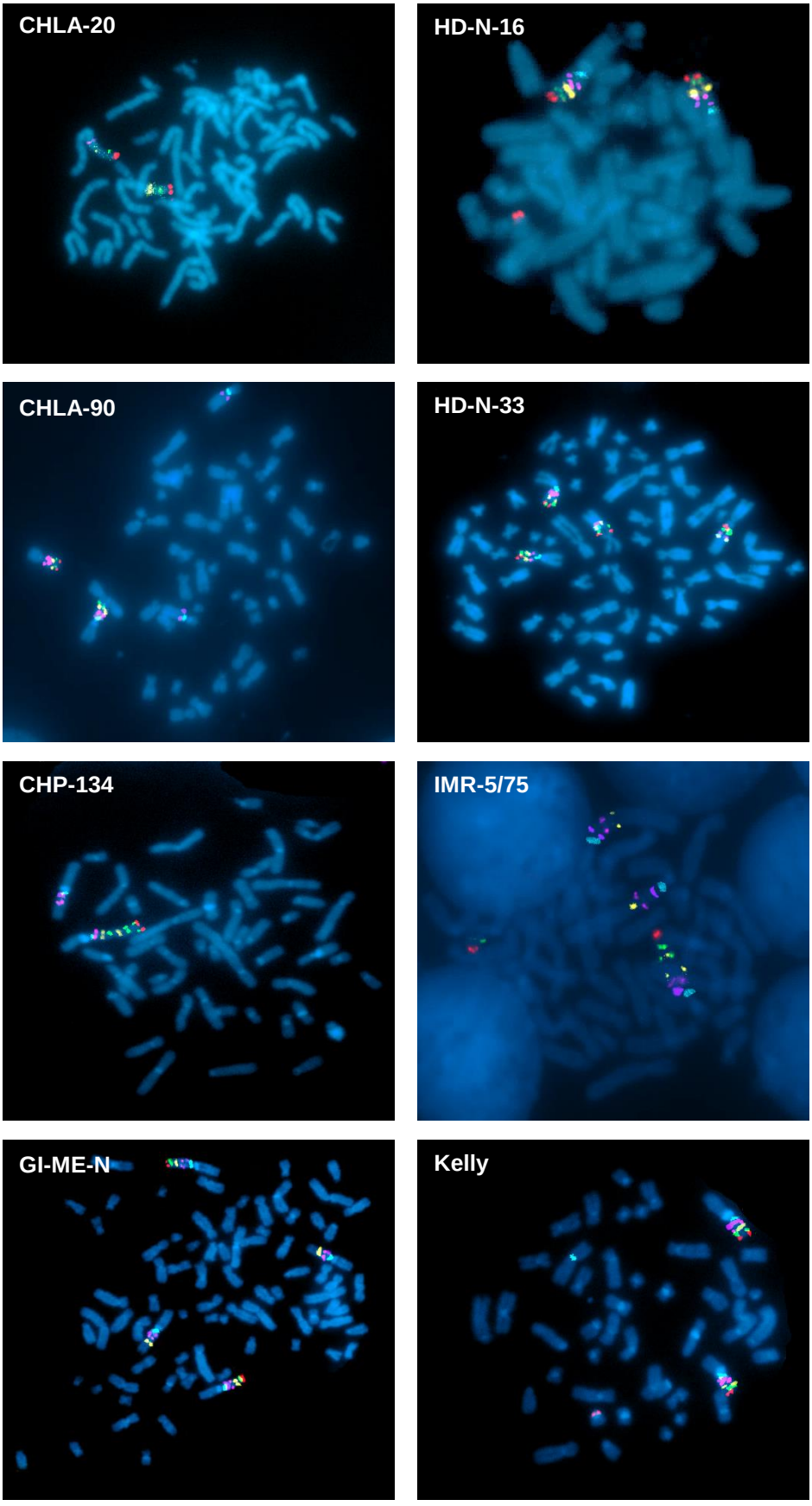

The figure continues on the next page

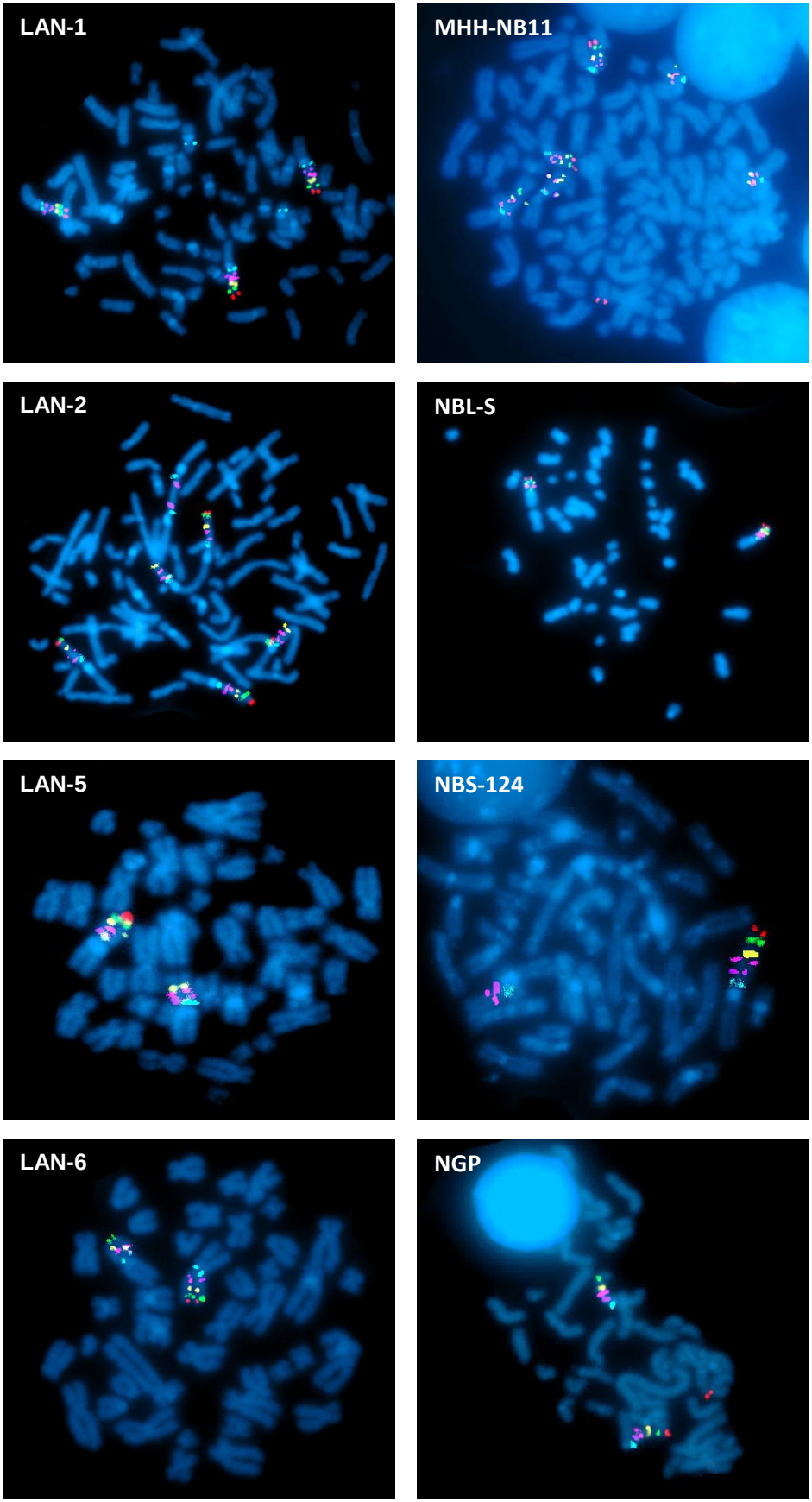

The figure continues on the next page

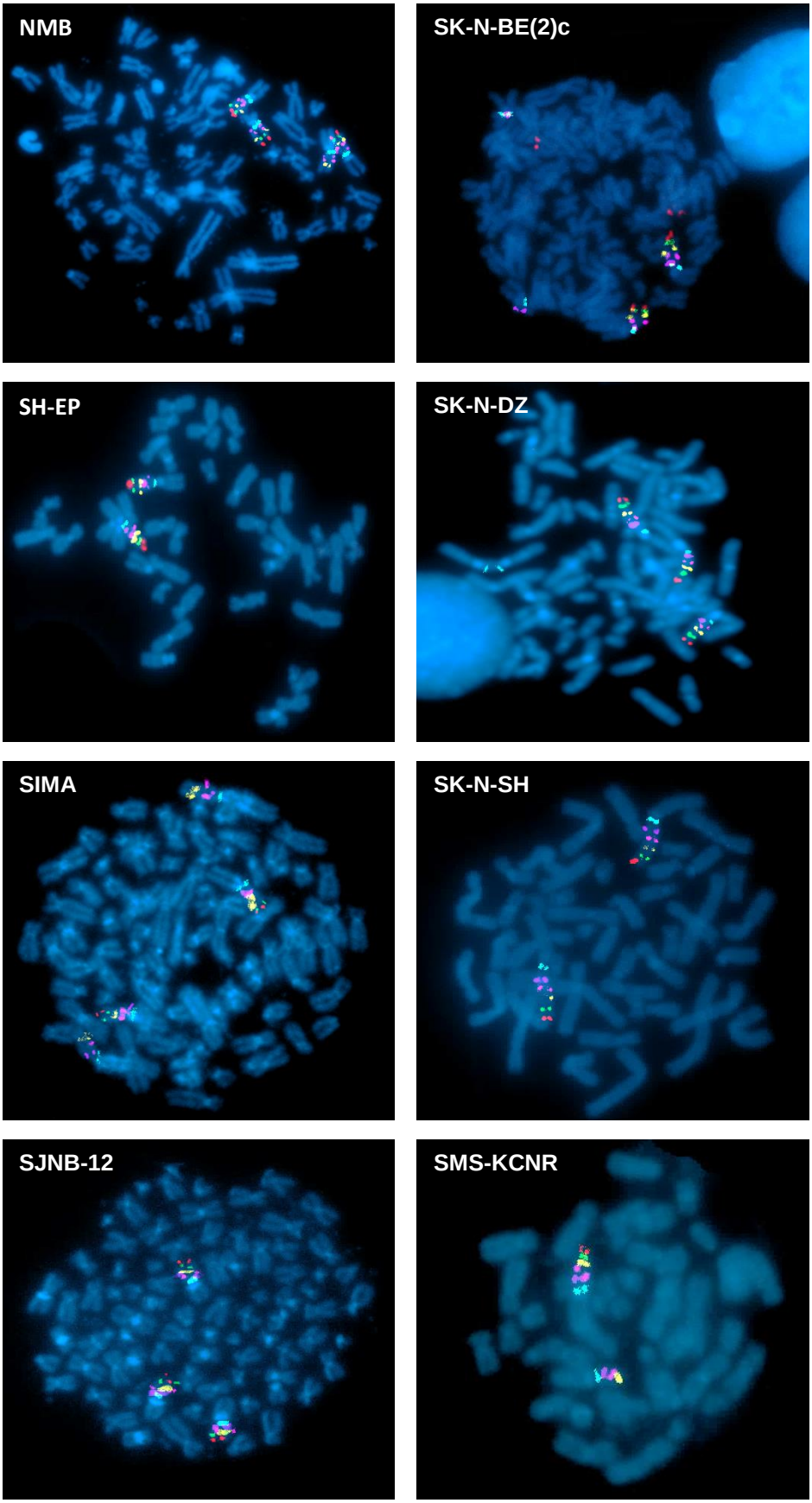

The figure continues on the next page.

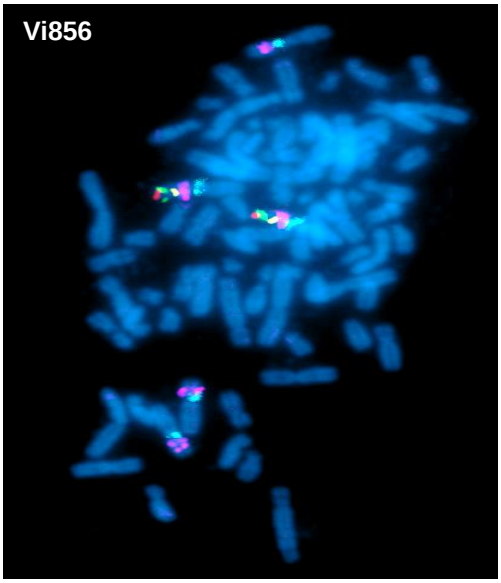

Fig. S 1: FISH analysis in neuroblastoma cell lines.

FISH analysis of 25 neuroblastoma cell lines reveals the copy number status of chromosome arm 1p. Six probes have been used (Cy3, FITC, Cy5, Cy3.4, DEAC, Cy5.5), the chromosomes are stained with DAPI.

Tab. S 2: Selected genes which knock-down reduces cell confluency in 1p-deleted and 1p non-deleted cells.

Function	Gene	concluency score 1p-deleted	concluency score 1p non-deleted
Neuonal genes and/or embryonic development	ARID1A	-0.27	-0.96
	ATP13A2	-0.54	-0.49
	CHD5	-0.36	-0.18
	EPHA2	-0.19	-0.15
	EPHA8	-0.15	0.00
	EPHB2	-0.28	-0.18
	FBXO44	-0.23	-0.05
	GABRD	-0.41	-0.22
	GRHL3	-1.37	-1.58
	HTR1D	-0.70	-0.22
	HTR6	-0.50	-0.35
	MMEL1	-0.45	-0.07
	MMP23B	-0.40	-0.46
	PAX7	-0.22	-0.61
	SCNN1D	-0.53	-0.38
	ZBTB17	-0.06	0.11
Cell growth and proliferation	ASAP3	-0.56	-0.72
	CDC42	-1.18	-0.73
	CDK11B	-1.96	-1.18
	CNKSR1	-0.14	-0.58
	DFFA	-0.70	-0.80
	CASP9	-0.79	-0.29
	EFHD2	-0.14	-0.27
	IL22RA1	-0.05	-0.48
	NR0B2	-0.09	-0.64
	NUDC	-0.65	-0.27
	SLC9A1	-0.84	-0.73
	TNFRSF18	-0.48	-0.55
	TNFRSF4	0.15	-0.34

Tab. S 3: Differentially expressed genes in IMR-32 after EphB2 siRNA knock-down.

Gene	p-value	Fold Change	Gene	p-value	Fold Change
FCF1P1	0.0096	6.48	STC2	0.0330	1.78
HGF	0.0096	6.19	RP11-244O19.1	0.0330	1.74
AC083867.4	0.0096	5.77	RPL23AP50	0.0105	1.74
RP11-548N1.1	0.0366	5.60	CTC-268N12.3	0.0330	1.71
LRRC4B	0.0096	5.19	SRGAP3	0.0190	1.70
GBP1	0.0176	4.68	RP11-317G6.1	0.0105	1.69
TCEAL7	0.0366	4.38	ABCC5-AS1	0.0190	1.68
NAV2-AS2	0.0187	2.83	AC138035.2	0.0105	1.67
RP11-778J15.1	0.0325	2.67	RP11-367O10.1	0.0105	1.64
NAV2-AS3	0.0103	2.56	RP4-633I8.1	0.0330	1.63
GDNF	0.0330	2.53	EEF1A1P25	0.0105	1.58
AC073109.2	0.0105	2.47	PCDHB18	0.0330	1.58
RBP1	0.0330	2.41	ZNF883	0.0330	1.55
RP11-134O21.1	0.0105	2.38	RP11-457M11.5	0.0190	1.52
CTD-2215E18.3	0.0103	2.34	RP11-326L2.1	0.0105	1.51
RPL7AP31	0.0325	2.33	CTB-176F20.3	0.0190	1.51
AC013472.3	0.0325	2.32	LL22NC03-2H8.5	0.0190	1.50
TRABD2B	0.0105	2.32	RPL5P3	0.0105	1.48
RP1-296L11.1	0.0105	2.30	RP3-472M2.2	0.0105	1.46
ZBTB12P1	0.0190	2.09	RP11-887P2.5	0.0105	1.41
KRT18P55	0.0330	2.06	ABCA12	0.0105	1.36
TTC18	0.0105	1.97	CTD-2293H3.1	0.0105	1.26
PCDHA6	0.0190	1.95	DHRS2	0.0330	-1.51
AC093390.1	0.0325	1.89	VN1R80P	0.0330	-1.68
AC106801.1	0.0325	1.87	P2RY6	0.0325	-2.02
IFIT3	0.0330	1.87	TMEM255B	0.0309	-2.48
RP11-764K9.1	0.0190	1.86	PRAME	0.0521	-2.64
RP11-354P11.8	0.0105	1.85	RAB33A	0.0176	-2.87
RP11-162A12.3	0.0105	1.84	YBX3	0.0477	-3.19
PSAT1	0.0190	1.83	RP11-120K18.2	0.0477	-3.25

Tab. S 4: Shared differentially expressed genes in IMR_shEphB2 #2/#3 in absence (EphB2 On) and presence (EphB2 Off) of doxycycline, all results are at least significant (p<0.05).

Gene	Fold change shEphB2 Off	Fold change shEphB2 On	Gene	Fold change shEphB2 Off	Fold change shEphB2 On	Gene	Fold change shEphB2 Off	Fold change shEphB2 On
ABCC8	2.037	1.835	EYA4	1.576	1.694	PITPNM3	-2.871	-2.875
ABCC9	-2.190	-2.069	F3	-2.391	-2.551	PLCB2	-1.841	-1.538
ADAMTS4	-2.376	-2.238	FBLN2	-2.195	-1.862	PPP1R17	-1.654	-1.535
AFF3	2.685	2.665	GKAP1	-2.344	-2.331	RAMP1	-2.176	-1.902
ALPK2	-2.691	-2.751	GLB1L3	1.675	1.527	RNF112	-2.128	-2.316
ANGPT1	1.653	1.596	GPX8	-2.952	-3.059	ROBO2	1.589	1.848
ANKFN1	-2.108	-2.145	GRIK3	1.818	1.725	RTL1	-1.744	-1.542
ANKRD18A	2.120	1.990	GRIP2	1.850	1.871	RXRG	-2.927	-2.508
ARHGEF28	1.718	1.702	HERC5	1.695	1.604	S100A6	1.640	1.748
BMP7	2.038	2.110	HS3ST3A1	1.730	1.509	SEMA5A	1.570	1.559
BOK	-2.094	-1.998	HTR3A	-1.587	-1.592	SHTN1	-1.816	-2.037
BTBD11	-3.373	-3.335	IFI44	-2.695	-2.577	SLC6A2	2.154	1.699
CA12	-1.743	-1.632	IL13RA1	2.069	2.155	SSFA2	-1.753	-1.660
CCKAR	-2.420	-1.906	IL1RAPL1	1.746	1.949	STIM2	-1.511	-1.576
CCSER1	2.159	2.142	ISLR2	-2.193	-2.340	STRA6	-2.424	-2.509
CDH10	1.964	2.158	ITPKB	-1.508	-1.506	STUM	-1.836	-2.053
CELF3	1.799	1.572	KAT2B	2.063	2.013	STX3	-2.651	-2.508
CHL1	-1.960	-2.106	KCNJ6	2.975	2.833	THSD7A	-2.268	-2.523
CHRNA9	-4.539	-4.590	KCNJ9	1.739	1.610	TIMP1	-3.044	-2.959
CNR1	-1.636	-1.591	LITAF	-2.302	-2.214	TMEFF2	1.728	1.549
CNTNAP3	1.559	1.571	LR	2.395	2.669	TOM1L1	-1.881	-1.953
COLEC12	2.148	1.959	MAMDC2	2.395	2.669	TUBA4A	-2.368	-2.302
CRABP1	-3.872	-3.612	ME3	-2.326	-2.263	UGT8	-1.791	-1.850
CRHR1	-1.801	-2.006	MEG3	-3.625	-3.646	VEGFD	-3.040	-2.929
CXCL12	-2.227	-2.398	MEG8	-2.779	-2.822	WNT5A	2.700	2.320
DLK1	-1.562	-1.591	MTTP	-1.555	-1.941	ZFAND4	-1.685	-1.828
DMRTA1	-1.839	-1.846	NELL1	1.971	1.744	ZIC5	1.561	1.694
DOCK11	2.695	2.925	NDRG2	1.688	1.630	ZNF264	-1.687	-1.605
ELOVL6	-1.907	-2.011	NEUROD2	-1.505	-1.500	ZNF334	2.284	1.897
EMC10	-2.206	-2.041	NEUROG2	-1.985	-1.971	ZNF521	-1.748	-1.709
EML5	2.538	2.559	NOS1AP	1.831	1.701	ZNF677	-2.964	-2.958
ENPP2	-2.240	-2.310	NRP1	2.457	2.472	ZNF835	-1.606	-1.538
EPHA4	1.813	1.903	NRP2	-2.683	-2.404	ZNF844	-2.505	-2.643
EPHB4	-3.886	-3.749	NWD2	3.827	3.703	ZNF876P	-2.842	-2.926
ESYT3	-1.810	-1.701	PIGM	1.896	1.824			

Tab. S 5: Genes uniquely differentially expressed in shEphB2 Off and EphB2 Off condition in IMR32_shEphB2 #2/#3, all results are at least significant (p<0.05).

shEphB2 Off		shEphB2 On	
Gene	Fold change	Gene	Fold change
BCAN	1.78229263	GJA1	3.10443033
C1orf226	1.69249093	PDE1A	2.23474781
PLPPR4	1.64018427	LMX1A	1.82782285
ZNF551	1.63885236	DNAH7	1.78796
CYTOR	1.5540148	PFKFB2	1.64740008
HS3ST3B1	1.54777595	CCDC80	1.60277526
POGZ	1.53871545	DPM3	1.58998197
GATA2	1.53773161	TMEM74B	1.58024689
ZNF107	1.53704625	PCDH9	1.57814376
CASQ1	1.52073287	EPB41L4B	1.54482017
KIAA1549L	1.50627167	TTC9B	1.52819272
KIF1A	-1.51074132	NACC2	1.51735093
ACKR3	-1.51242559	TBX2	1.51516316
SERINC2	-1.51488745	MYCBP2	1.50123209
TNC	-1.51930241	CORO2B	-1.50790262
CSPG4	-1.51999631	BAALC	-1.52427941
NHLH2	-1.52426802	PDE3A	-1.52550556
GOLGA7B	-1.53114532	PLEKHA6	-1.54563012
CD163L1	-1.53417393	ARHGAP28	-1.56324447
HIST3H2A	-1.57005974	PXDNL	-1.57761276
PID1	-1.5821893	JPH4	-1.61196847
SRPX	-1.58592947	GPR26	-1.63474383
IGDCC3	-1.58874127	KCNK3	-1.71459188
GPC1	-1.60263508		
ETV5	-1.6387073		
HES6	-1.65091155		
HIST3H2BB	-1.6533431		
NHS	-1.67565417		
PCSK9	-1.68112456		
AL353743.1	-1.69400468		
DCLK3	-1.7122369		
APCDD1	-1.72587985		
CNN1	-1.77051922		
DUSP6	-1.78283935		
AL117190.1	-1.80888155		

Tab. S 6: Differentially expressed genes in TR14 after EphB2 siRNA knock-down

Gene	p-value	Fold Change
C10orf53	0.0176	5.87
CSMD2	0.0366	5.29
RNU6-31P	0.0366	5.27
ADAMTS14	0.0366	4.86
TMEM178A	0.0366	4.50
CHST13	0.0325	2.89
GUCY1A2	0.0103	2.77
PARK2	0.0190	2.70
RP11-736K20.5	0.0187	2.59
RP11-617D20.1	0.0325	2.31
CTB-33G10.1	0.0330	1.98
RNF180	0.0330	1.94
PGBD4P3	0.0190	1.94
INSM1	0.0330	1.80
RP11-181C3.1	0.0325	1.69
ASPRV1	0.0105	1.68
DAB1	0.0330	1.64
DISC1FP1	0.0330	1.51
RP11-586D19.1	0.0190	1.51
MEIS1-AS1	0.0105	1.51
RP11-74C1.4	0.0190	-1.52
MEIS1-AS2	0.0103	-1.52
PCDP1	0.0187	-1.56
LMCD1	0.0330	-1.57
CD101	0.0187	-1.60
PCDH19	0.0190	-1.70
RP11-3D4.3	0.0190	-1.83
RNU6-875P	0.0105	-2.08
ERP27	0.0105	-2.10
AMER2	0.0325	-2.24
ADAM21	0.0309	-2.70
RP11-382A20.1	0.0477	-3.84
LINC00444	0.0083	-3.91
CTC-268N12.3	0.0477	-4.74

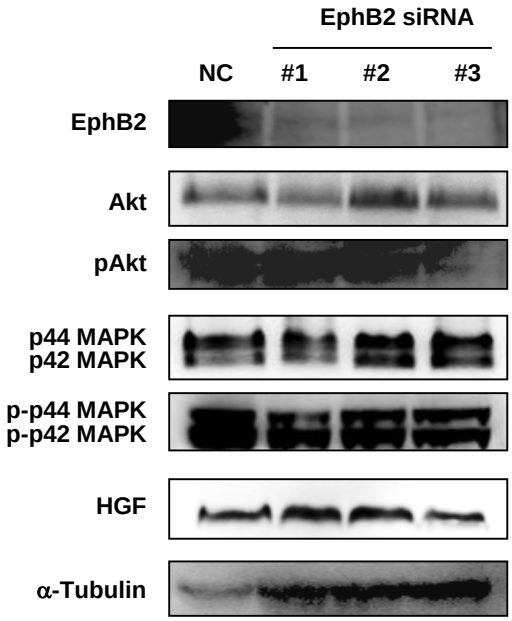

Fig. S 2: EphB2 knock-down has no impact on phosphorylated MAPK and Akt levels in 1p non-deleted cell lines.

EphB2 was knocked-down in the 1p non-deleted cell line TR14 with three different siRNAs. After 96 h the protein levels of HGF, MAPK, Akt and EphB2 through western blot. All results were compared to a non-targeting scrambled siRNA as negative control (NC).

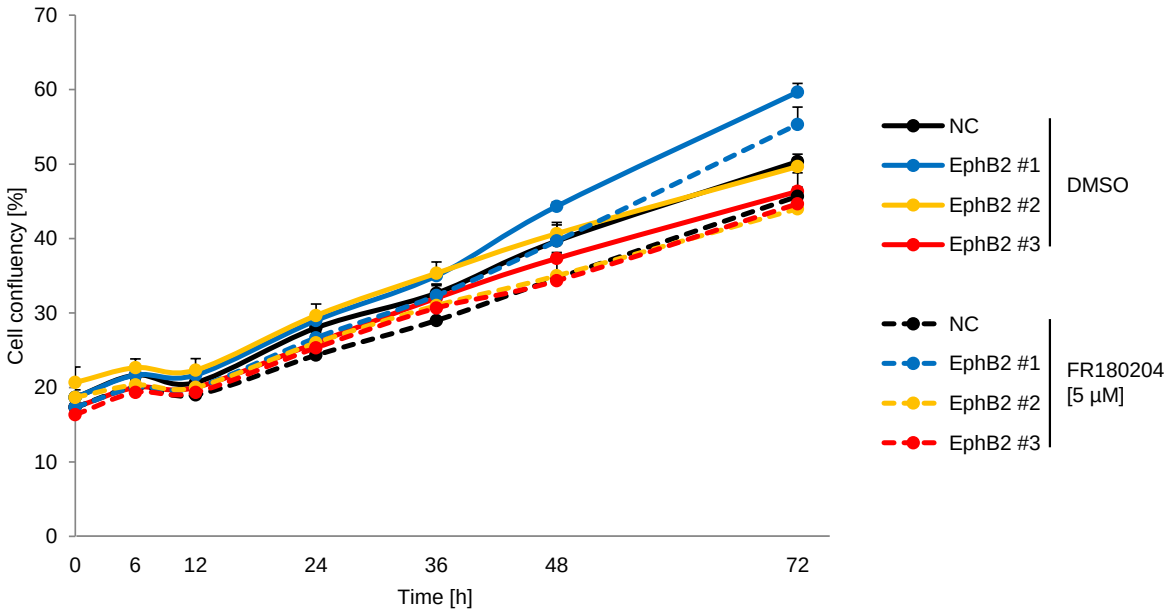

Fig. S 3: EphB2 knock-down in combination with MAKP inhibition has no impact on cell confluency in 1p non-deleted cell lines.

The 1p non-deleted cell line TR14 was treated with three different siRNAs against EphB2 in combination with the selective MAPK inhibitor FR180204 [5 µM]. All results are compared to a non-targeting scrambled siRNA as negative control (NC). The cell confluency was assessed after 0, 6, 12, 24, 36, 48 and 72 h. One exemplary result in triplicates, +SD.

6.2 Abbreviations

A, C, T, G, U, N	adenine, cytosine, guanine, thymine, uracile, any nucleotide
APS	ammoniumpersulfate
ATP	adenosine-5´-triphosphat
BAC	bacterial artificial chromosome
BCR	RhoGEF and GTPase activating protein
Bp	base pair
BSA	bovine serum albumin
cDNA	complementary DNA
cm	centimeter
CPM	counts per million
Cy3/ Cy3.5/ Cy5/ Cy 5.5	Cyanine 3/ 3.5/ 5/ 5.5
CYCLOPS	copy number alterations yielding cancer liabilities owing to partial loss
DAPI	4,6-diamino-2-phenylindol
dATP	2'-deoxyadenosine 5’-triphosphate
DAVID	database for annotation, visualization and integrated discovery tool
dCTP	2'-deoxycytidine 5’-triphosphate
DEAC	7-diethylaminocoumarin-3-carboxylic acid
dGTP	2'-deoxyadenosine 5’-triphosphate
DM	double minutes
DMSO	dimethylsulfoxid
DNA	deoxyribonucleic acid
DNA	desoxyribonucleic acid
DNase	desoxyribonuclease
dNTP	2'-deoxyribonucleoside 5’-triphosphate
dTTP	2'-deoxythymidine 5’-triphosphate
dUTP	2'-deoxyuracil 5’-triphosphate
E. coli	*Escherischia coli*
EDTA	ethylendiamintetraacetic acid, Na-salt
ELISA	Enzyme-linked Immunosorbent Assay
et al.	et alii (and other)
FACS	fluorescence activated cell sorting
FBS	fetal Bovine serum

FISH	fluorescence *in situ* hybridization
FITC	fluorescein isothiocyanate
for	forward
FSC	forward scatter
g	gram
$G_0/G_1/G_2$	gap 0/ gap 1/ gap 2 phase in cell cycle
GO	gene ontology
h	hour
H_20_{dd}	double-distilled water
HDACs	histone deacetylases
HPV	human papilloma virus
HRP	horseradish peroxidase
HSR	homogeneously stained region
INSS	International Neuroblastoma Staging System
kDa	kilodalton
l	liter
LB	Luria-Bertani
LOH	loss of heterozygosity
m	milli
M	molar
mA	millampere
min	minute(s)
miRNA	microRNA
ml	milliliter
mRNA	messenger RNA
mRNA	messenger RNA
n	nano
nm	nanometer
p	piko
PAGE	polyacrylamide gel electrophoreses
PBS	phosphate buffered saline
PCR	polymerase chain reaction
pH	*potentia Hydrogenii*
PI	propidium iodide
qRT-PCR	quantitative real-time PCR
rev	reverse

RISC	RNA-induced silencing complex
RNA	ribonucleic acid
RNA	ribonucleic acid
RNase	ribonuclease
rpm	rotation per minute
RPMI1640	Rosvell Park Memorial Institute, medium formulation 1640
RT	room temperature
RT-PCR	real time PCR
s	second
S.D.	standard deviation
SDS	sodiumdodecylsulfat
SE	super enhancer
sec	second(s)
siRNA	small interfering RNA
SRO	smallest region of overlapping deletion
SSC	side scatter
TBE	Tris/Borate/EDTA,
TBS-T	tris-buffered saline with Tween 20
TEMED	N, N, N´, N´-tetramethylethylendiamin
TF	Transcription factor
Tris	tris-(hydroxymethyl)-aminomethan
Triton X-100	octyl-phenoxy-ethylenoxide
TSG	tumor suppressor gene
U	unit (a determinate of an enzyme activity)
UV	ultra violet
UV	ultraviolet
V	Volt
W	Watt
z-VAD-FMK	carbobenzoxy-valyl-alanyl-aspartyl-[O-methyl]-fluoromethylketone
µ	micro

6.3 Figures

6.4 Publications

Afanasyeva EA, Gartlgruber M, Ryl T, Mönke G, Florez A, **Torkov A**, Dreidax D, Herrmann C, Okonechnikov K, Toprak U, Sagulenko V, Henrich KO, Decaesteker B, Denecker G, Speleman F, Ek S, Westermann F: Kalirin-RAC controls nucleokinetic migration in ADRN-type neuroblastoma. In submission.

Henrich KO, Bender S, Saadati M, Dreidax D, Gartlgruber M, Shao C, Herrmann C, Wiesenfarth M, Parzonka M, Wehrmann L, Fischer M, Duffy DJ, Bell E, **Torkov A**, Schmezer P, Plass C, Höfer T, Benner A, Pfister SM, Westermann F: Integrative Genome-Scale Analysis Identifies Epigenetic Mechanisms of Transcriptional Deregulation in Unfavorable Neuroblastomas. Cancer Res. 2016, 76(18): 5523-37.

Czaplinski S, Abhari BA, **Torkov A**, Seggewiß D, Hugle M, Fulda S: Differential role of RIP1 in Smac mimetic-mediated chemosensitization of neuroblastoma cells. Oncotarget 2015, 6(39): 41522-34.

6.5 Acknowledgements

Mein erster Dank geht an Frank Westermann. Ich freue mich, dass ich meine Arbeit in deiner Gruppe absolvieren durfte, in der es eine gute Balance zwischen wissenschaftlicher Herausforderung und freundschaftlicher Atmosphäre gibt. Deinen wissenschaftlichen Rat weiß ich sehr zu schätzen, sowie die Ermöglichung der Teilnahme an verschiedenen internationalen Konferenzen.

Ich danke Thomas Höfer für die Übernahme der Aufgabe als Erstgutachter, sowie die Bereitstellung von Bioinformatikern zur Datenauswertung. Außerdem danke ich an dieser Stelle Stefan Wiemann und Michael Boutros, die sich ebenfalls als Prüfer dieser Arbeit zur Verfügung gestellt haben.

Meine Arbeit wäre nicht möglich geworden ohne das starke Erfle-Team. Danke Nina und Jürgen für euren unermüdlichen Einsatz im Labor, obwohl ich und die „Kackbratzen“ euch des Öfteren zur Verzweiflung gebracht haben. Danke Manuel für die Auswertungen und vor allem das Sressmanagement danach. Ihr seid die lustigste und liebenswürdigste Gruppe!

Ganz besonders bedanke ich mich bei meiner Arbeitsgruppe B087. An erster Stelle steht hier Elisa, ohne Dich wäre diese Arbeit nie möglich geworden, da ich vermutlich einfach nur weinend in einer Ecke unseres brennenden Labors sitzen würde. Danke auch an Steffen, denn obwohl Du nicht mehr bei uns arbeitest, hast Du dir spät abends die Zeit genommen um mit mir telefonisch auf Fehlersuche zu gehen, wenn sich mal wieder gar nichts kloniert hat. Umut thank you for data analysis, especially for producing bee hives (who needs volcano blots anyway?). Ein Dankeschön auch an YG und die vier lieben Görls aus dem Call Center für gemeinsame Mittagessen, Kaffeetrinken und gegenseitiges Verständnis, wenn mal wieder die kleine Welt eines Doktoranden zusammenbricht. Insbesondere danke ich hier Lea, ohne Dich wäre die eine oder andere RT-PCR in einem Nervenzusammenbruch geendet. Ich danke Larissa für wissenschaftlichen Rat, die Einführung in die geheimnisvolle FISH-Methode, für kulturelle Tipps und Reiseführer. Elena, thank you for scientific advice, for being always a good companion and for your Russian awesomeness! Mona, Dir möchte ich danken für deine beratende Funktion als Chef-Korrektorin und -Nachrechnerin und hervorragende Ausflüge nach Griechenland, Bali und Australien.
Nun zu den Brudis: Daniel, Du warst immer beste. Ich hoffe, dass wir uns noch in der Weststadt sehen und alle umliegenden Menschen mit HipHop-Gesprächen nerven.

Moritz, Dir danke ich für ganz viele Sachen, z.B. Rudern, Bali/Australien/Schweden/ Berlin/New York..., BioContact, Äppelwoi,...aber vor allem, dass wir das ganze zusammen durchgestanden haben. Kai, Du bist eine ganz besondere Type, danke, dass Du mit mir die Vorliebe für Trash, verrückte Hobbies und düschtere Musik geteilt hast.

Außerdem danke ich Felix, Du warst immer ein guter Freund und „Geschäftspartner“. Ich hoffe, dass wir mal zusammen ein echtes Startup gegen die Wand fahren!

Ich möchte noch einigen Leuten aus meinem privaten Umfeld danken. Dazu zählen die darmstädter Rabauken Miriam, Farena, Sophia und Thalitz, die verrückten Katzenladies Näddlie und Janina und meine ehemaligen Mitbewohner Läppold und Anke. Jeder von euch hätte einen ganzen Absatz verdient, da es sich hierbei aber um eine seriöse Arbeit handelt, verschiebe ich das Ganze auf meine Memoiren. Nur so viel sei gesagt: ihr seid alle ganz außergewöhnliche Menschen und ohne euch und euren Support wäre mein Leben ziemlich trist.

An letzter Stelle, aber an wichtigster, danke ich meinen Eltern. Ihr seid wie eine eiserne Wand, die hinter mir steht. Mein Dank geht an den bedingungslosen Rückhalt und den Glauben an mich. Möge diese Arbeit euch gewidmet sein, meine lieben Eltern.